

DTIC  
**AD-A229 508**

WRDC-TR-90-3063



**TWIN JET SCREECH SUPPRESSION CONCEPTS TESTED FOR  
4.7% AXISYMMETRIC AND TWO-DIMENSIONAL NOZZLE CONFIGURATIONS**

Steven H. Walker  
Aerodynamics and Airframe Branch  
Aeromechanics Division

29 September 1990

Final Report for Period July 1987 - September 1989

Approved for Public Release; Distribution Unlimited

FLIGHT DYNAMICS LABORATORY  
WRIGHT RESEARCH AND DEVELOPMENT CENTER  
AIR FORCE SYSTEMS COMMAND  
WRIGHT-PATTERSON AIR FORCE BASE, OHIO 45433-6553

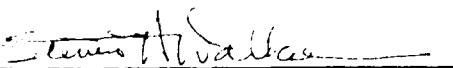
**DTIC**  
**ELECTE**  
**DEC 05 1990**  
**S B D**

NOTICE

When Government drawings, specifications, or other data are used for any purpose other than in connection with a definitely Government-related procurement, the United States Government incurs no responsibility or any obligation whatsoever. The fact that the government may have formulated or in any way supplied the said drawings, specifications, or other data, is not to be regarded by implication, or otherwise in any manner construed, as licensing the holder, or any other person or corporation; or as conveying any rights or permission to manufacture, use, or sell any patented invention that may in any way be related thereto.

THIS REPORT HAS BEEN REVIEWED BY THE OFFICE OF PUBLIC AFFAIRS (ASD/PA) AND IS RELEASABLE TO THE NATIONAL TECHNICAL INFORMATION SERVICE (NTIS). AT NTIS IT WILL BE AVAILABLE TO THE GENERAL PUBLIC INCLUDING FOREIGN NATIONS.

This technical report has been reviewed and is approved for publication.

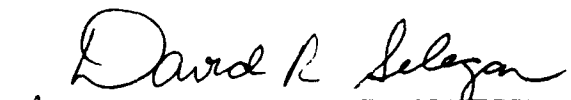


STEVEN H. WALKER  
Project Engineer



RUSSELL OSBORN, Acting Chief  
Aerodynamics and Airframe Branch  
Aeromechanics Division

FOR THE COMMANDER



for ALFRED C. DRAPER, Acting Chief  
Aeromechanics Division  
Flight Dynamics Laboratory

If your address has changed, if you wish to be removed from our mailing list, or if the addressee is no longer employed by your organization please notify WRDC/FIMM, WPAFB, OH 45433-6553 to help us maintain a current mailing list.

Copies of this report should not be returned unless return is required by security considerations, contractual obligations, or notice on a specific document.

# REPORT DOCUMENTATION PAGE

Form Approved  
OMB No 0704 0188

Public reporting burden for this collection of information is estimated to average 1 hour per response, including the time for reviewing instructions, searching existing data sources, gathering and maintaining the data needed, and completing and reviewing the collection of information. Send comments regarding this burden estimate or any other aspect of this collection of information, including suggestions for reducing this burden, to Washington Headquarters Services, Directorate for Information Operations and Reports, 1215 Jefferson Davis Highway, Suite 1204, Arlington, VA 22202-4302, and to the Office of Management and Budget, Paperwork Reduction Project (0704-0188), Washington, DC 20503.

1. AGENCY USE ONLY (Leave blank)		2. REPORT DATE September 1990		3. REPORT TYPE AND DATES COVERED Final Technical Report, Jul 87 - Sep 89	
4. TITLE AND SUBTITLE Twin Jet Screech Suppression Concepts Tested for 4.7% Axisymmetric and Two-Dimensional Nozzle Configurations				5. FUNDING NUMBERS PE 62102F PR 2404 TA 10 WU B4	
6. AUTHOR(S) Steven H. Walker , (513)255-6207					
7. PERFORMING ORGANIZATION NAME(S) AND ADDRESS(ES) Flight Dynamics Laboratory (WRDC/FIMM) Wright Research and Development Center				8. PERFORMING ORGANIZATION REPORT NUMBER TR-90-3063	
9. SPONSORING/MONITORING AGENCY NAME(S) AND ADDRESS(ES) Wright Research and Development Center Aerodynamics and Airframe Branch WRDC/FIMM WPAFB OH 45433-6553				10. SPONSORING/MONITORING AGENCY REPORT NUMBER WRDC-TR-90-3063	
11. SUPPLEMENTARY NOTES					
12a. DISTRIBUTION/AVAILABILITY STATEMENT Approved for public release, distribution unlimited.				12b. DISTRIBUTION CODE A	
13. ABSTRACT (Maximum 200 words) The sonic fatigue of nozzle flaps on F-15 and B-1 aircraft has demanded an increase in aeroacoustics research. A 4.7% scale, cold, static test was conducted at the Wright Research and Development Center (WRDC) to investigate noise suppression concepts on F-15 axisymmetric and two-dimensional nozzle configurations. These concepts included lateral spacing, secondary air jets, and tab suppression. Nozzle orientation parametrics included nozzle canting and pitch deflection. Design guideline charts are presented showing screech amplitude variation for each suppression and orientation concept.					
14. SUBJECT TERMS Twin jets, screech, mode coupling, axisymmetric, two-dimensional, suppression, helical, toroidal, flapping, secondary air jets, tabs, axial shift, nozzle cant, lateral spacing				15. NUMBER OF PAGES 116	
				16. PRICE CODE N/A	
17. SECURITY CLASSIFICATION OF REPORT Unclassified	18. SECURITY CLASSIFICATION OF THIS PAGE Unclassified	19. SECURITY CLASSIFICATION OF ABSTRACT Unclassified	20. LIMITATION OF ABSTRACT Unlimited		

## PREFACE

This report was prepared by Mr. Steven H. Walker of the Aerodynamics and Airframe Branch, Aeromechanics Division of the Wright Research and Development Center Flight Dynamics Laboratory (WRDC/FIMM), Wright-Patterson Air Force Base, Ohio. This research was accomplished under Job Order Number 240410B4, "Twin Jet Screech Analysis." The effort recorded in this report was conducted during the period of July 1987 through Sep 1989.

Special acknowledgment is extended to Mr. Leonard Shaw of the Structures Division and Mr. Michael Compton of the Aeromechanics Division who created the static test facility and generated the wealth of acoustic data. A special thanks to both gentlemen for their guidance and patience. Also, a word of thanks to Mr. Robert Gillgrist who spent many hours reducing acoustic data and plotting nozzle design guideline charts. Without the above people, this report would not have been possible.

Accession For	
NTIS GRA&I	<input checked="checked" type="checkbox"/>
DTIC TAB	<input type="checkbox"/>
Unannounced	<input type="checkbox"/>
Justification	
By	
Distribution/	
Availability Codes	
Dist	Avail and/or Special
A-1	

## TABLE OF CONTENTS

Section	Page
INTRODUCTION	1
Historical Perspective	1
WRDC Test Objective	9
DESCRIPTION OF TEST APPARATUS, INSTRUMENTATION, AND PROCEDURES	12
Model Description	12
Test Apparatus Description	13
Test Instrumentation Description	16
Test Procedures	16
ACOUSTIC DATA REDUCTION	19
Acoustic Spectrum Data	19
Data Reduction Challenges	22
Data Reduction Process	24
AXISYMMETRIC NOZZLE RESULTS	40
Single Axisymmetric Baseline Configuration	40
Twin Axisymmetric Baseline Configuration	42
Lateral Spacing Suppression	47
Twin Axisymmetric Secondary Air Jet Suppression	57
Twin Axisymmetric Tab Suppression	59
Twin Axisymmetric Axial Shift Suppression	66

TWO-DIMENSIONAL NOZZLE RESULTS	68
Single 2D Baseline Configuration	68
Twin 2D Baseline Configuration	72
Twin 2D Lateral Spacing Suppression	74
Twin 2D Secondary Air Jet Suppression	81
Twin 2D Tab Suppression	84
Twin 2D Axial Shift Suppression	87
Twin 2D Cant Angle Orientation	87
Twin 2D Vectored Thrust	89
CONCLUSIONS	95
REFERENCES	98
APPENDIX	101

## LIST OF ILLUSTRATIONS

Figure	Page
1. F-15 Afterbody Solution	3
2. Powell's Screech Feedback Mechanism	3
3. Powell's Frequency Jump Chart	5
4. Multiple Stages of Screech	5
5. Axisymmetric Modes	7
6. Two-dimensional Modes	8
7. Single versus Twin Nozzle Comparison	10
8. Hose-No Hose Effect	14
9. Test Setup	14
10. Comparison of Data Measurement Methods	17
11. Typical Acoustic Spectrum, (NPR=2.8)	20
12. Single Axisymmetric Baseline, (NPR=3.1)	23
13 (a,b). Peak Trend Methodology	26
14. Single Axisymmetric Baseline, First Pass (Modal Frequency Plot)	29
15 (a,b). Examples of Harmonics	30
16. Single Axisymmetric Baseline (Modal Frequency Plot)	31
17. Single Axisymmetric Baseline (SPL vs. Mach # Plot)	33
18. First Modal Transfer	35

19. Second Modal Transfer	36
20. Third Modal Transfer	37
21. Single Axisymmetric Baseline, Modes Identified (SPL vs. Mach # Plot)	39
22. Single Axisymmetric Baseline (Modal Frequency Plot)	41
23. Single Axisymmetric Baseline (SPL vs. Mach # Plot)	41
24. Dual Axisymmetric Baseline, $s/d=2.25$ (Modal Frequency Plot)	43
25. Dual Axisymmetric Baseline, $s/d=2.25$ (SPL vs. Mach # Plot)	43
26 (a,b). Single versus Dual SPL Plots	45
27. Single versus Dual Axisymmetric Configurations, (NPR=3.0)	46
28. Schlieren Photo of Mode Coupling, (NPR=3.0)	47
29 (a-1). Modal Frequency Plots for Various Spacing Ratios, ( $2.25 < s/d < 7.00$ )	49
30 (a-1). SPL vs. Mach # Plots for Various Spacing Ratios, ( $2.25 < s/d < 7.00$ )	52
31. Lateral Spacing Suppression for Dual Axisymmetric Configurations, (OASPL vs. $s/d$ )	56
32 (a-d). Modal Frequency Plots for Various Secondary Air Pressures (0 psig - 60 psig)	58



33 (a-d). SPL vs. Mach # Plots for Various Secondary Air Pressures (0 psig - 60 psig)	60
34. Secondary Air Suppression for Dual Axisymmetric Configurations, (SPL vs. Secondary Jet Pressure)	61
35 (a-d). SPL vs. Mach # Plots for Various Tab Configurations (0 tab - 3 tabs)	63
36. Tab Suppression for Dual Axisymmetric Configurations, (SPL vs. Mach # Plot)	64
37 (a,b). Schlieren Photos of Tab Suppression (a) No Tabs, (b) Two Tabs	65
38. Axial Shift Suppression for Dual Axisymmetric Configurations	67
39. Single Two-dimensional Baseline (Modal Frequency Plot)	70
40. Single Two-dimensional Baseline (OASPL vs. Mach # Plot)	70
41. Directivity Instrumentation	71
42. Dual Two-dimensional Baseline, $s/w=3.25$ (Modal Frequency Plot)	73
43. Dual Two-dimensional Baseline, $s/w=3.25$ (OASPL vs. Mach # Plot)	73
44 (a-k). OASPL versus NPR Plots for Various Spacing Ratios, ( $2.75 < s/w < 7.00$ )	75
45. Lateral Spacing Suppression for Dual Two-dimensional Configurations, (OASPL vs. $s/w$ )	79
46 (a-d). OASPL versus NPR for Various Secondary Air Pressures, (0 psig - 60 psig)	82

47. Secondary Air Suppression for Dual Two-dimensional Configurations	83
48. Tab Suppression for Dual Two-dimensional Configurations, (OASPL vs. NPR Plot)	85
49. Tab Suppression for Dual Two-dimensional Configurations, (OASPL vs. # Tabs)	86
50. Axial Shift Suppression for Dual Two-dimensional Configurations, (OASPL vs. Axial Shift Distance)	88
51. Cant Angle Comparison for Dual Two-dimensional Configurations, (OASPL vs. NPR Plot)	90
52. Cant Angle Effect (OASPL vs. Cant Angle Plot)	91
53. Vectoring Nozzle Effect (OASPL vs. NPR Plot)	92
54. Vectoring Nozzle Effect (SPL vs. Pitch Deflection)	94

## LIST OF SYMBOLS

c	Speed of Sound
d	Axisymmetric Nozzle Exit Diameter
dB	Decibel Units
f	Frequency
$h_t$	2D Nozzle Throat Height
M	Jet Mach Number
NPR	Nozzle Pressure Ratio
NVOLT	Instrumentation Measurement
OASPL	Overall Sound Pressure Level
PSIA	Atmospheric Pressure ( $\text{lb}_f/\text{in}^2$ )
RMS	Root Mean Squared Value
s	Center-To-Center Nozzle Spacing
s/d	Axisymmetric Nozzle Spacing Ratio
s/w	2D Nozzle Spacing Ratio
SPL	Sound Pressure Level
w	Two-dimensional Nozzle Exit Width
$\gamma$	Specific Heat Ratio
$\lambda$	Wavelength

## INTRODUCTION

In recent years, structural damage to nozzle flaps on the F-15 and B-1 aircraft has generated considerable interest in the acoustical environment of closely spaced twin jet aircraft. Acoustic wave instabilities originating in the supersonic plume have been found to propagate upstream causing structural failure of the nozzle flaps. A solution for the F-15 aircraft was to remove the nozzle flaps exposing the nozzle mechanical system to the freestream flow (Figure 1). This solution is not acceptable for the B-1 aircraft, since the removal of the nozzle flaps would increase the boattail drag and thus severely limit the B-1 range capability.

### Historical Perspective

The acoustical phenomenon associated with nozzle flap sonic fatigue is produced by supersonic jets, because the shock wave structure serves as a catalyst for generating narrowband and broadband shock-associated noise.<sup>1</sup> Shock-associated noise was first investigated by Powell who studied choked jet noise associated with axisymmetric and two-dimensional nozzles.<sup>2</sup>

Powell found that turbulent mixing within the jet shear layer was responsible for producing jet noise.<sup>2</sup> This jet noise had no discrete frequency and no discrete maxima over a continuous spectrum. Powell observed a dominant pure tone over certain ranges of pressure ratio for supersonic jet plumes. Powell discovered that increasing nozzle pressure ratios produced increasing pure tone wavelengths, and that these pure tone wave structures had a tendency to propagate upstream towards the nozzle exit.<sup>3</sup>

Powell is credited with observing a self-sustained aeroacoustic feedback loop in which the pure tone or screech tone, generated by the interaction of large scale turbulent eddies and the shock wave structure, is propagated upstream past the nozzle exit. As the sound waves pass the nozzle exit, embryotic disturbances originate at the nozzle exit and are amplified as they pass downstream. These disturbances complete the cycle by sending the pure tone instabilities upstream again<sup>2</sup> (Figure 2).

In testing the axisymmetric and two-dimensional cases, Powell measured frequency instability regions for the axisymmetric case and a fully stable frequency region for the two-dimensional case. Powell believed the screech feedback



Figure 1. F-15 Afterbody Solution

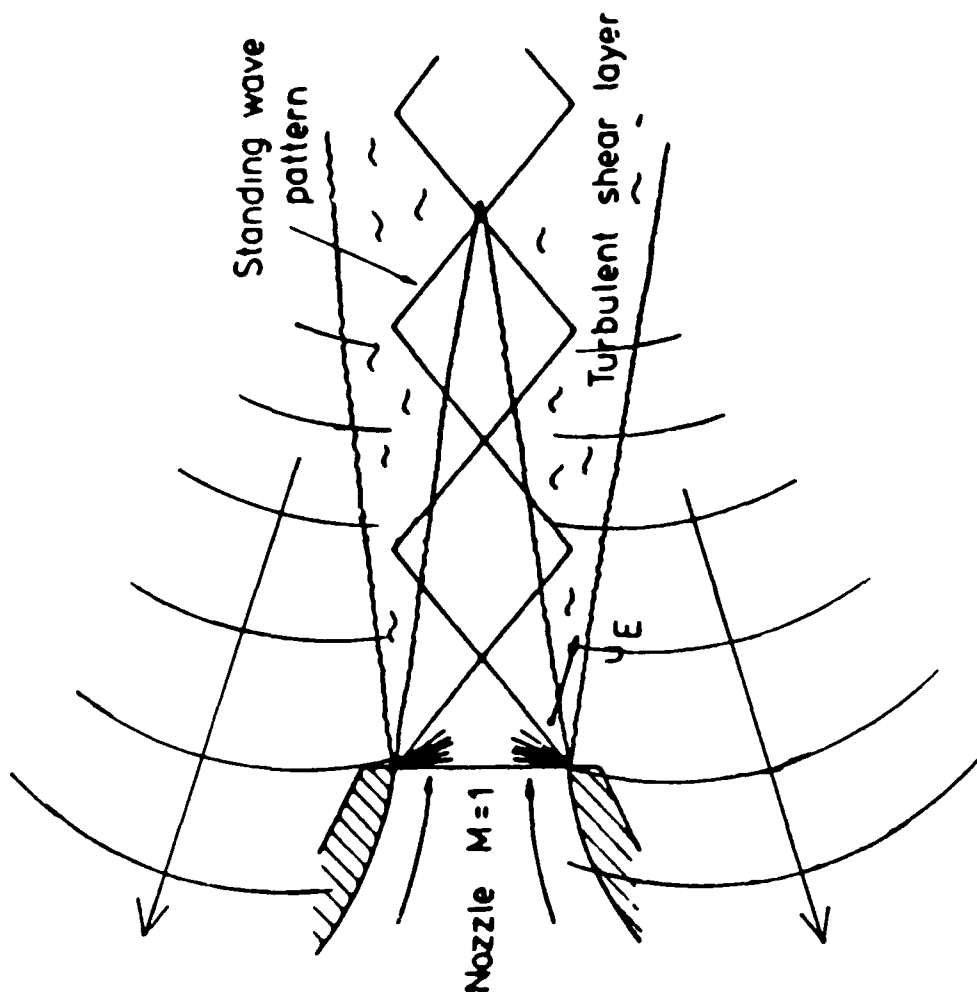


Figure 2. Powell's Screech Feedback Mechanism

process would only operate under certain conditions of phase and gain. For the two-dimensional case, Powell suggested that screech would occur over the entire range of nozzle pressure ratios tested, whereas for the axisymmetric case, he believed frequency jumps existed where screech could not be present<sup>2</sup> (Figure 3).

Davies and Oldfield suggested that various modes of screech existed, and that these modes could occur over the same operating range.<sup>4</sup> Norum investigated modes of screech, when these modes occurred, and how to suppress amplitudes of the screech tone for axisymmetric choked nozzles. He found that multiple stages of screech could exist for a given nozzle configuration and operating condition (Figure 4).<sup>5</sup> Westley and Woolley showed that multiple modes can exist for one configuration and one operating condition, but that one mode was always dominant over the others.<sup>6</sup>

For the axisymmetric case, two different spatial mode structures have been identified. The helical spatial structure, or B mode, possesses longer wavelengths (lower frequencies) and normally produces the highest screech sound amplitudes. The toroidal spatial structure, or A mode, possesses shorter wavelengths (higher frequencies) and normally produces the lower

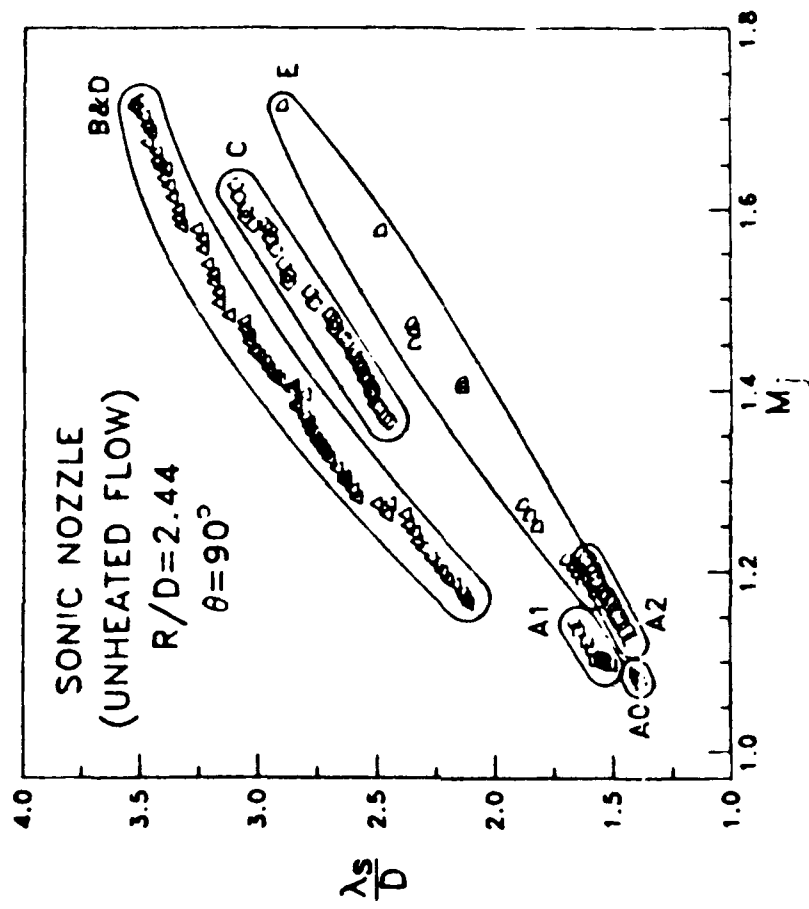


Figure 4. Multiple Stages of Screech

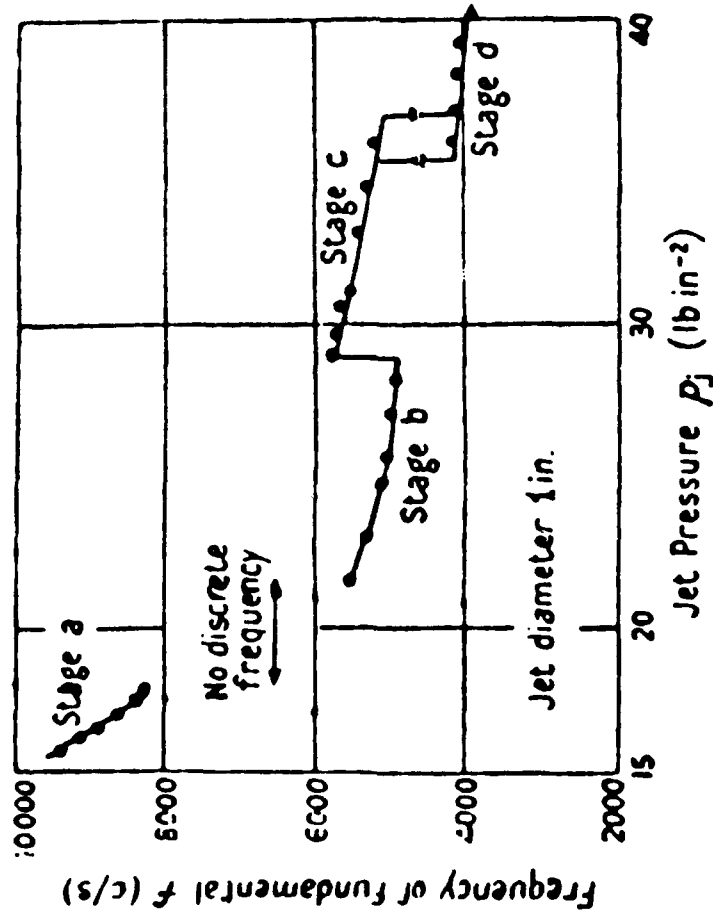


Figure 3. Powell's Frequency Jump Chart



screech sound amplitudes. The two spatial mode shapes in the region of the jet plume are shown in Figure 5.

For the two-dimensional case, Seiner and Norum agreed with Powell's findings that only a single mode structure existed.<sup>7</sup> Seiner, Manning, and Ponton later found a convergent-divergent rectangular nozzle to have at least three modes of screech.<sup>8</sup> Zilz, in a recent report, suggested that four screech modes existed for several two-dimensional nozzle configurations.<sup>9</sup> Zilz studied the jet operating conditions over which the two-dimensional mode combinations existed and measured the directivity of the sound waves to determine the dominant screech mode. A diagram of these four flapping modes is sketched in Figure 6.

The amplitudes of shock-associated noise and the various modes of screech are normally increased when two jets are spaced closely to one another. Seiner, Manning and Ponton determined that screech modes of the two closely spaced jet plumes can become coupled with each other, and that this mode coupling mechanism produces dynamic pressures exceeding the fatigue failure limit for metallic aircraft structures.<sup>10</sup> In a related study, Wlezien showed that a strong helical mode coupling existed for convergent-divergent axisymmetric nozzles at certain jet Mach

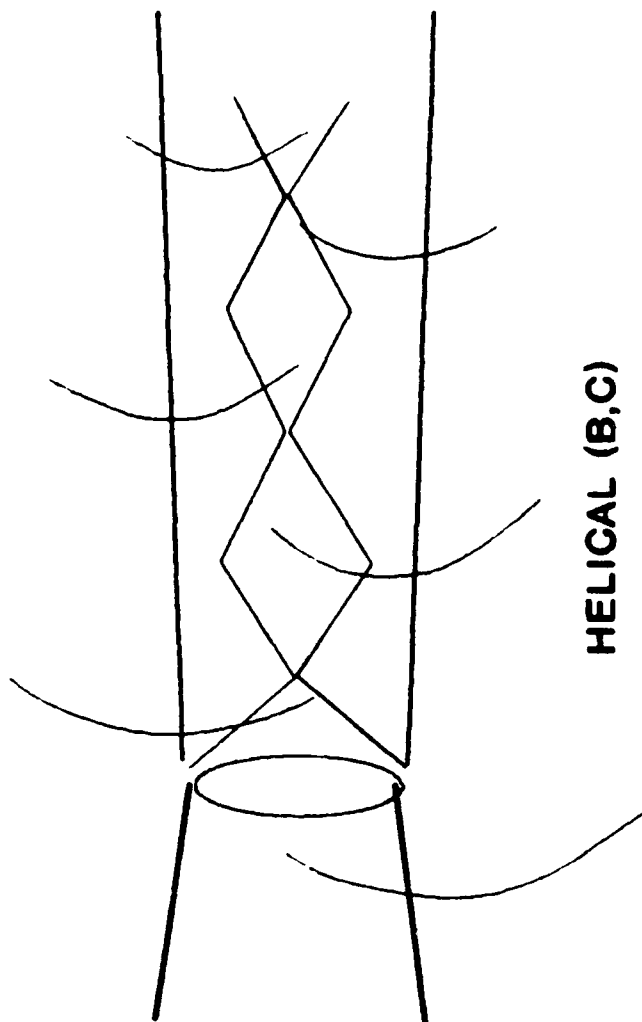
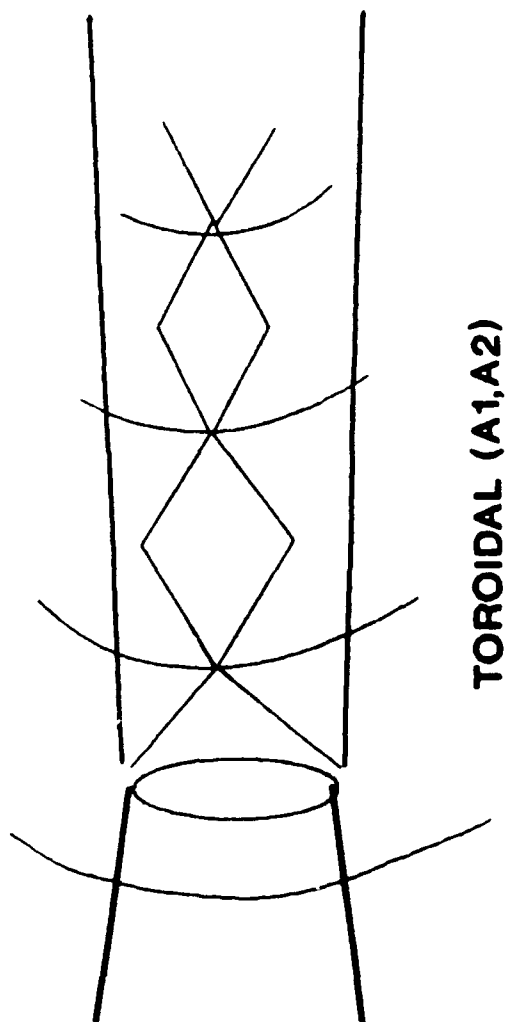
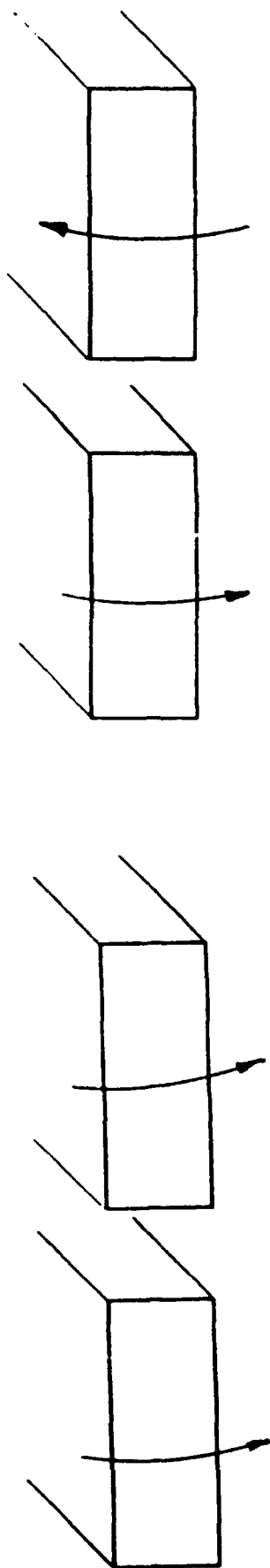
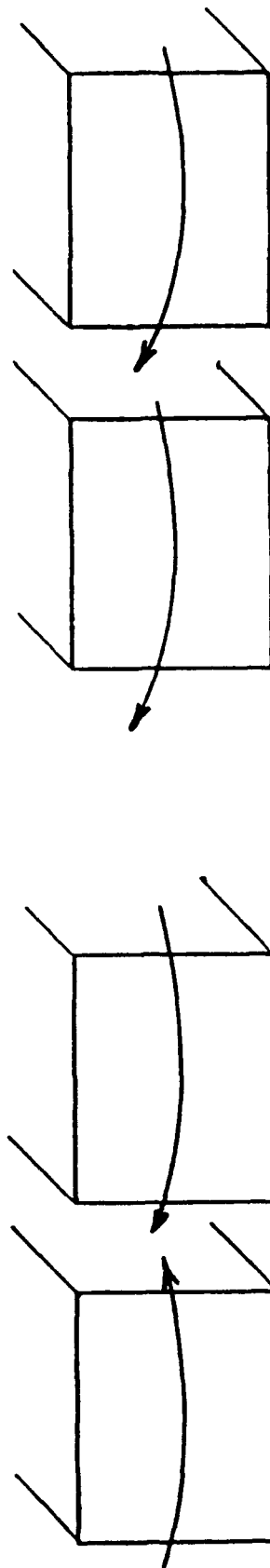


Figure 5. Axisymmetric Modes



NORMAL ANTISYMMETRIC (NA)

NORMAL SYMMETRIC (NS)



LATERAL ANTISYMMETRIC (LA)

LATERAL SYMMETRIC (LS)

Figure 6. Two-dimensional Modes

numbers.<sup>11</sup> Shaw investigated twin jet axisymmetric configurations and observed that for one particular comparison, the twin jet configuration resulted in a sound pressure amplitude 20 dB higher than the single jet configuration (Figure 7).<sup>12</sup> This sound amplitude difference of 20 dB is significant considering that the dual configuration produced a sound level of 160 dB which is large enough to cause structural fatigue.

#### WRDC Test Objective

A 4.7% scale, cold, static test was conducted at the Wright Research and Development Center (WRDC) to investigate the acoustic environment of closely spaced jet plumes. The objective of this test was to complement the existing screech database by contributing suppression and nozzle orientation results. Axisymmetric and two-dimensional nozzle configurations for several screech suppression concepts and nozzle orientations were tested. Among the test parameters were screech suppression techniques such as lateral spacing, secondary air jet, tab suppression, and axial shift. Other control parameters include nozzle orientations, such as canting the nozzle about the longitudinal axis, and pitching the nozzle about the lateral

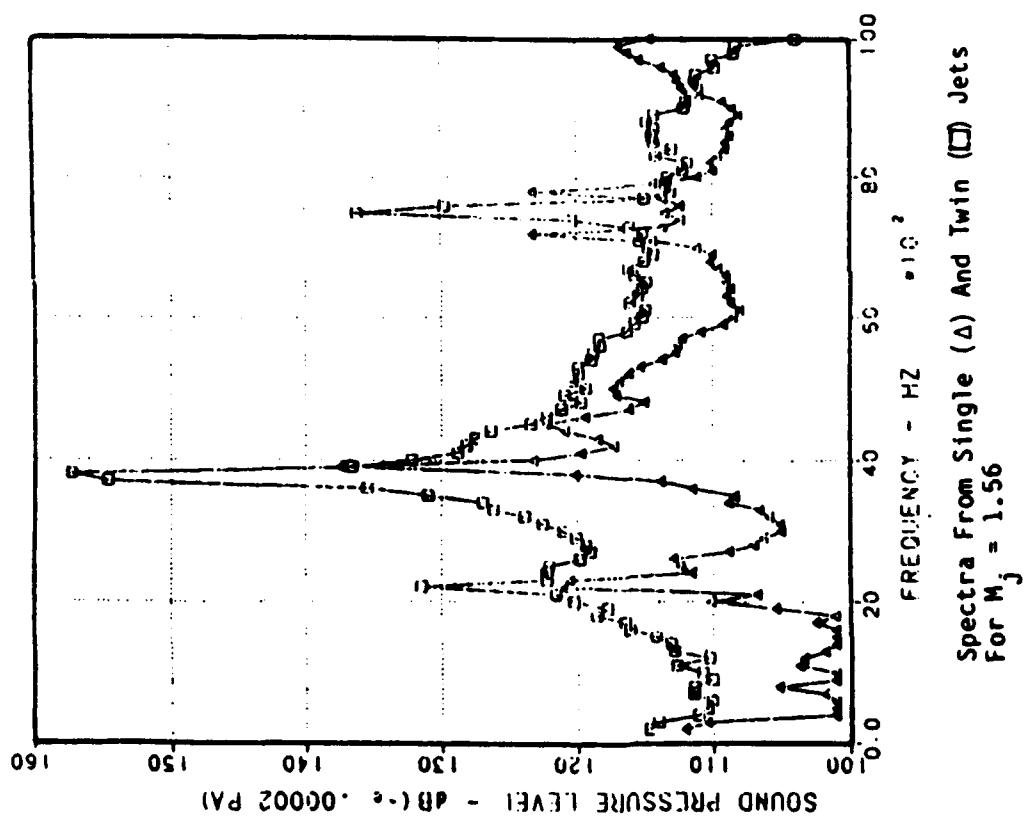


Figure 7. Single versus Twin Nozzle Comparison

axis. Design guidelines for screech reduction in various nozzle configurations were obtained.

## DESCRIPTION OF TEST APPARATUS, INSTRUMENTATION, AND PROCEDURES

This experiment was performed in the Flight Dynamics Laboratory at the Wright Research and Development Center (WRDC), Wright-Patterson AFB, Ohio. This cooperative research effort, sponsored by the Aeromechanics Division and the Structures Division, generated acoustic data using 4.7% scale axisymmetric and two-dimensional F-15 nozzles.

### Model Description

The axisymmetric nozzles were convergent in nature having a nozzle exit diameter of 1 in (2.54 cm) and an exit to throat area ratio of 1. The geometry dictated a fully expanded jet plume at an exit Mach number of 1. The two-dimensional nozzles were convergent-divergent in nature having a nozzle throat aspect ratio of 3.71 and an exit to throat area ratio of 1.11. This area ratio dictates a design jet Mach number of 1.4 or a design nozzle pressure ratio (NPR) of 3.23. This convergent-divergent geometry allowed for both overexpanded and underexpanded exhaust

plumes. For a complete description of test configurations and suppression concept configurations refer to the Appendix.

### Test Apparatus Description

The test facility apparatus consisted of an 18in (45.7cm) diameter by 48in (121.9cm) long plenum chamber with the nozzle configuration mounted at one end. High pressure air entered the chamber at the other end and was straightened using 4in (10.16cm) honeycomb flow straighteners. Two flexible hoses each approximately 17.7in (45cm) long were used between the plenum chamber and each nozzle to allow for variable spacing of twin nozzle configuration (Figure 8).

Tests were conducted using the test apparatus with and without the hoses. In Figure 9, a sound pressure level (SPL) vs. NPR plot shows a single hose-no hose comparison for the single axisymmetric case. The hose configuration resulted in increased screech amplitudes of more than 10 dB over the no hose configuration for a large portion of the NPR range. In past tests, it was shown that the addition of hoses increases the thickness of the boundary layer at the nozzle exit, which increases the thickness of the jet shear layer. The increased thickness of the shear layer results in higher screech sound



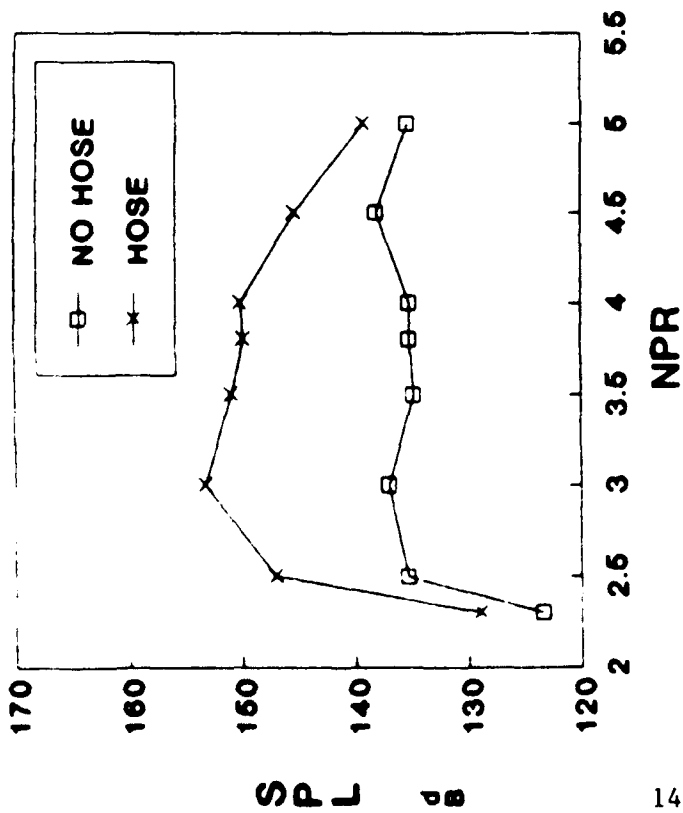


Figure 8. Hose-No Hose Effect

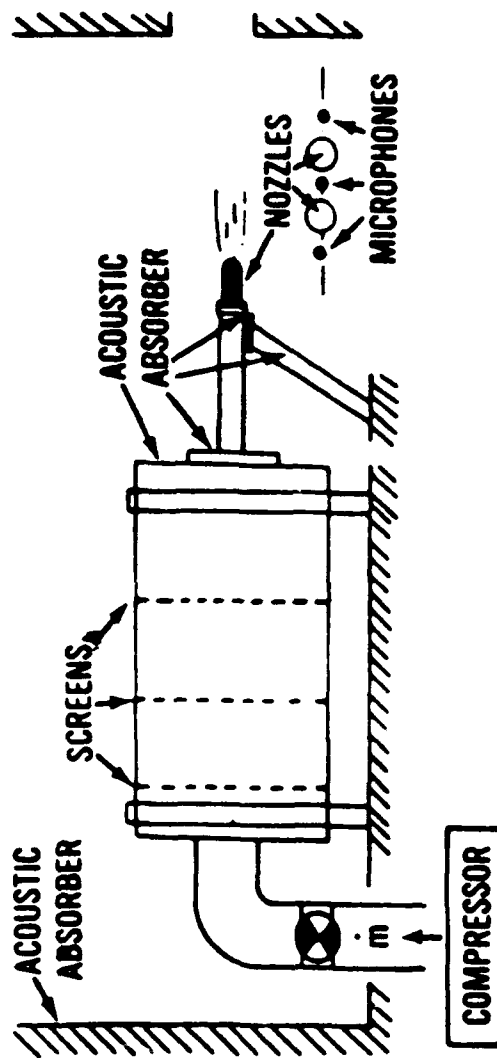


Figure 9. Test Setup

levels. Since the objective of this test was to observe the effect of screech suppression techniques and not to measure exact screech amplitudes, all acoustic data were taken using the flexible extension hoses.

An extensive quantification of the uncertainties present in the data was not conducted based on the above objective. The effect on SPL trends and frequency positions of the suppression techniques tested was more important than measuring exact SPL levels. Possible errors occurred in the measurement of acoustic signals using the microphones and in the determination of critical peaks at certain frequencies during the data reduction process. An uncertainty of 5 dB is assigned to each SPL value to represent instrumentation error. This uncertainty value translates into 3-5% error depending on the measured SPL amplitude. The data reduction error is much more difficult to quantify, since this is primarily human error. An uncertainty of 3 dB was assigned to SPL values, and an uncertainty of 100 Hz was assigned to frequency position values. These uncertainty values translate into 2-3% error on SPL values and 1-5% error on frequency position values depending on the selected SPL and frequency values.

### Test Instrumentation Description

The instrumentation for this experiment included three 1/4in (0.63cm) Gulton microphones which were located as seen in Figure 8. The center microphone remained fixed throughout the test while the outboard microphones moved with the nozzle exit translations. The signals from the microphones were routed to a real-time analyzer in order to monitor sound amplitudes during the test and were also recorded on analog tape for data reduction purposes. All the acoustic data presented here were measured in the region between the nozzles using the center microphone.

### Test Procedures

High pressure air was supplied to the plenum chamber using a manual valve. Two methods of data measurement were used: one a steady-state method, and the other, a dynamic method. The steady-state method allowed the pressure in the plenum chamber to stabilize before recording an acoustic data point. The dynamic method allowed the recording of a series of acoustic data points as the plenum chamber pressure was varied from a high NPR to a low NPR setting. This method saved time and money, since a

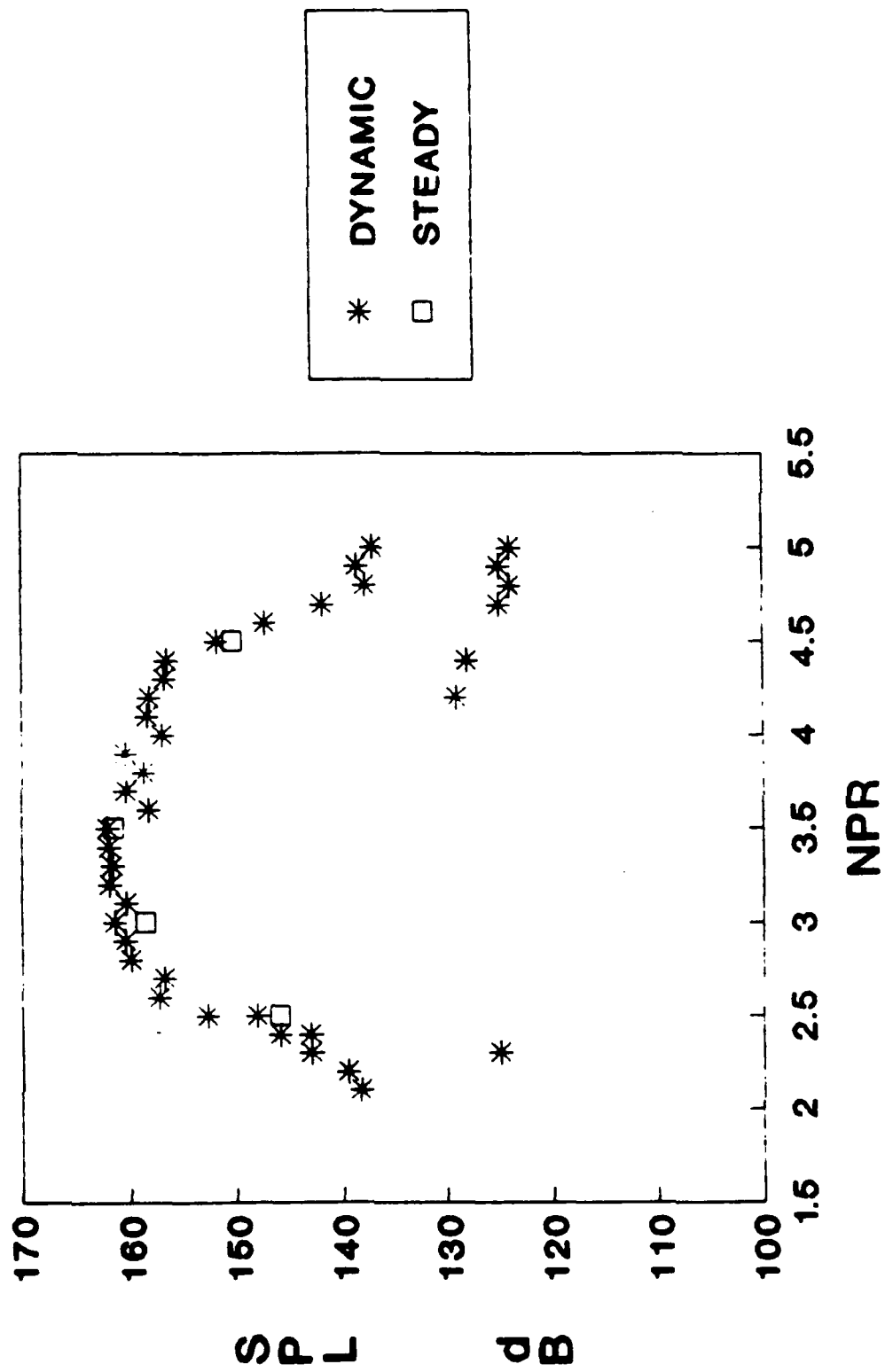


Figure 10. Comparison of Data Measurement Methods

maximum amount of acoustic data was measured quickly. In Figure 10, a comparison of the steady-state and dynamic measurement methods is shown for the dual axisymmetric baseline configuration. The dynamic measurement technique allowed for the measurement of more acoustic data in shorter run times. Also, the agreement for many of the configurations between data measurement techniques was fairly good. Despite this fact, when two or more data sets for different configurations were compared, the data sets were generated using one measurement technique or the other but not both.

## ACOUSTIC DATA REDUCTION

The acoustic signals measured by the center microphone were amplified and monitored on an oscilloscope. These dynamic data were recorded using hard copy plots showing the relation of sound pressure level in decibel units to a frequency spectrum of 0 to 10,000 Hz. Plots of sound pressure level (SPL) versus frequency (f) were recorded for an NPR range of 1.4 to 5.0 for each configuration.

### Acoustic Spectrum Data

A typical acoustic spectrum plot for the single axisymmetric baseline configuration at an NPR of 2.8 is shown in Figure 11. The measured voltage reading, NVOLT=0.257, at the top of the plot is converted to an NPR setting using the following pretest calibration equation:

$$\text{NPR} = \frac{\text{NVOLT} \times 100. + \text{PSIA}}{\text{PSIA}} \quad (1)$$

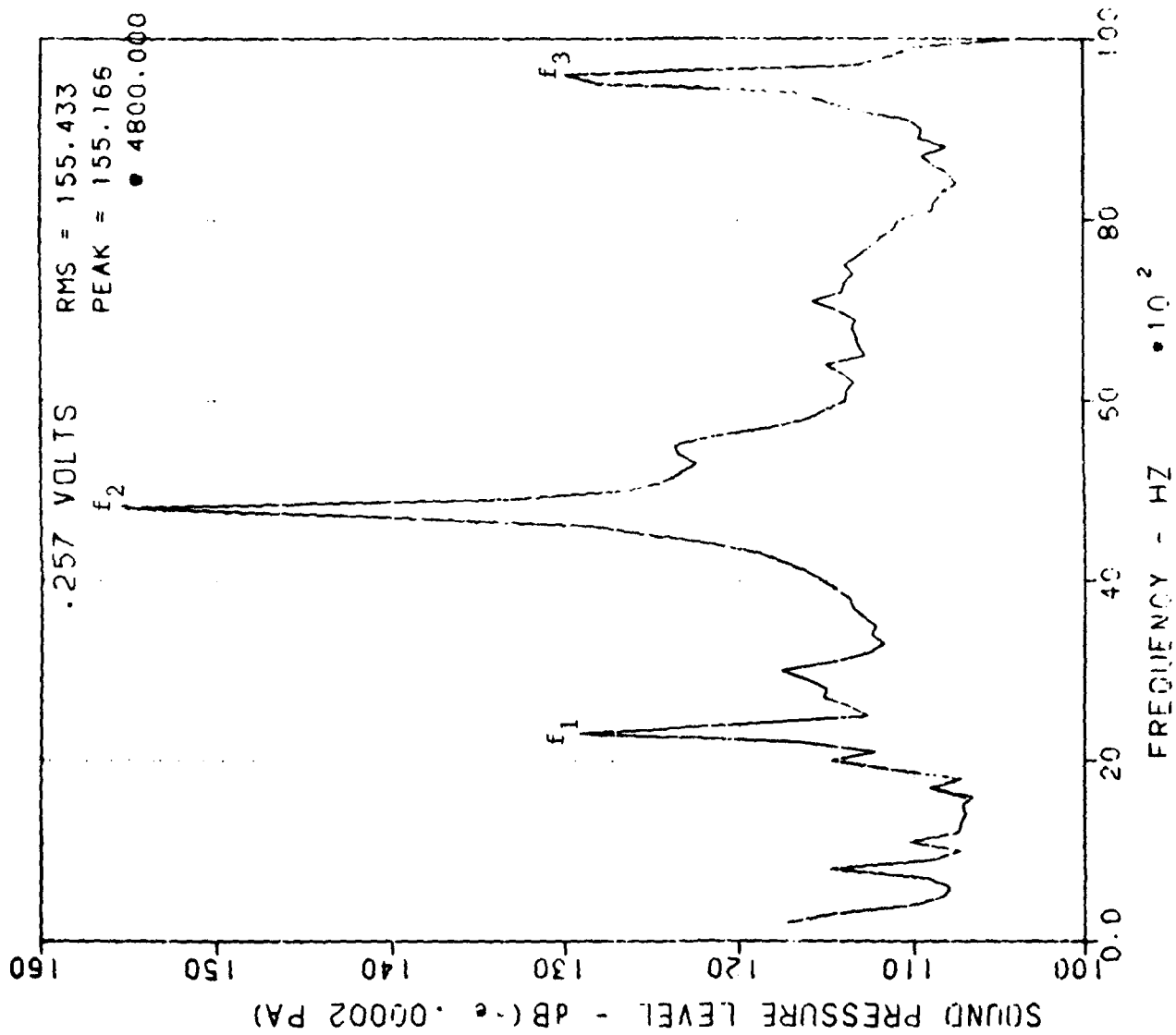


Figure 11. Typical Acoustic Spectrum, (NPR=2.8)

where PSIA is the measured ambient atmospheric pressure ( $\text{lb}_f/\text{in}^2$ ). In the upper right-hand corner of the data plots, the frequency and peak amplitude of the dominant, narrowband frequency peak over the given frequency spectrum is displayed. The root mean squared value (RMS) or Overall Sound Pressure Level (OASPL) which is an integrated value of sound amplitudes over the entire spectrum is also displayed. In Figure 11, three narrowband frequency peaks are observed. The amplitudes are approximately 129.0 dB, 155.166 dB, and 131.0 dB respectively. The frequencies are approximately 2400 Hz, 4800 Hz, and 9600 Hz respectively. The second narrowband peak,  $f_2$ , is defined to be the screech peak or the fundamental peak of the spectrum. This screech peak is the dominant peak over the frequency spectrum. The third peak,  $f_3$ , occurs exactly 4800 Hz later in the spectrum and is defined to be a harmonic of the screech peak,  $f_2$ . Harmonic peaks occur at frequency multiples of the fundamental peak over a given spectrum. The first narrowband frequency peak,  $f_1$ , occurs at 2400 Hz at every NPR setting for the entire configuration. Since  $f_1$  remains at a constant frequency over the entire operating range, it is believed to be a function of the



constant jet noise and unrelated to the screech feedback mechanism.

### Data Reduction Challenges

There are many challenges associated with the reduction of dynamic acoustic data from the acoustic spectra hard copy plots. The first and foremost problem is the size of the database. A total of 34 data plots were generated for each configuration studied over an NPR range of 1.4 to 5.0. This results in a total of 102 frequencies, dominant peaks, and OASPL values for just the single axisymmetric configuration.

A second problem which complicates the first is that most of the acoustic spectra possess more than one critical peak. The acoustic spectrum for the single axisymmetric configuration at an NPR setting of 3.1 is shown in Figure 12. This data plot shows 14 narrowband peaks which is an extreme case. However, if on the average each data plot showed four peaks, then a total of 408 frequencies, screech peaks, and OASPL values would have to be recorded for this configuration.

When multiple peaks are considered in the process, the question arises as to how to determine which peak values are critical peak values. Limitations are usually placed on the

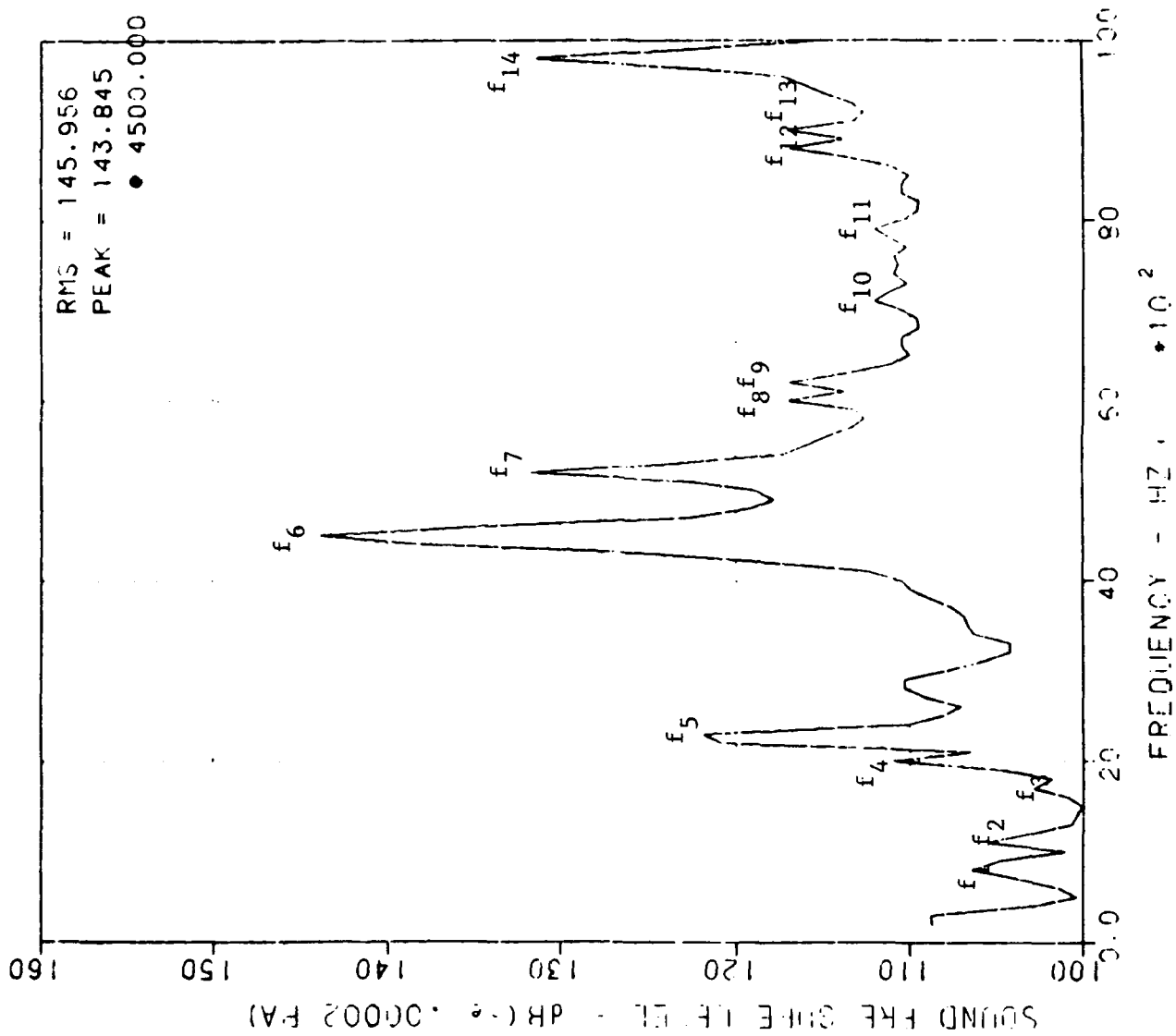


Figure 12. Single Axisymmetric Baseline, (NPR=3.1)

acoustic data such as a specified frequency range or a minimum peak amplitude. For this test, narrowband peaks over 120 dB were recorded. This minimum SPL requirement has been used by other researchers who use automated search algorithms to process their spectra plots.<sup>9</sup> A threshold of 120 dB is used because it generally represents the upper limit of broadband shock-associated noise and the lower limit of narrowband shock-associated noise.

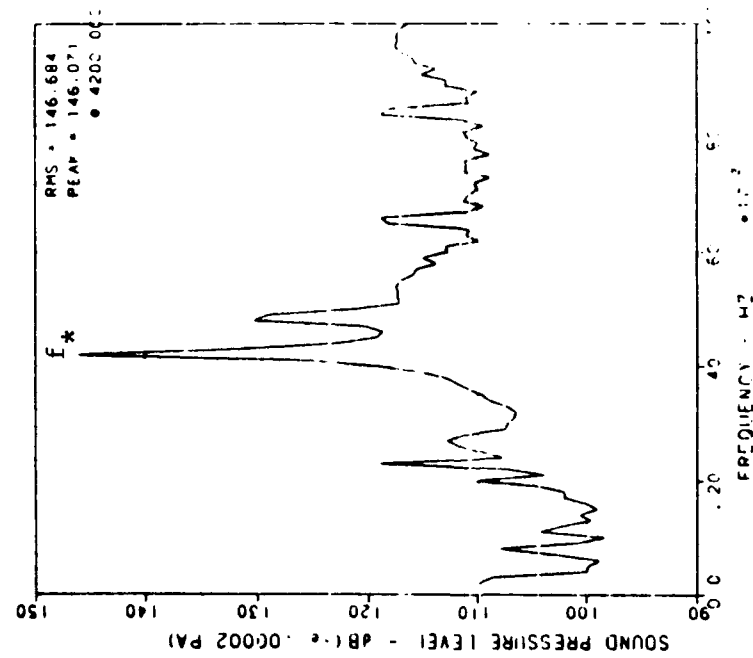
An equally complicated problem is how to display screech data in a parametric form that can accurately quantify and qualify the screech phenomenon. The measured quantities such as frequency, sound amplitude, and OASPL must be converted into meaningful parameters that describe modal transformations, sound variations versus configuration changes, and nozzle orientations.

#### Data Reduction Process

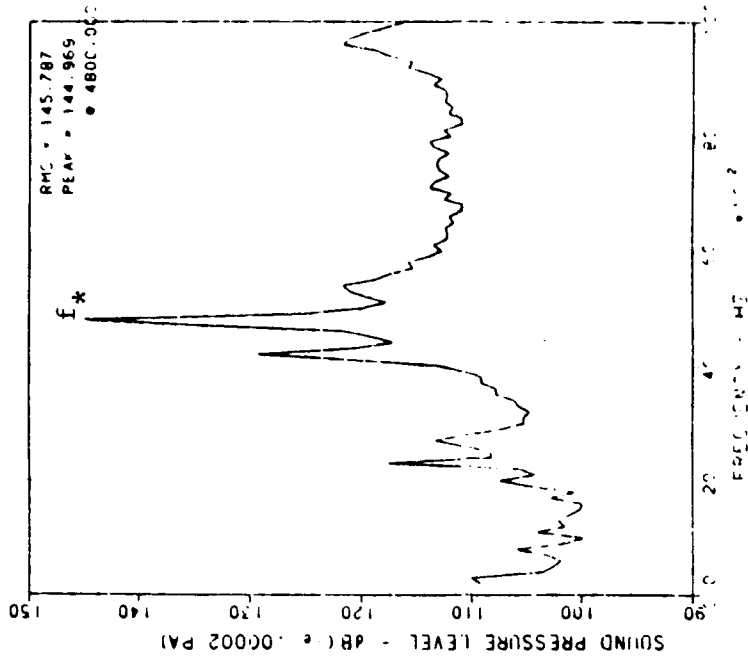
A personal computer in conjunction with a spreadsheet software program was used to record the large screech database which contained NPR, frequency, SPL, and OASPL values. The spreadsheet program was used to incorporate column formulas, so that data could easily be converted to desired parameters and compared using a separate plotting package.

Hard copy spectra plots being the only available data format, the reduction of the acoustic spectra data is a slow and tedious process not amenable to automation. The data reduction process originated with the organization of hardcopy plots in NPR sequence for each configuration. The narrowband frequency peaks must not only be registered, but the frequency and peak amplitude trends from NPR to NPR must be observed. An example of this type of analysis is shown in Figures 13 (a,b). Using the single axisymmetric nozzle configuration, the narrowband dominant peak occurred at a frequency of 4200 Hz at the NPR condition of 3.5. At the next NPR setting of 3.6, the dominant peak energy transferred to a frequency of 4800 (Hz). The peak frequency positions should be monitored closely in the reduction process, since these positions are related to the various screech modes and structural resonant frequencies. Therefore, for every NPR data point, the frequency and SPL values for each critical peak as well as the OASPL of the entire spectrum were entered into a spreadsheet program.

Once the significant data for a configuration had been recorded, the next step in the process was to display the screech data qualitatively. Several researchers have determined a parameter that shows the particular modes of the screech phenomenon such as the toroidal or helical modes and their linear



(a) NPR=3.5



(b) NPR=3.6

Figure 13 (a,b). Peak Trend Methodology

dependence on jet Mach number. This parameter is known as the modal frequency parameter and is defined in the following equation:

$$\frac{\lambda}{d} = \frac{c}{f d} \quad (2)$$

where  $d$  is the nozzle exit diameter,  $f$  is the frequency, and  $c$  is the speed of sound. The above formula was entered into the spreadsheet package and a column of frequencies was transformed into the above parameter. Also, the measured NPR values were transformed into ideal jet Mach numbers ( $M_j$ ) using the following isentropic flow equation:

$$\text{NPR} = [1 + (\gamma - 1)/2 \times M_j^2]^{\gamma/(\gamma - 1)} \quad (3)$$

where  $\gamma$  is the specific heat ratio of 1.4 for air, and  $M_j$  is the Mach number of the jet. The data were converted into these meaningful parameters and plotted for a first pass through the data plots (Figure 14). Some linear trends were visible, yet much of the plot seemed to be a collection of scattered data. A

second pass through the data plots was completed to examine the peaks at these data points more closely. In the second pass, many of the peaks that were recorded during the first pass were identified to be harmonics of the fundamental peaks. These peak amplitude measurements were deleted from the database, since the harmonic peaks were not a representation of the critical screech modes. Two examples of data points that include harmonics are shown in Figures 15 (a,b).

In Figure 14, the collection of data points at the top of the plot seemed to be independent of the jet Mach number. There was no appreciable increase or decrease in the frequency position of this peak with Mach number variation. This peak corresponded to the  $f_1$  peak of Figure 11 remaining at a frequency of 2400 Hz over the entire operating range for this configuration, hence it was neglected from further consideration. After the harmonics and the jet independent peaks were neglected, the  $\lambda/d$  versus Mach number plot for this configuration was complete and is shown in Figure 16. This final modal frequency plot showed good agreement with a modal frequency plot for a similar single axisymmetric nozzle over similar operating conditions.<sup>11</sup> The presentation of  $\lambda/d$  versus jet Mach number clearly showed the occurrence of various screech modes over various segments of the operating range. As mentioned in the literature, the toroidal

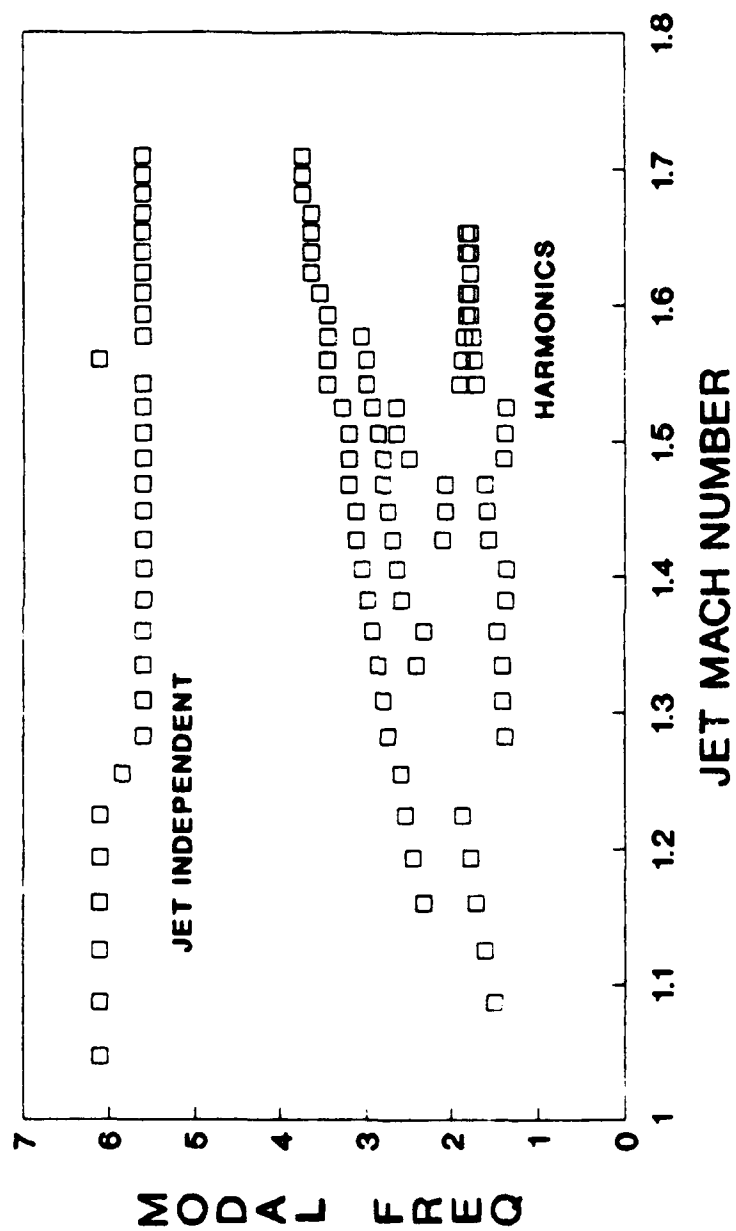
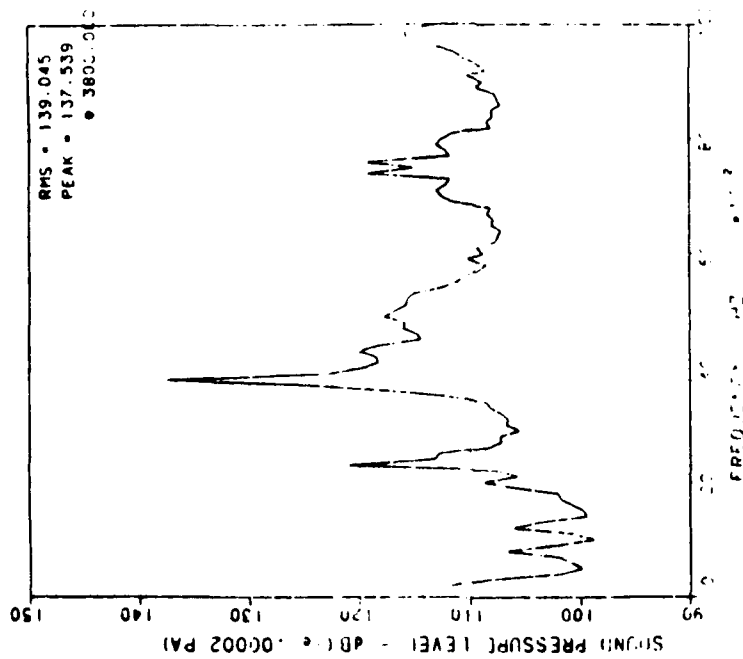
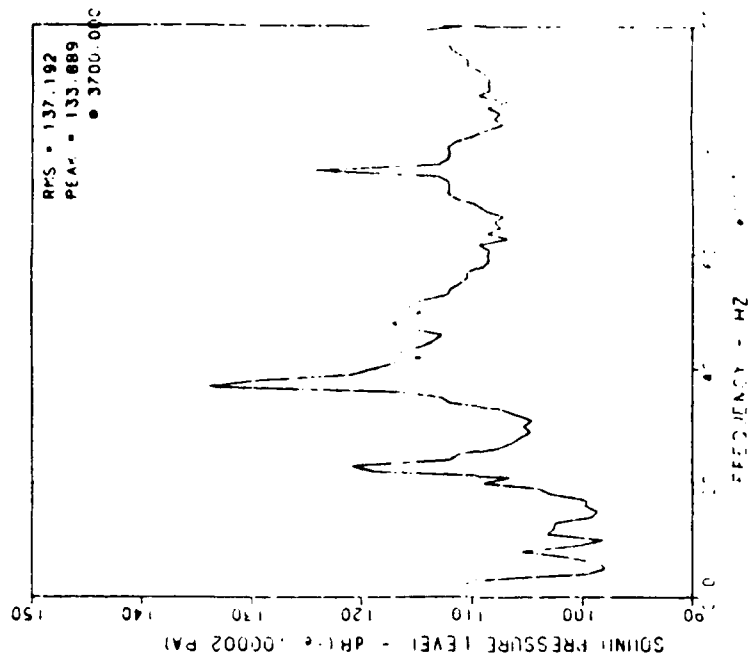


Figure 14. Single Axisymmetric Baseline, First Pass  
(Modal Frequency Plot)





(a)



(b)

Figure 15 (a,b). Examples of Harmonics

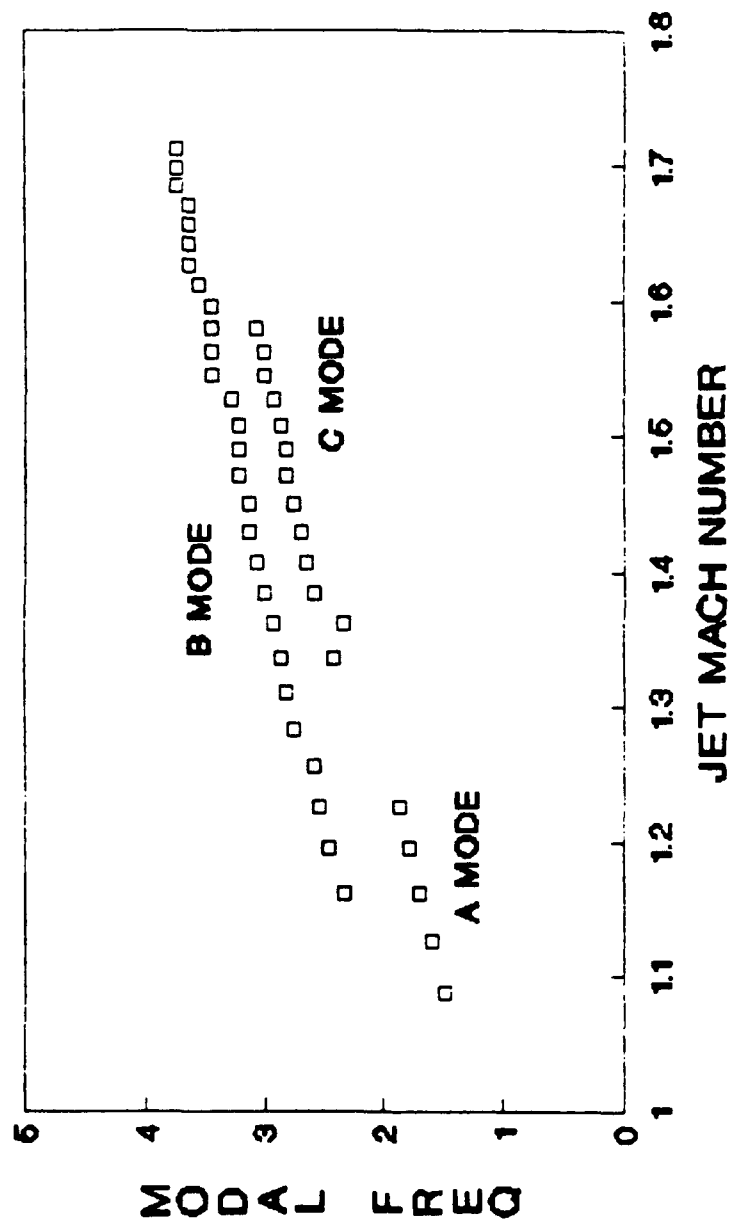


Figure 16. Single Axisymmetric Baseline  
(Modal Frequency Plot)

mode or A mode is a high frequency, low wavelength phenomenon that occurs at low jet Mach numbers. The helical mode can occur in two variations: B and C modes. These modes generally occur at high jet Mach numbers and are low frequency, high wavelength phenomena. The linear dependence on jet Mach number was clearly evident for the A, B, and C modes. As the jet Mach number was increased, the wavelength of the acoustic instabilities increased causing the degradation of the A mode and the realization of the B and C modes.

The second major result gained from this analysis was a plot of SPL versus jet Mach number (Figure 17). At first glance, this plot presented purely quantitative results as no appreciable trends in the data were visible. However, using the  $\lambda/d$  versus Mach number plot in conjunction with the spreadsheet database of recorded frequencies and peak amplitudes produced a qualitative representation of the data as well.

A third pass is made through the data plots to understand the screech mode variation and at what NPR settings these changes occur. For example, the spreadsheet database for the single axisymmetric nozzle configuration was searched from low NPR to high NPR. The first modal transfer from toroidal to helical modes is shown in Figure 18 over a jet Mach number range of 1.16 to 1.19. At  $M_j = 1.16$ , the  $f_3$  peak was the dominant screech peak

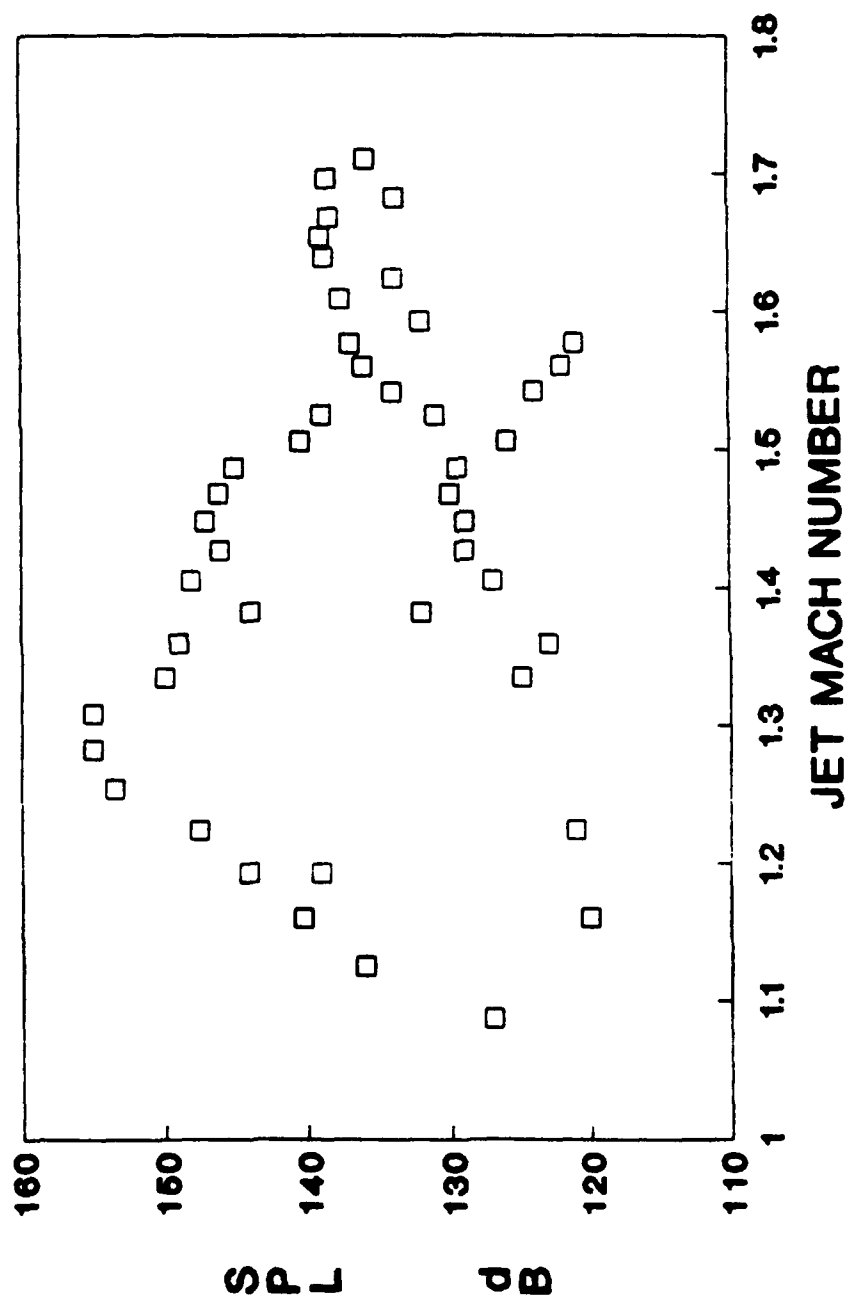


Figure 17. Single Axisymmetric Baseline  
(SPL vs. Mach # Plot)

with an SPL of 140.236 dB. This peak was a high frequency, low jet Mach number phenomenon and thus was labelled toroidal or A mode based on the  $\lambda/d$  versus Mach number plot of Figure 16. At the next jet Mach number of 1.19, the  $f_2$  peak had the highest amplitude at a middle frequency position suggesting the dominant screech mode to be the helical mode at this condition. Considering the frequency position and amplitude information obtained from the above analysis, the data points on the SPL versus jet Mach number plot could be identified (Figure 17). At  $M_j = 1.16$ , the data point at the higher peak amplitude must represent the toroidal mode, whereas the data point at the lower amplitude must represent the helical mode. At  $M_j = 1.19$ , the data point at the higher peak amplitude must represent the helical mode, whereas the data point at the lower amplitude must represent the toroidal mode. Two more modal transfer points were found in the database for this configuration and are shown in Figures 19 and 20. After these modal transfer points were analyzed for amplitude and frequency, a qualitative SPL versus  $M_j$  plot was constructed over the entire operating condition to show the variation in screech mode and amplitude simultaneously (Figure 21).

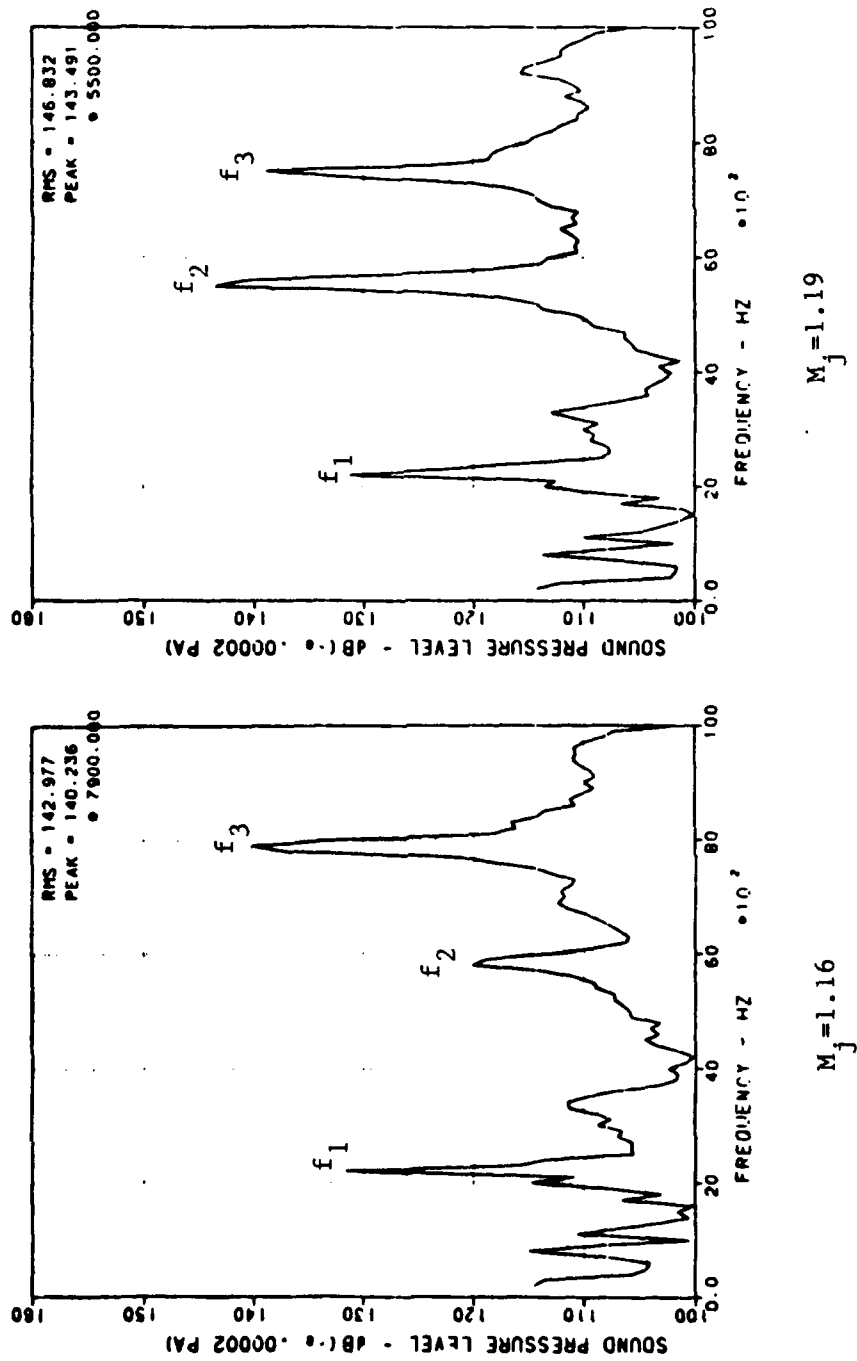


Figure 18. First Modal Transfer

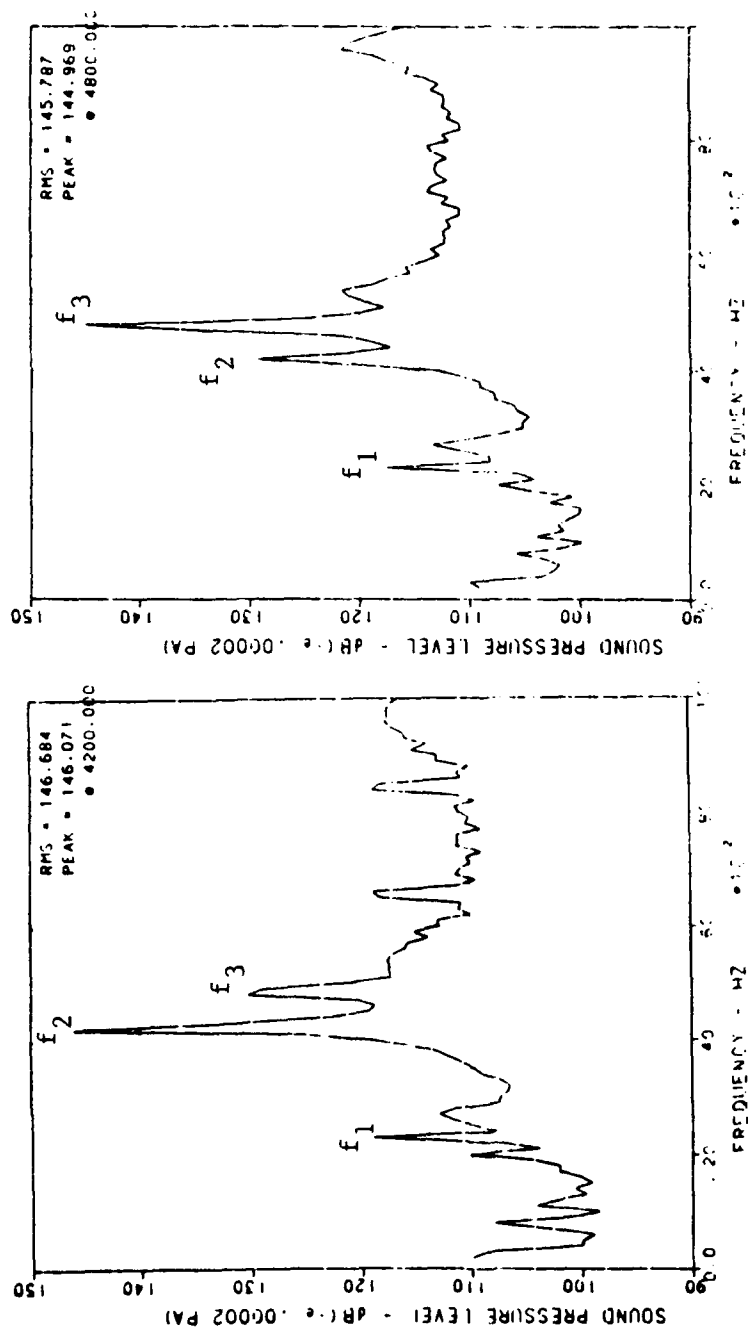


Figure 19. Second Modal Transfer

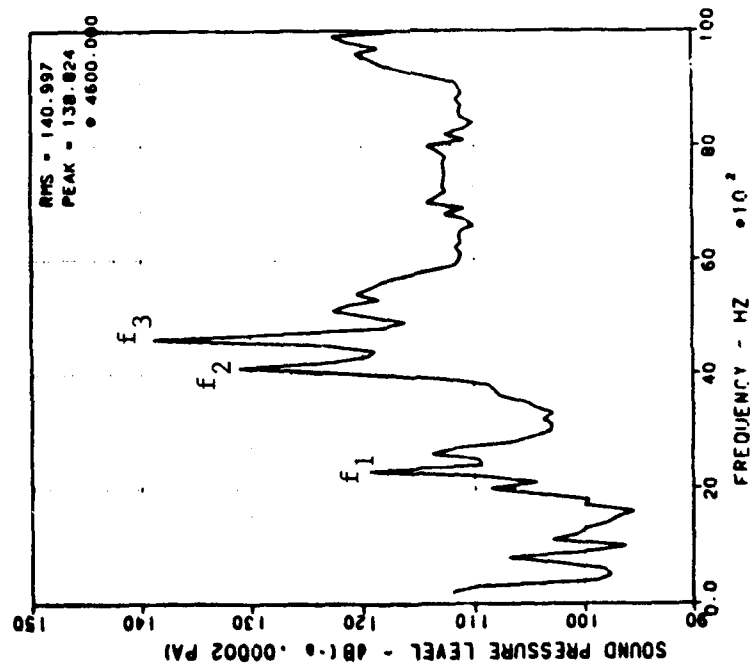
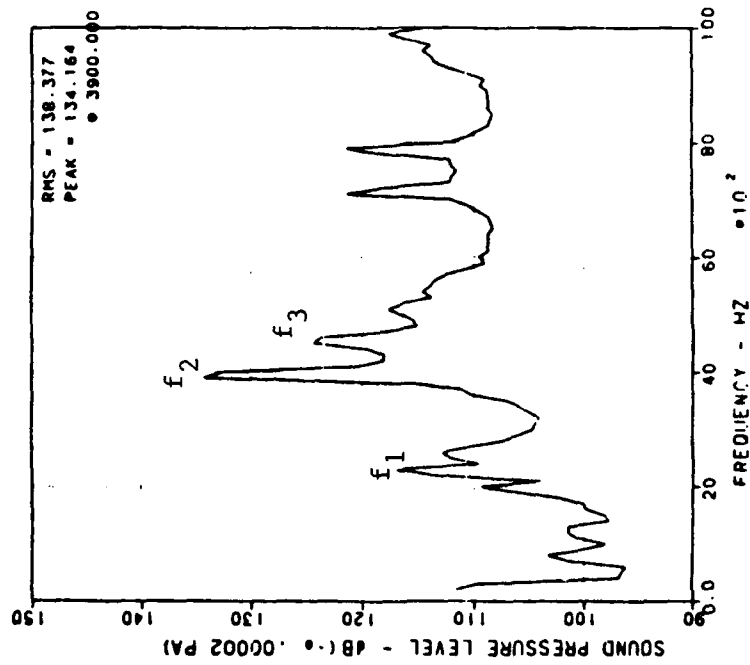


Figure 20. Third Modal Transfer



The reduction and presentation of dynamic jet screech data requires the ability to determine the critical frequency and peak amplitudes from a wealth of data. The dynamic data plots must be reviewed several times to understand the frequency, peak amplitude, and modal trends. Parameters must be investigated to present the recorded data in a meaningful way, so that variations in screech modes, frequency positions and peak amplitudes are seen with changing jet conditions and nozzle configurations.

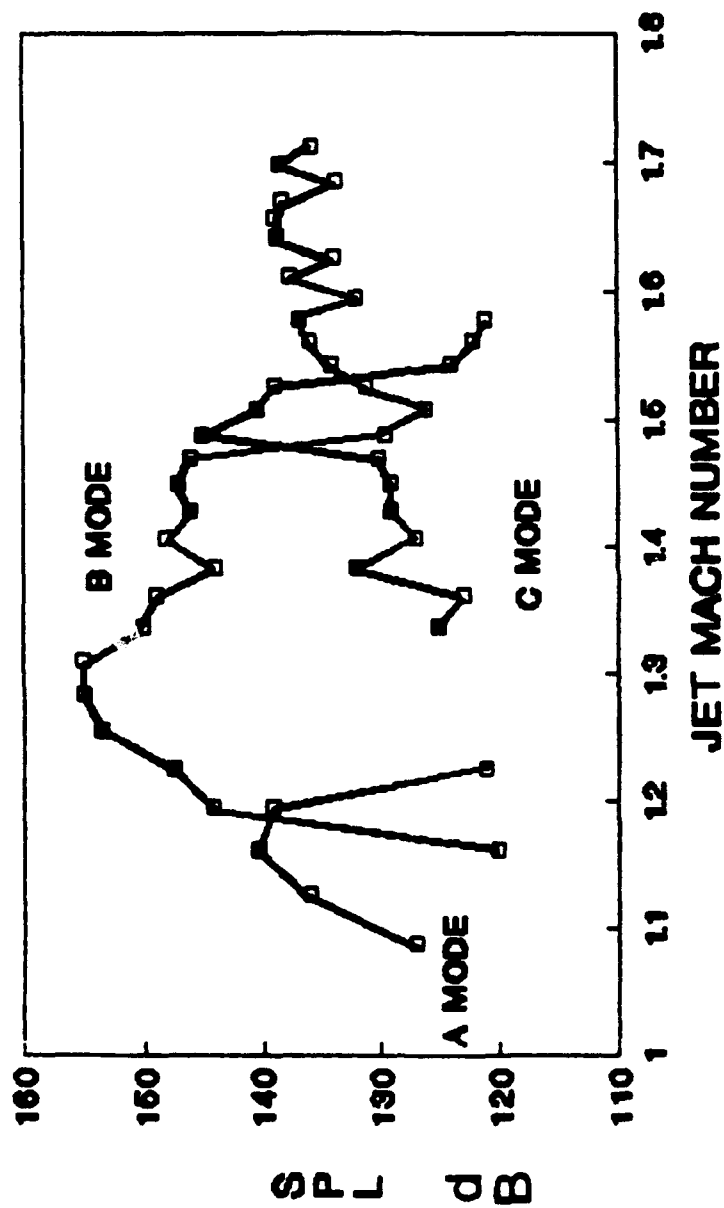


Figure 21. Single Axisymmetric Baseline, Modes Identified (SPL vs. Mach # Plot)

## AXISYMMETRIC NOZZLE RESULTS

The 4.7% scale axisymmetric nozzles were used to investigate various methods of screech suppression. These methods included lateral spacing of the twin jets, a secondary air jet in one nozzle, tabs positioned at a nozzle exit, and longitudinal shifting of one nozzle. The single and twin baseline nozzle configurations were tested followed by various screech suppression configurations.

### Single Axisymmetric Baseline Configuration

The single axisymmetric baseline configuration results will be repeated here for presentation completeness. The modal frequency plot for this configuration is shown in Figure 22. The toroidal A mode occurred at the lower jet Mach numbers and higher sound frequencies, while the helical B and C modes occurred at the higher jet Mach numbers and lower sound frequencies. These wave instabilities were linearly dependent with jet Mach number, and the modal frequency transition points were evident at three locations as discussed in the previous section.

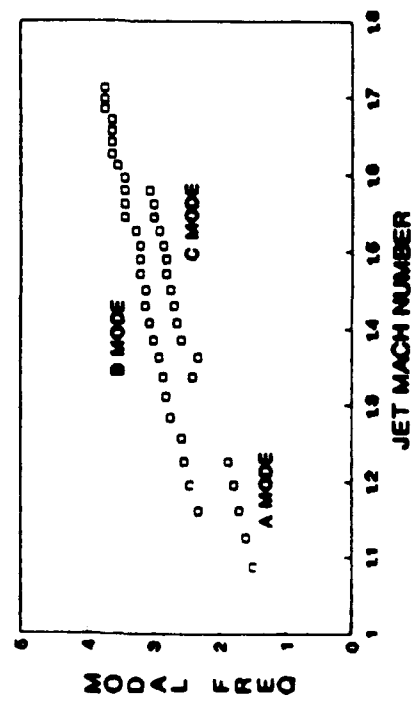


Figure 22. Single Axisymmetric Baseline  
(Modal Frequency Plot)

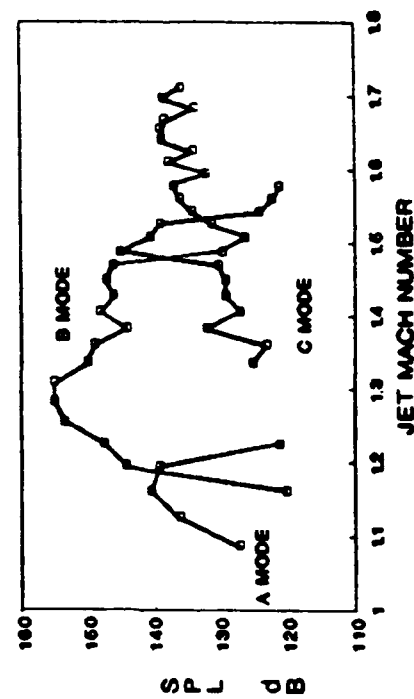


Figure 23. Single Axisymmetric Baseline  
(SPL vs. Mach # Plot)

The screech amplitude levels are shown in Figure 23. The helical B mode resulted in the highest levels of screech for most of the jet Mach number region. A maximum SPL of approximately 156 dB was measured. The C mode became dominant in the vicinity of  $M_j = 1.5$  producing a maximum SPL of approximately 146 dB; however, the C mode produced relatively low levels of sound over most of the Mach number region.

These single axisymmetric baseline results were necessary to compare the effective screech levels of a single configuration to a twin nozzle configuration. These comparisons were accomplished and are presented in the next section.

#### Twin Axisymmetric Baseline Configuration

The data reduction procedure used for the single nozzle baseline configuration was used for the twin nozzle baseline configuration which had a spacing ratio,  $s/d$ , of 2.25. The axisymmetric nozzle spacing ratio is the center-to-center distance between the nozzles divided by the nozzle exit diameter. Using the modal frequency parameter,  $\lambda/d$ , to visualize the jet Mach number dependency of the various modes resulted in Figure 24. For this configuration, a second toroidal mode was observed and was labelled A2 based on previous conventions in the

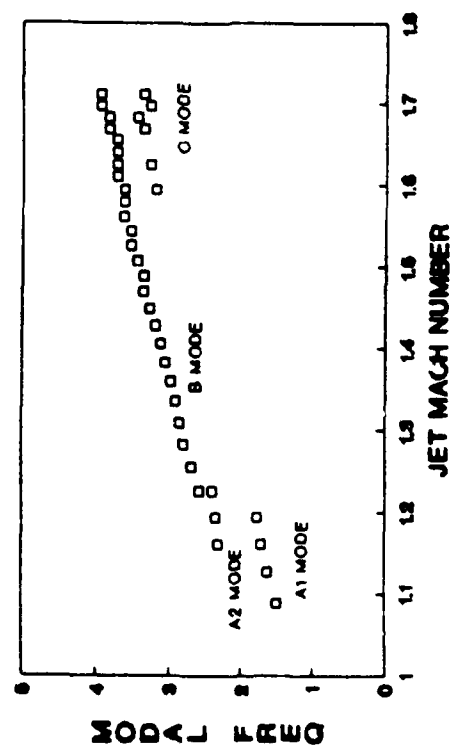


Figure 24. Dual Axisymmetric Baseline,  $s/d=2.25$   
(Modal Frequency Plot)

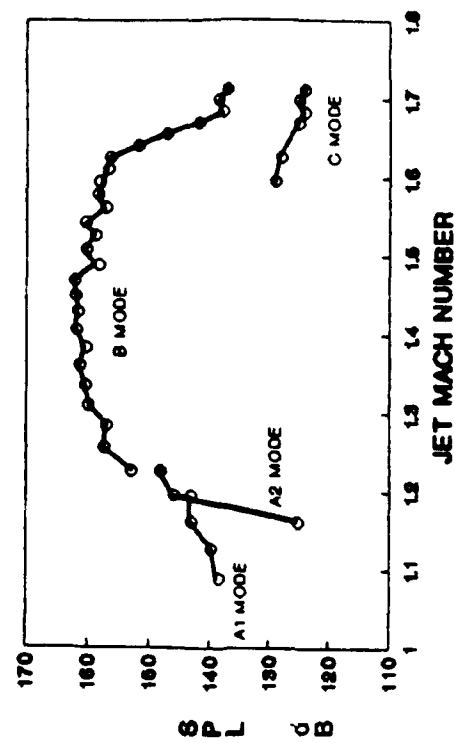
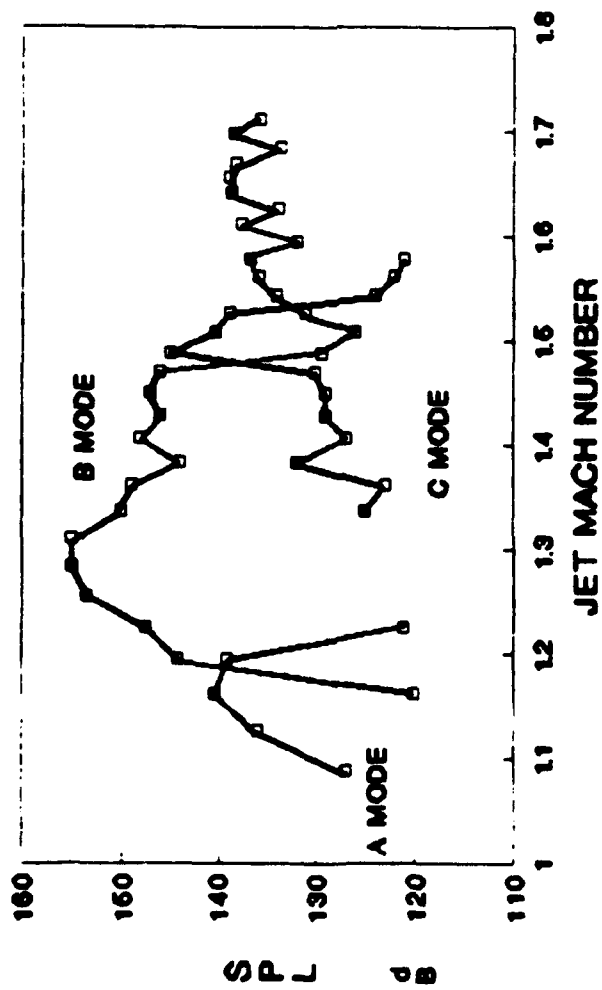


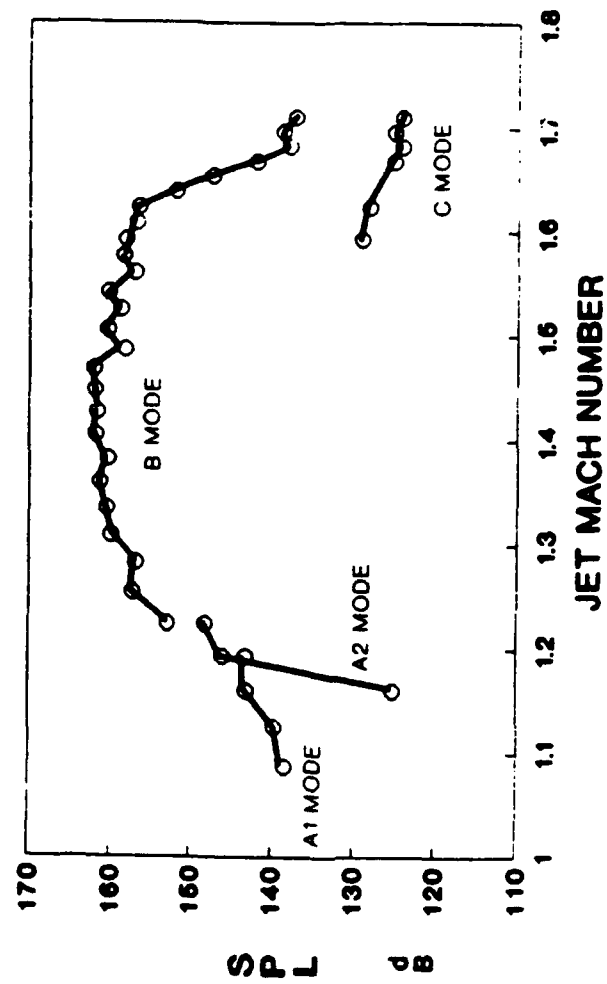
Figure 25. Dual Axisymmetric Baseline,  $s/d=2.25$   
(SPL vs. Mach # Plot)

literature. This qualitative representation of the screech modes for the twin configuration showed the instabilities in the jet plumes to be essentially the same as the structures in the single configuration plume. The toroidal modes occurred at the lower jet Mach numbers and at the higher sound frequencies (lower wavelengths). The helical modes occurred at the higher jet Mach numbers and at the lower sound frequencies (higher wavelengths).

Since the helical modes occurred at higher jet Mach numbers where the shock cell structure was the strongest, these modes should produce the higher screech levels based on Powell's screech feedback mechanism. A quantitative SPL vs.  $M$  plot for this configuration is shown in Figure 25. The B helical mode dominated the entire jet Mach number regime and produced substantially higher SPL levels than did the B mode for the single nozzle configuration as seen in Figures 26 (a,b). The twin configuration SPL levels remained high over a much wider Mach number region than did the SPL levels of the single jet configuration. Many of the SPL amplitudes exceeded 160 dB over several different Mach number data points. An example of the single configuration versus the twin configuration acoustic spectrum is shown in Figure 27 for the NPR=3.0 condition. A difference of over 10 dB existed in the sound pressure level of the narrowband tone for this NPR. The increase in SPL for the



(a)



(b)

Figure 26 (a,b). Single versus Dual SPL Plots



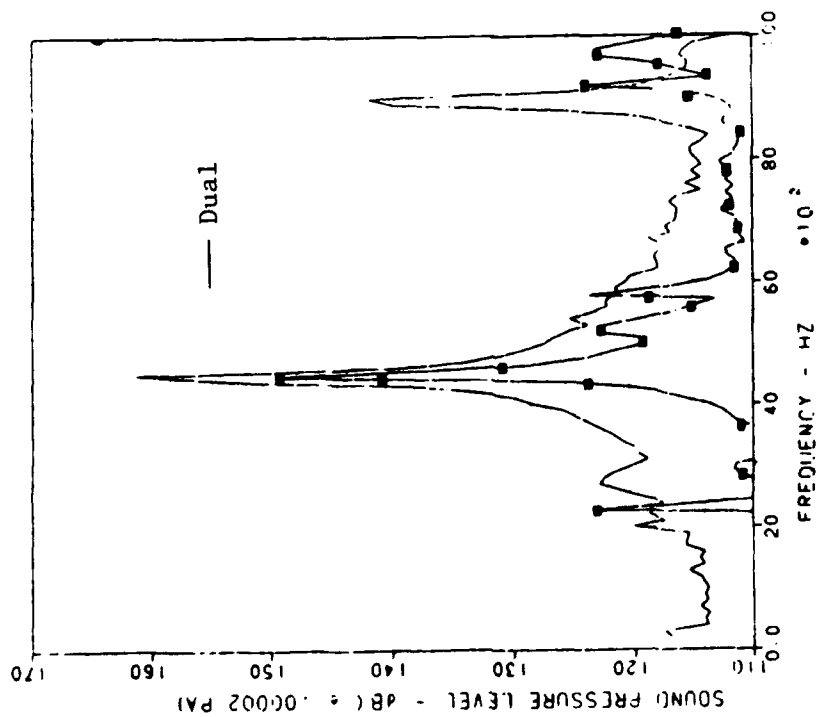


Figure 27. Single versus Dual Axisymmetric Configurations,  
(NPR=3.0)

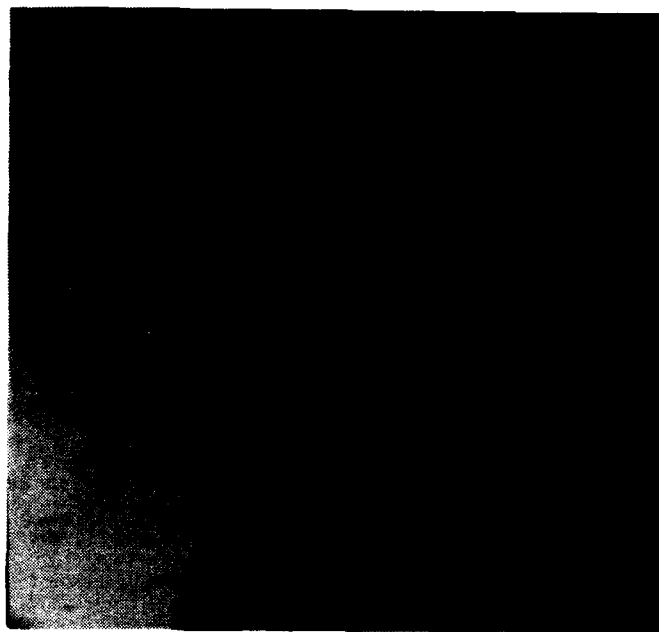


Figure 28. Schlieren Photo of Mode Coupling, (NPR=3.0)

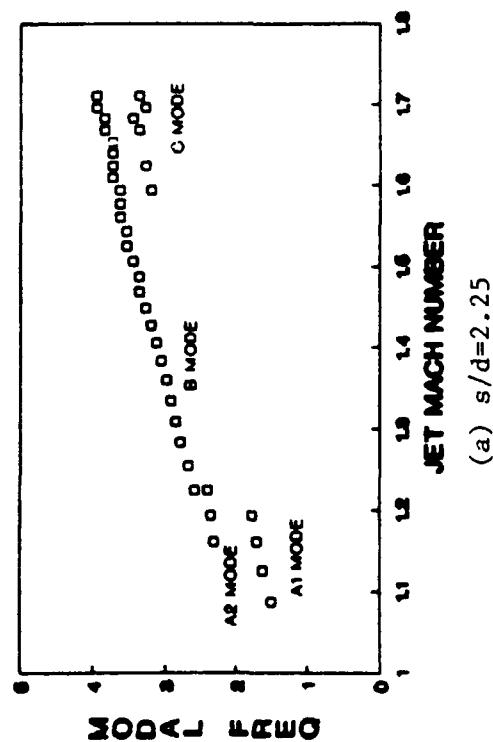
twin jet case was due to the coupling of the wave instabilities in the twin jet plumes. Because the coupling of the jet instabilities increases the jet screech tone considerably, structural response and fatigue are a possibility. This coupling mechanism is visualized in Figure 28 for the twin baseline configuration at the NPR=3.0 condition.

#### Lateral Spacing Suppression

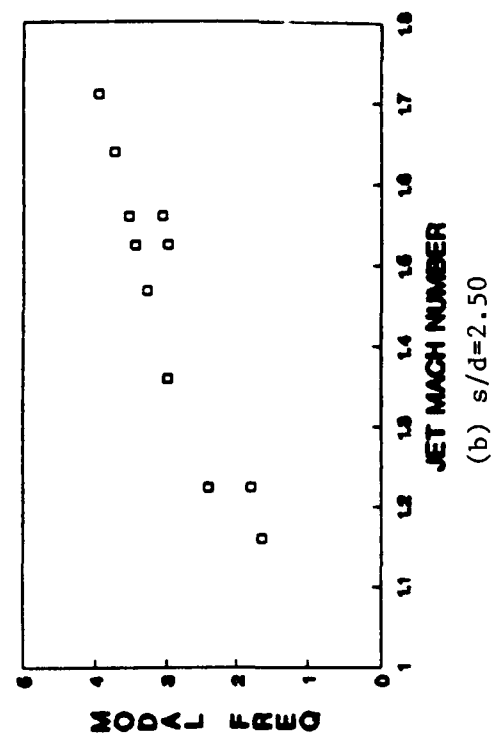
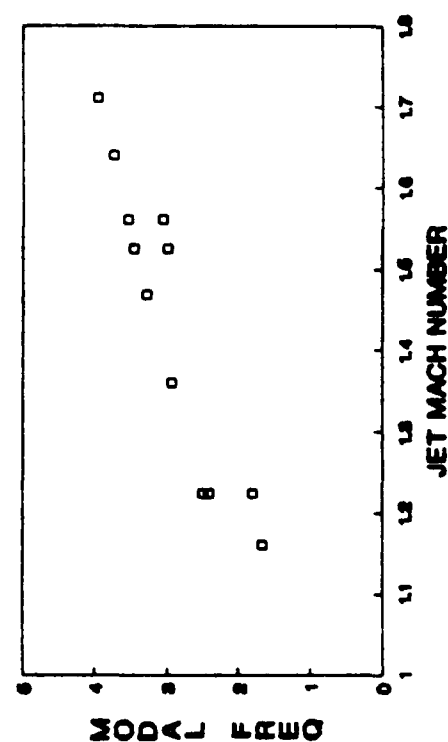
The coupling of wave instabilities of closely spaced jets results in higher pressure amplitudes which continually subject the nozzle flaps to higher sonic loadings. If the coupling phenomenon could be prevented using screech suppression techniques, the nozzle hardware would be less stressed and presumably more reliable. Variable lateral spacing of the two nozzles in a twin nozzle configuration was accomplished in the attempt to suppress the coupling mechanism of closely spaced nozzles. Lateral spacing was investigated by Wlezien and was found to have a profound effect on the SPL levels of a twin configuration.<sup>11</sup> Wlezien found that a composite plot of modal wavelength as a function of Mach number could be constructed for eight different spacings. The modal frequency trends and Mach ranges were identical for each of the eight different spacings.

For this test, the  $s/d$  was varied from 2.25 to 7.0 to investigate the effect of lateral spacing on a twin jet configuration. The modal frequency plots for the various spacings are shown in Figures 29 (a-1). For this test, the modal frequency plots confirm the baseline frequency and Mach number ranges for each of the various modes. In general, these plots were similar to Wlezien's results in that the A, B, and C modes were measured at similar frequencies and over similar jet Mach number ranges for every spacing ratio.

Although the modal frequencies and jet Mach number ranges were similar for the twin configuration at various spacing ratios, the SPL levels for the various spacing ratio configurations were extremely distinct. The SPL versus M plots for the lateral spacings of 2.25 to 7.0 are shown in Figures 30 (a-1). For the lower spacing ratios of 2.25 to 2.75, the B mode was dominant and possessed high SPL levels over a wider Mach range. The C mode was suppressed and had much lower SPL levels relative to the isolated single jet of Figure 23. For the next spacing ratio range of 3.0 to 3.5, the B mode was lower for the lower jet Mach numbers, then increased sharply at the higher Mach numbers. The A toroidal mode amplitudes remained relatively low over this range. For the acoustic runs that included the measurement of many data points, the A2 mode can be observed. In



(c)  $s/d=2.75$



(d)  $s/d=3.00$

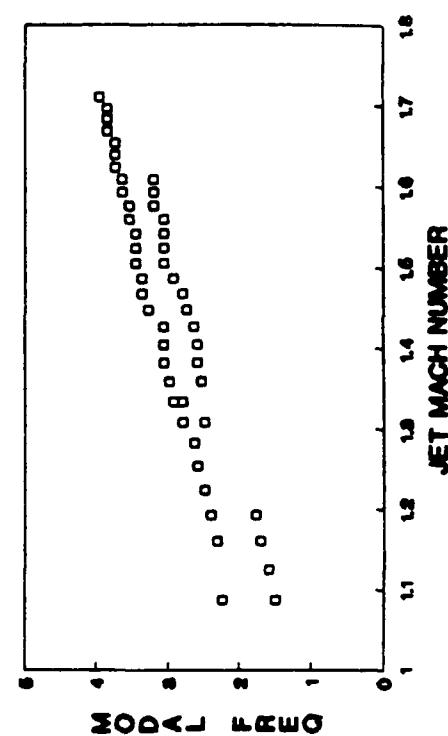
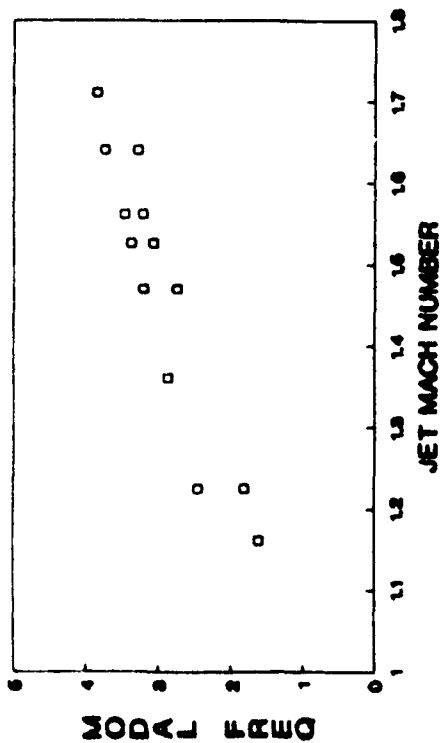
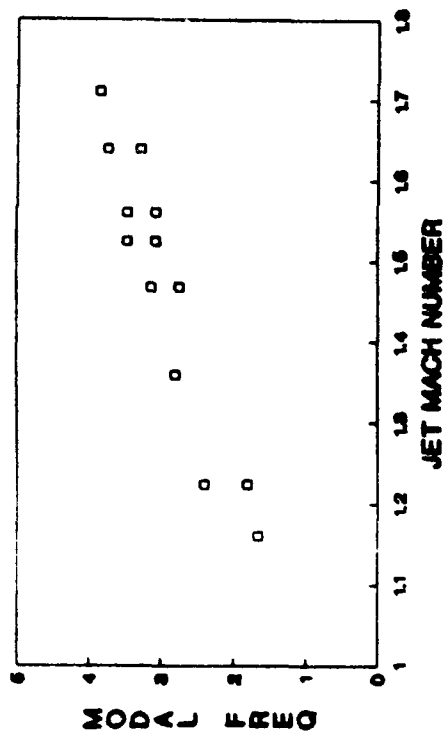


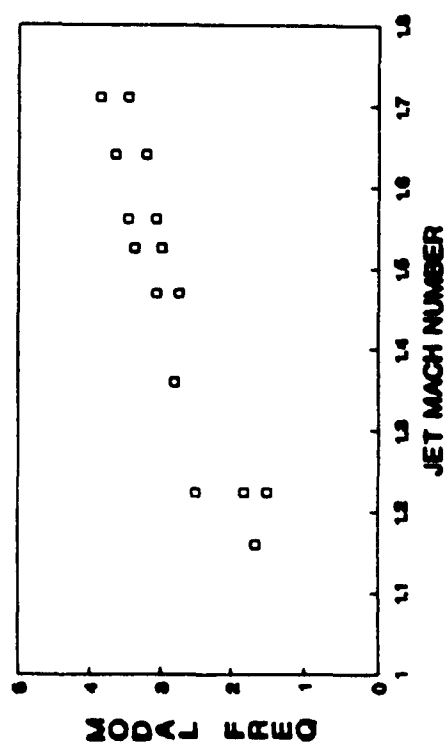
Figure 29 (a-l). Modal Frequency Plots for Various Spacing Ratios, ( $2.25 < s/d < 7.00$ )



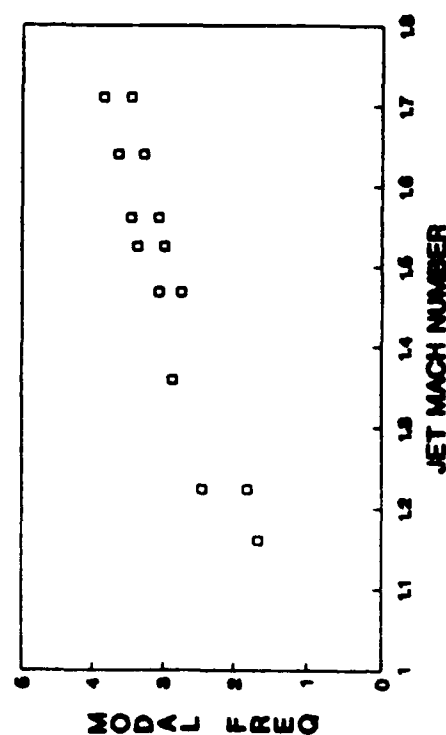
(e)  $s/d=3.25$



(f)  $s/d=3.50$

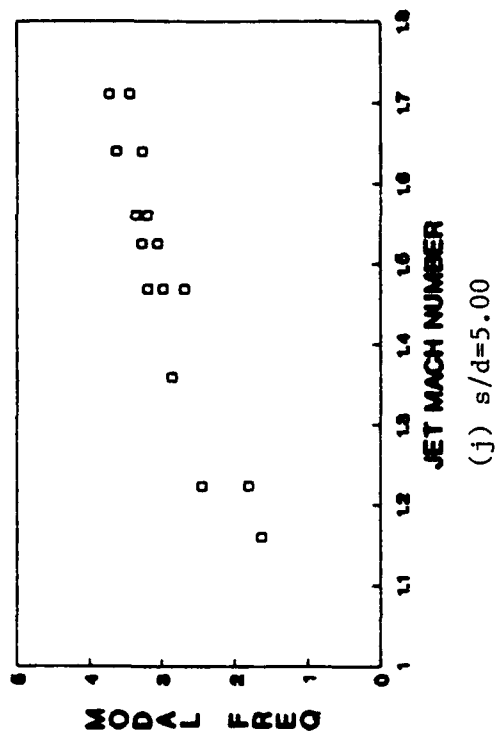


(g)  $s/d=3.75$

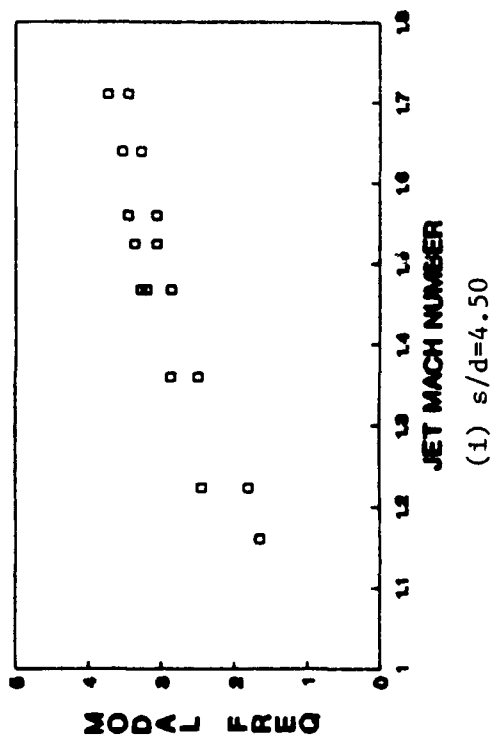
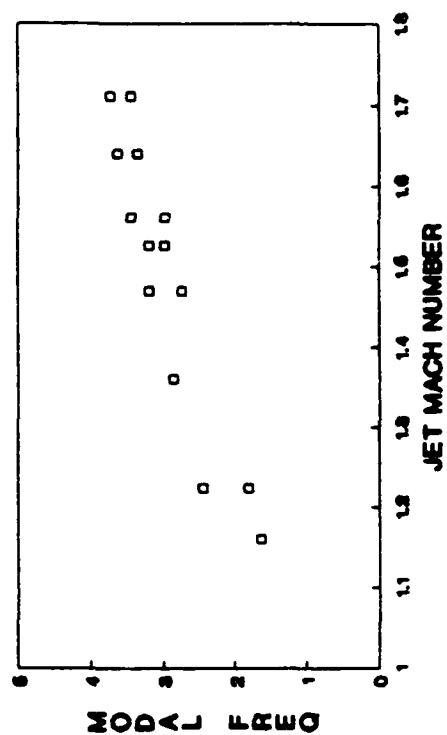


(h)  $s/d=4.00$

Figure 29 (Cont'd)



(1)  $s/d=7.00$



(1)  $s/d=6.00$

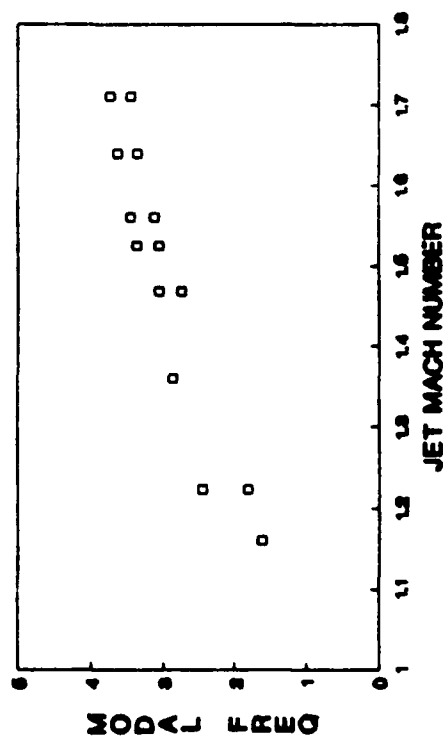


Figure 29 (Cont'd)

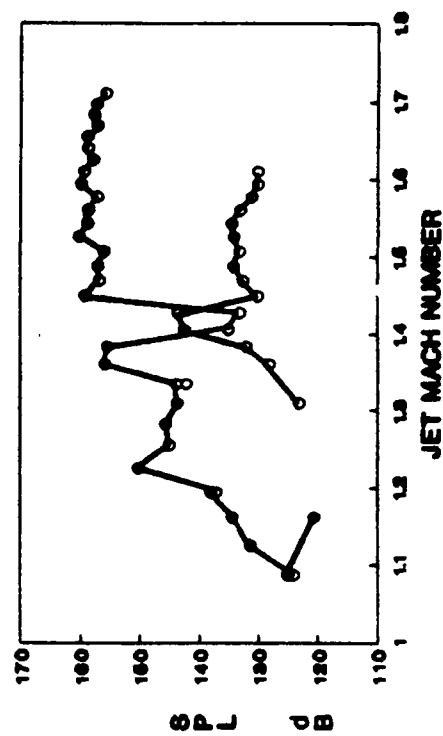
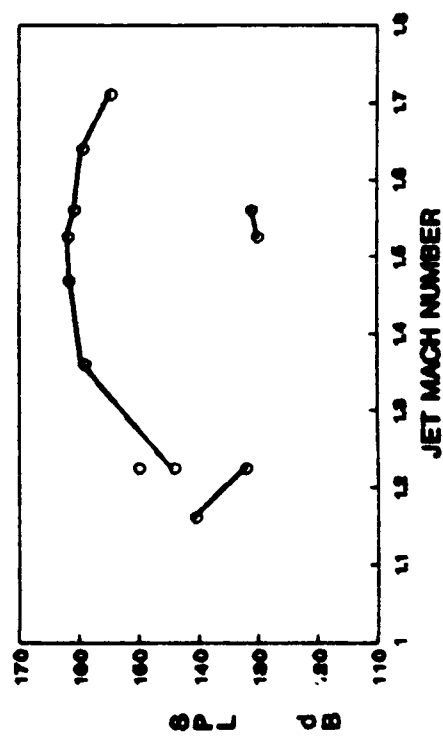
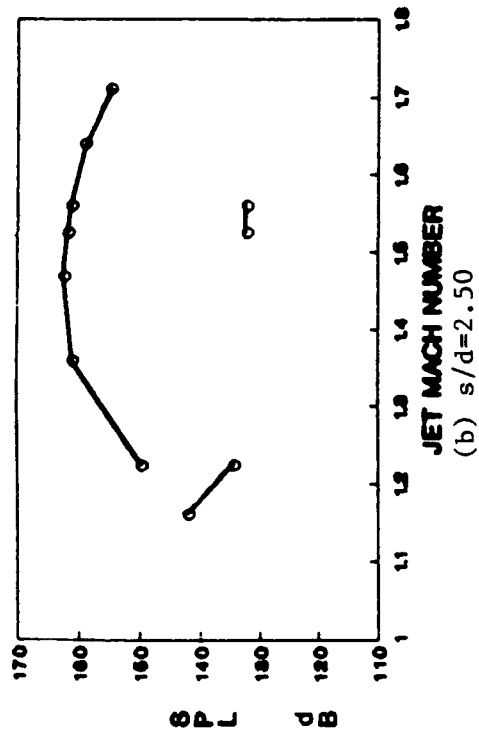
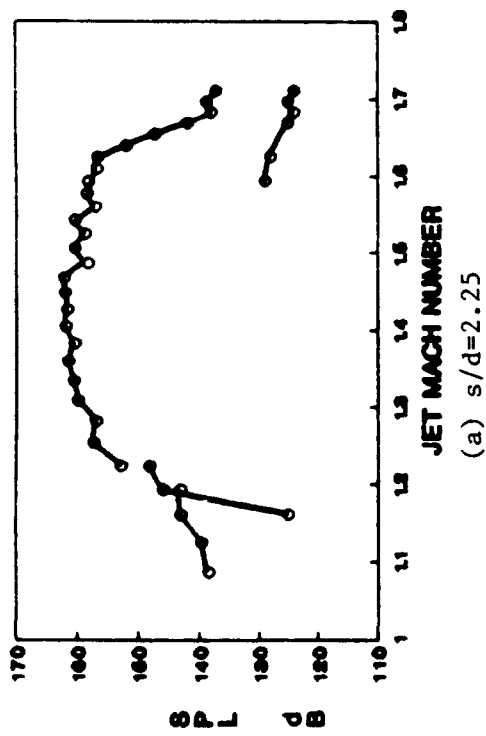
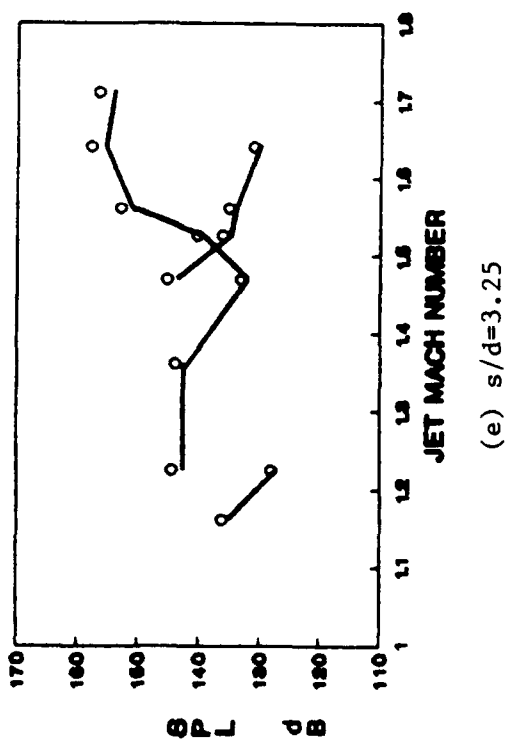
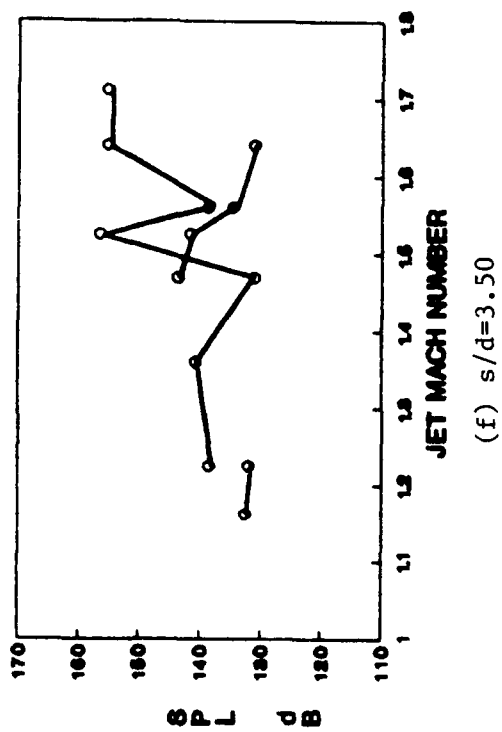
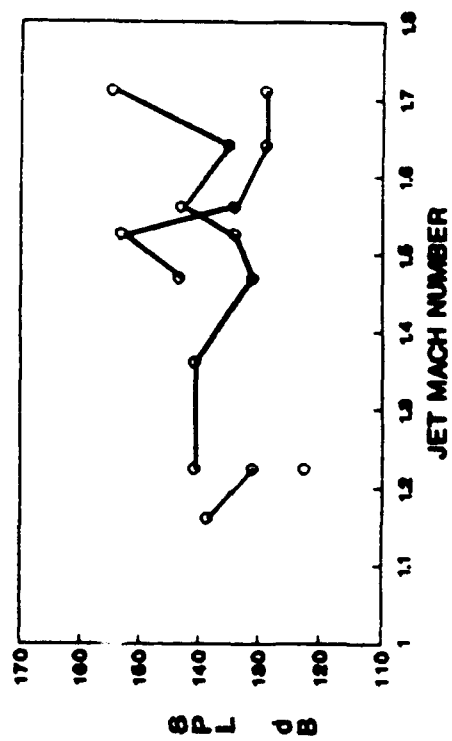


Figure 30 (a-l). SPL vs. Mach # Plots for Various Spacing Ratios,  $(2.25 < s/d < 7.00)$



(g)  $s/d=3.75$



(h)  $s/d=4.00$

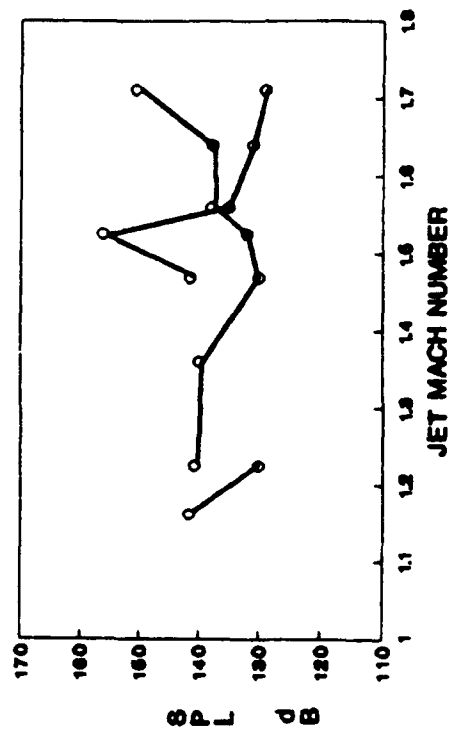
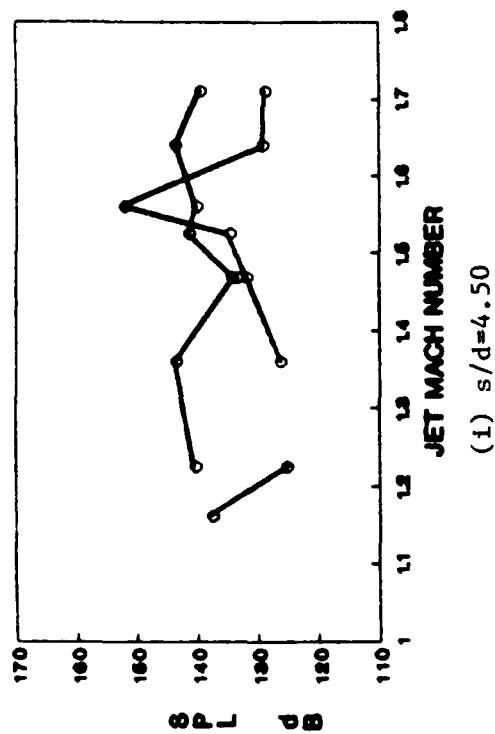


Figure 30 (Cont'd)





(1)  $s/d=7.00$

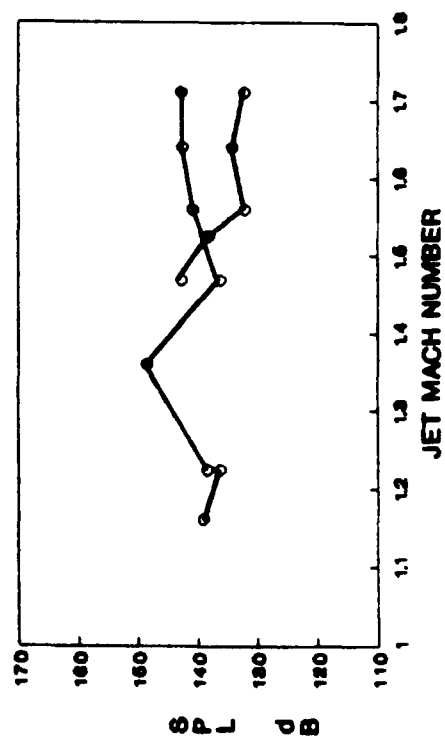


Figure 30 (Cont'd)

the next spacing ratio range of 3.75 to 4.5, the C mode peaked sharply between  $M=1.5$  and 1.6 and was actually the dominant mode in this Mach number range, whereas the B mode was fairly stable over the entire Mach number range. Finally, for the spacing range of 5.00 to 7.00, both B and C helical modes were fairly constant over the Mach range with most of the amplitudes remaining below 150 dB.

Design guidelines for screech suppression using a twin nozzle configuration was the ultimate goal of this experiment. Design plots of Overall Sound Pressure Level (OASPL) versus  $s/d$  were developed to show the effect of the lateral screech suppression technique. This OASPL value approximates the highest peak magnitude of the spectrum or usually the screech peak magnitude; however, it is a purely quantitative measurement since it is not representative of any one frequency position. For the twin axisymmetric configurations tested here, a plot of OASPL versus  $s/d$  was constructed for several NPR conditions (Figure 31). Initial results showed that at the lower spacing ratios of 2.25 to 3.00, the OASPL levels were high with many recorded above the 160 dB level. For a spacing ratio of 3.5, a decrease in OASPL occurred at every NPR except for  $NPR=5.0$ . At spacing ratios equal to 5.0 or greater, the OASPL level remained fairly constant and low suggesting that the larger spacing gap resulted

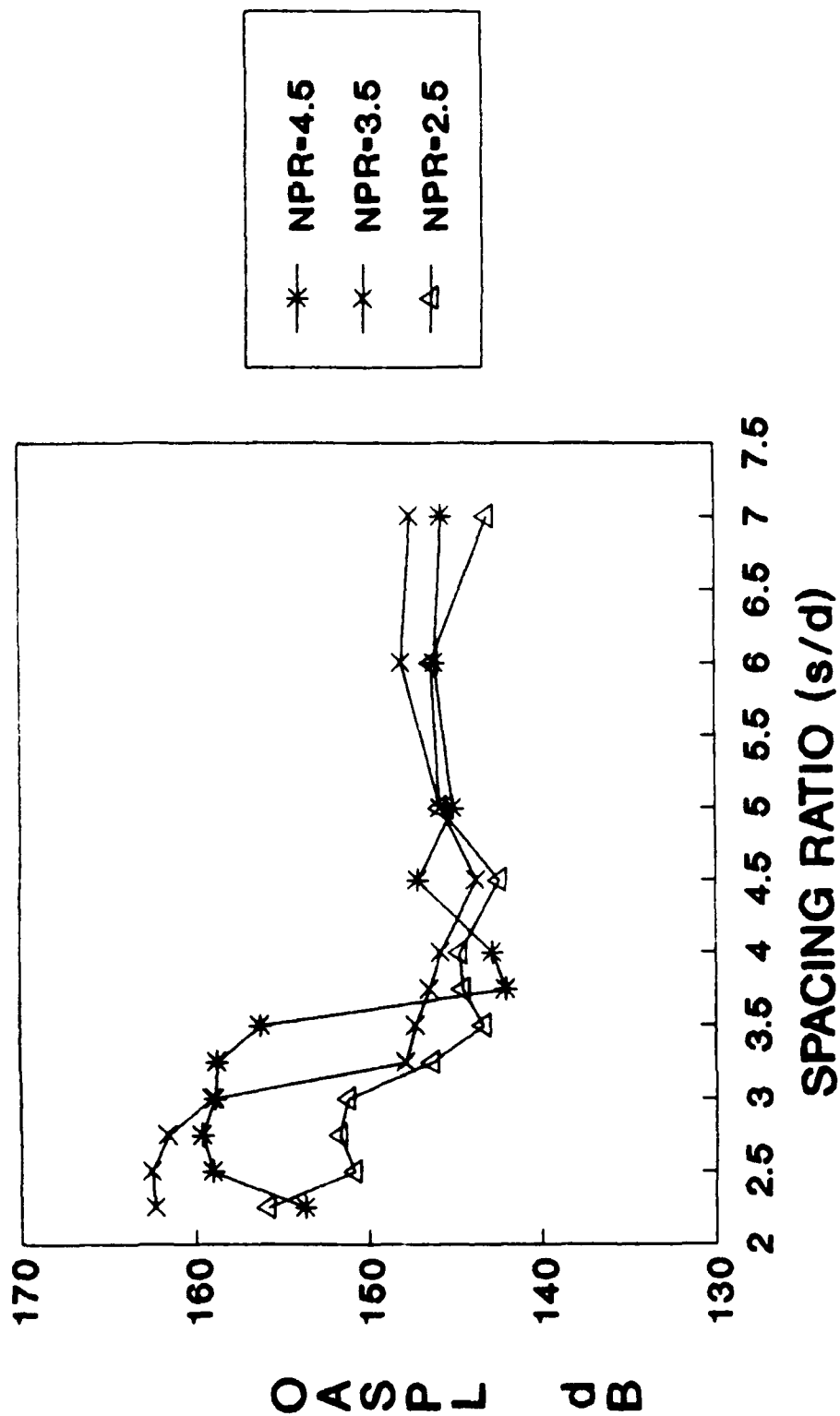


Figure 31. Lateral Spacing Suppression for Dual Axisymmetric Configurations, (OASPL vs. s/d)

in a decoupling of the plume instabilities. Lower OASPL amplitudes occurred at NPR=2.5 over all the spacing ratios due to the weaker shock cell structure of the plumes at this condition.

These lateral spacing results showed that for all the twin configurations tested, the modal types and frequency ranges were essentially the same for the various spacing ratios. The SPL and OASPL amplitudes differed over the range of spacing ratios and remained high for the small spacings. For the larger spacings, the OASPL amplitudes decreased generally with some local increases occurring at specific NPR values.

#### Twin Axisymmetric Secondary Air Jet Suppression

Because an aftbody configuration is designed using many aerodynamic, performance, and control parameters, a screech suppression concept that does not alter the external geometry of the configuration is preferred. A secondary air jet was investigated as an alternative suppression technique for a twin nozzle configuration. The secondary jet tube inside diameter measured 0.1875 in (0.476 cm). The secondary jet was fixed to one of the two primary nozzles and secondary jet pressure was varied from 0 psig to 60 psig. (Appendix). The  $\lambda/d$  versus  $M_j$  plots for the secondary air jet are shown in Figures 32 (a-d).

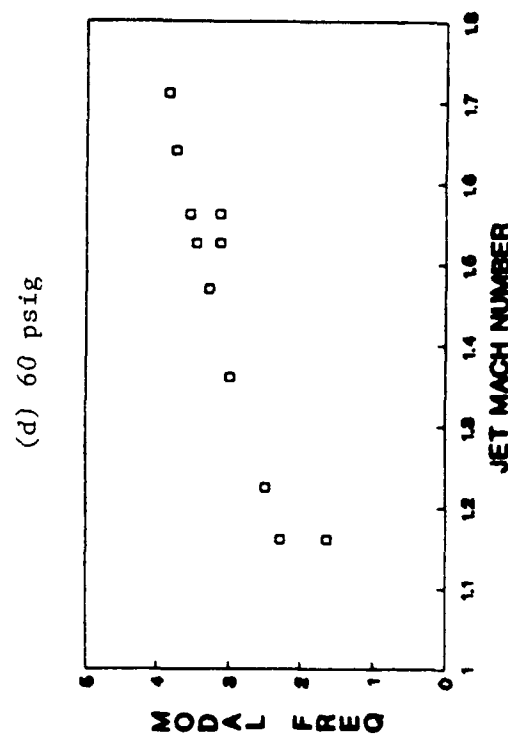
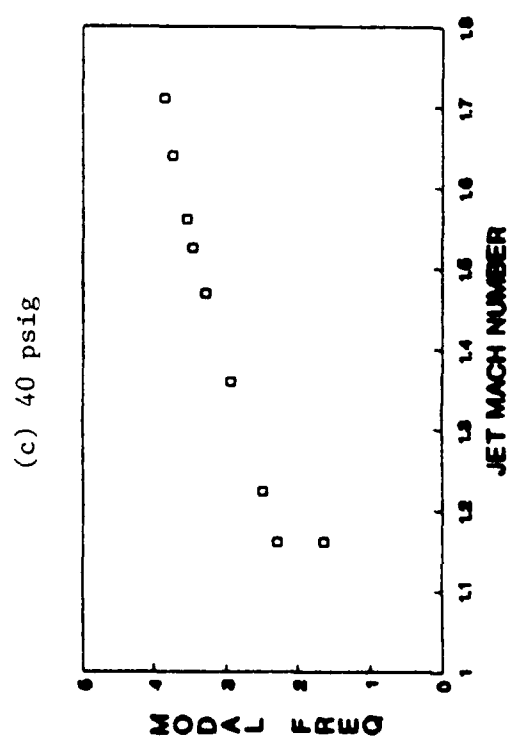
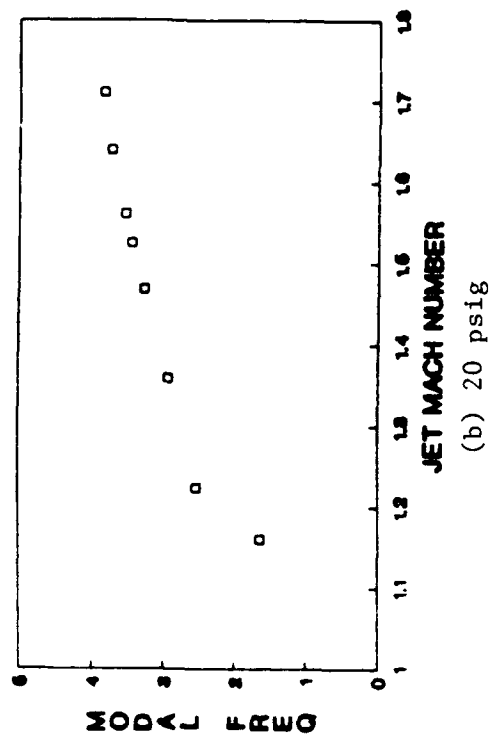
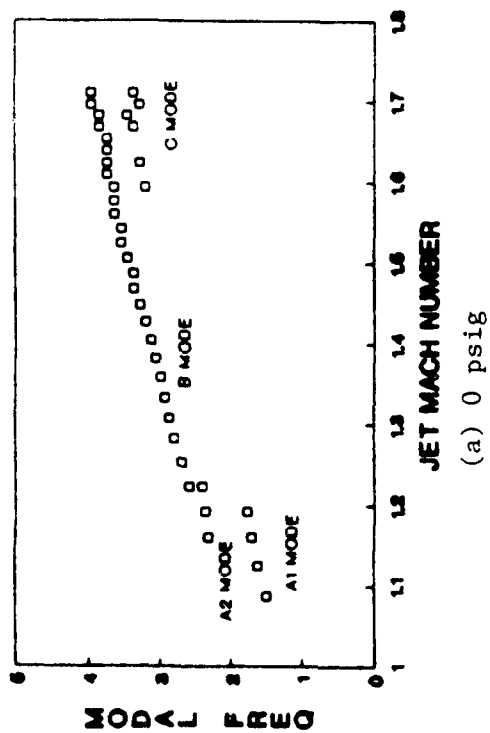


Figure 32 (a-d). Modal Frequency Plots for Various Secondary Air Pressures (0 psig - 60 psig)

The secondary air jet configurations reflected modal frequency ranges similar to the twin axisymmetric baseline configuration.

Sound pressure level plots were completed for the 20-60 psig cases which show a decrease in the SPL levels compared to the unsuppressed configuration of 0 psig. The dominant peak amplitudes are plotted versus jet Mach number in Figures 33 (a-d). The peak levels at low  $M_j$  and at high  $M_j$  were reduced from the levels of the unsuppressed configuration. Also, as the secondary jet pressure increased, the SPL levels decreased for most NPR data points (Figure 34). In this figure, the unsuppressed peak level of the twin axisymmetric baseline configuration ( $s/d=2.25$ ) is shown relative to the suppressed peak levels at certain NPRs over the secondary air pressure range. For the  $NPR=2.5$  condition, the reduction in sound intensity is over 15 dB. In all cases, the highest secondary air jet pressure of 60 psig produced the most screech suppression.

#### Twin Axisymmetric Tab Suppression

Various methods to suppress screech tones have been used in the past including adding small tabs to the nozzle exit plane. Three different tabs of various sizes were used to determine which style tab would be used in further suppression tests. The

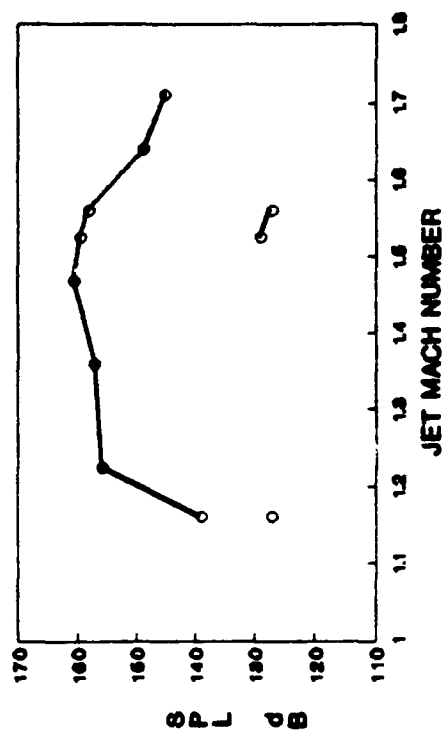
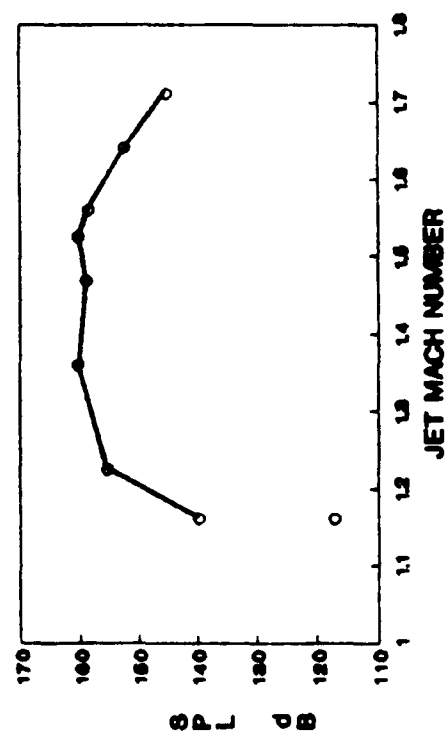
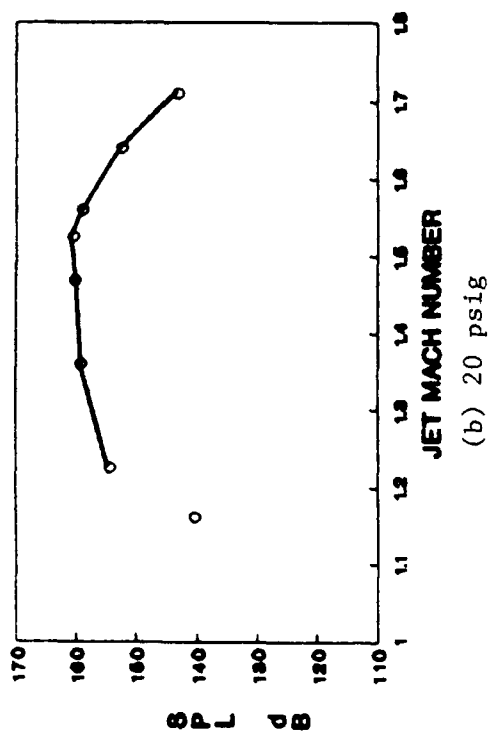
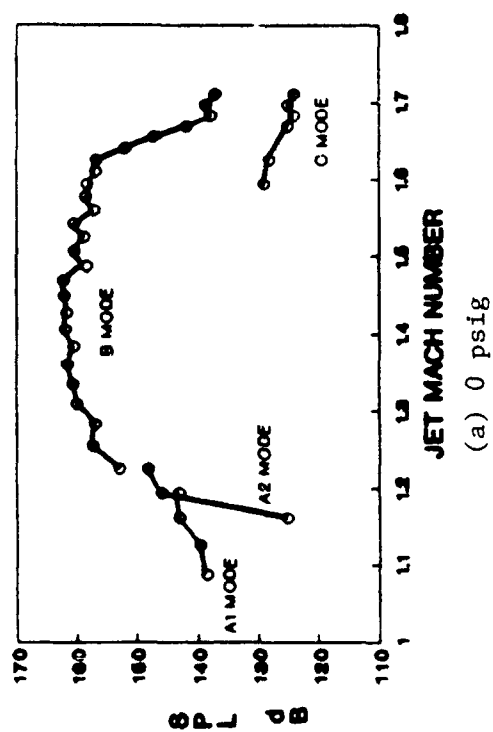


Figure 33 (a-d). SPL vs. Mach # Plots for Various Secondary Air Pressures (0 psig - 60 psig)

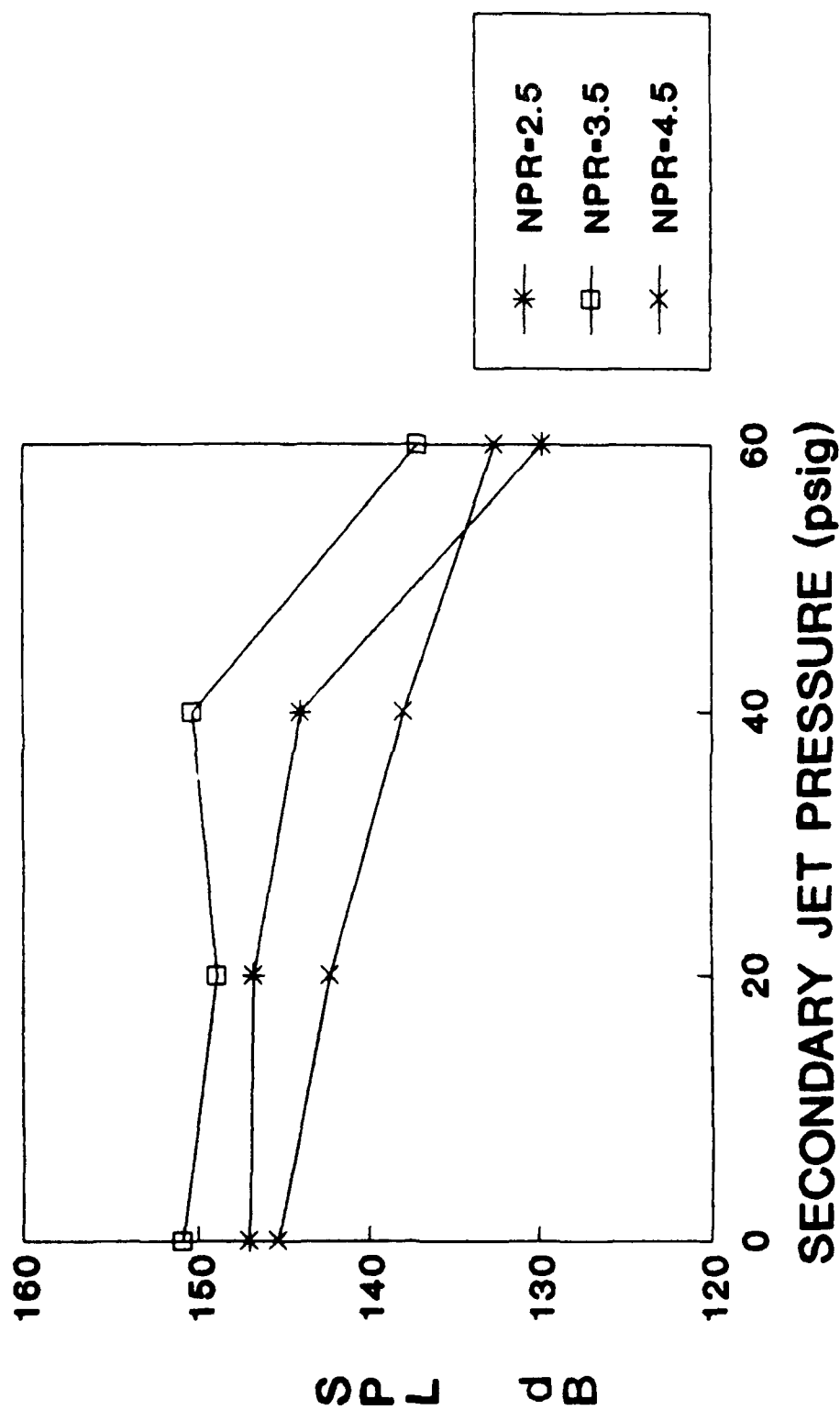
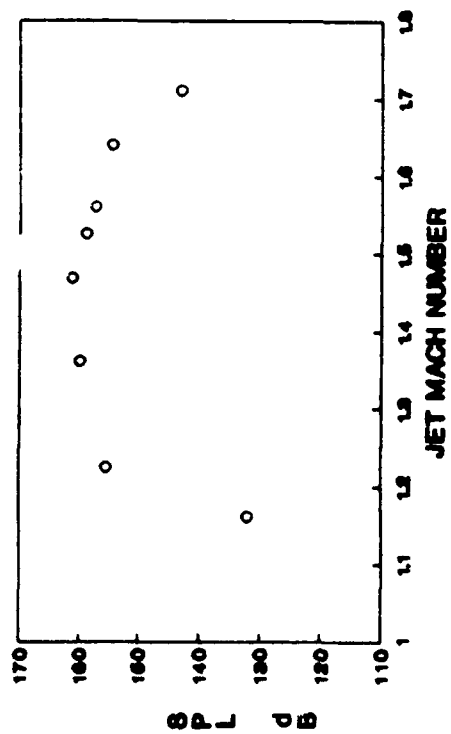


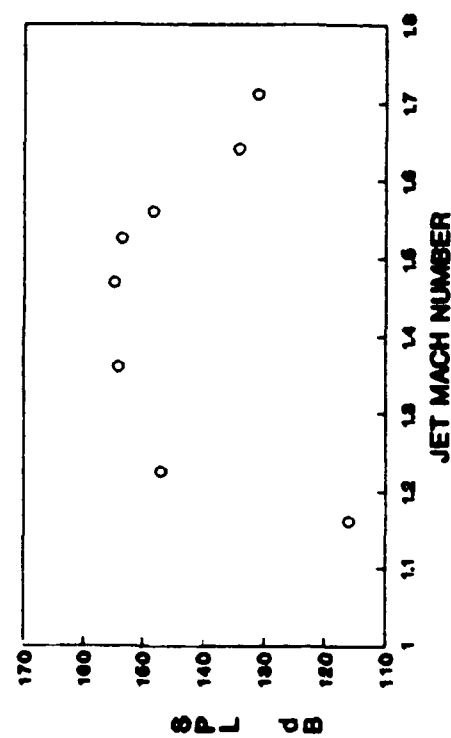
Figure 34. Secondary Air Suppression for Dual Axisymmetric Configurations, (SPL vs. Secondary Jet Pressure)



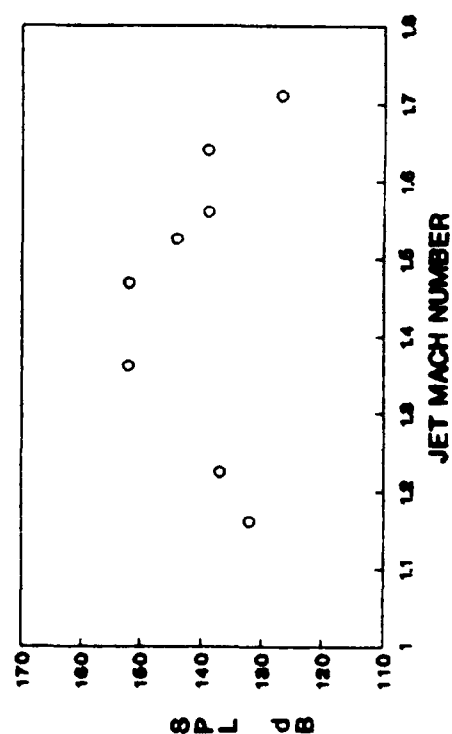
size and dimensions of the tabs are given in the Appendix. These three tab sizes in groups of 1,2, or 3 tabs were attached to a single nozzle exit. Steady-state results were obtained that showed tab number 3 to be the most effective for suppressing screech. A decision was made to use the largest tab in area, tab 3, and to use it in 1,2, or 3 number configurations on a single nozzle in a dual axisymmetric configuration of  $s/d=2.25$ . The SPL versus  $M_j$  plots for 0,1,2, and 3 tabs are shown in Figures 35 (a-d). An overlay plot of these graphs is shown in Figure 36. These SPL values corresponded to B mode values, since the B mode was normally the strongest screech producer in these tests. The top curve is the unsuppressed SPL values of the twin axisymmetric configuration at a nozzle spacing ratio of 2.25. The 1-tab suppression test resulted in lower values of SPL; however, the 2-tab and 3-tab configurations resulted in still lower SPL values. For the 2- and 3-tab configurations, the SPL levels were significantly reduced at the lower and higher jet Mach number ranges. Schlieren photographs of the 0-tab and 2-tab configurations for the  $NPR=3.0$  condition are shown in Figures 37 (a-b). Mode coupling is clearly seen in the unsuppressed case, whereas the plumes are decoupled for the tab configuration cases. Generally, more than 1-tab was needed for screech suppression reduction of more than 15 dB.



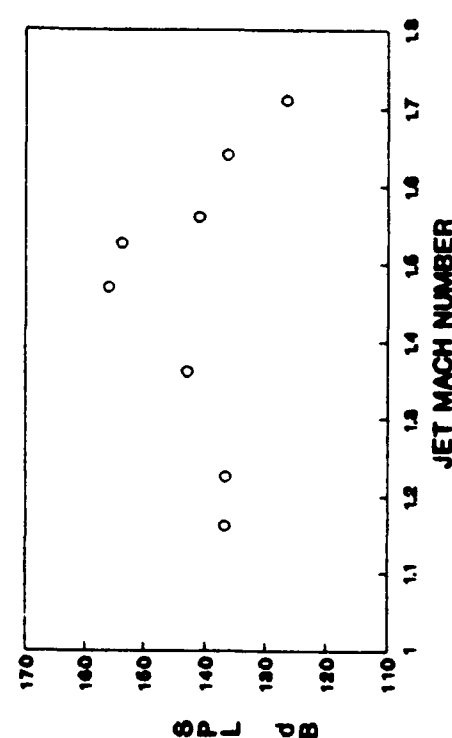
(a) 0 tabs



(b) 1 tab



(c) 2 tabs



(d) 3 tabs

Figure 35 (a-d). SPL vs. Mach # Plots for Various Tab Configurations (0 tab - 3 tabs)

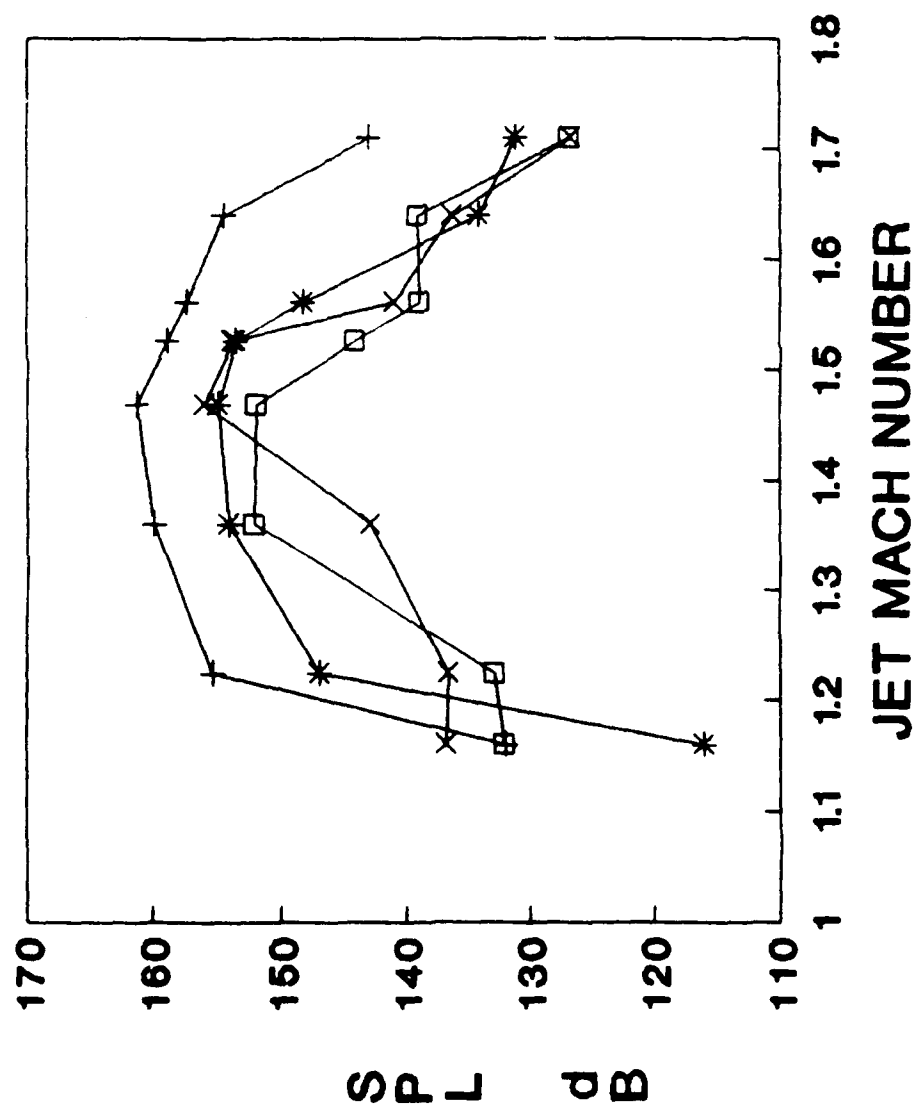
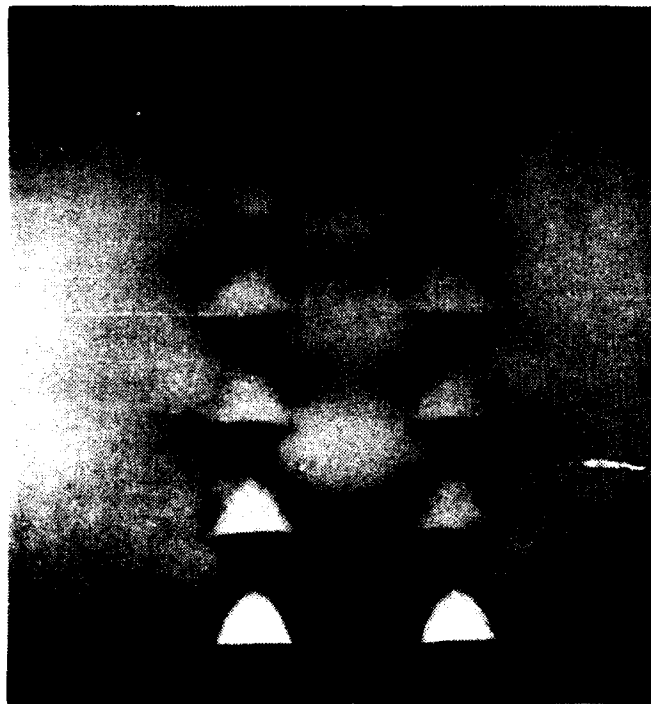
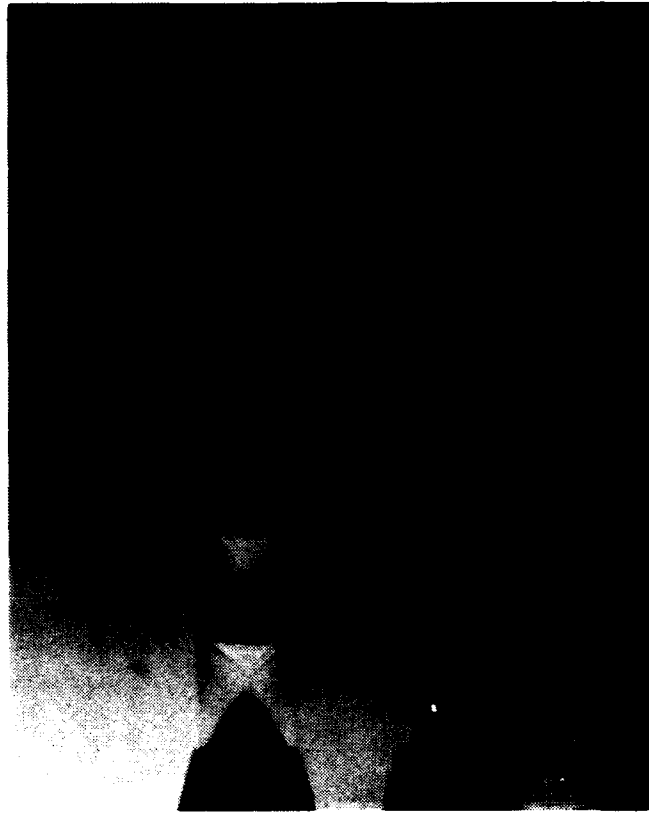


Figure 36. Tab Suppression for Dual Axisymmetric Configurations, (SPL vs. Mach # Plot)



(a) 0 tabs



(b) 2 tabs

Figure 37 (a,b). Schlieren Photos of Tab Suppression  
(a) No Tabs, (b) Two Tabs

### Twin Axisymmetric Axial Shift Suppression

Axial shifting of one of the two nozzles in the longitudinal direction was thought to prevent the in phase coupling of the wave instabilities in the jet plumes. Axial shift intervals of 0.25 in (0.635 cm) and 0.5 in (1.27 cm) were used and are described in the Appendix. The axial shift results are compared to the twin baseline configuration of no suppression in Figure 38. The results showed that the shifting of one nozzle produced no appreciable suppression of the screech amplitudes except at the low NPR condition of 2.5. At the NPR=4.5 condition, the 0.25in (0.635cm) axial shift actually increased the SPL by close to 10 dB.

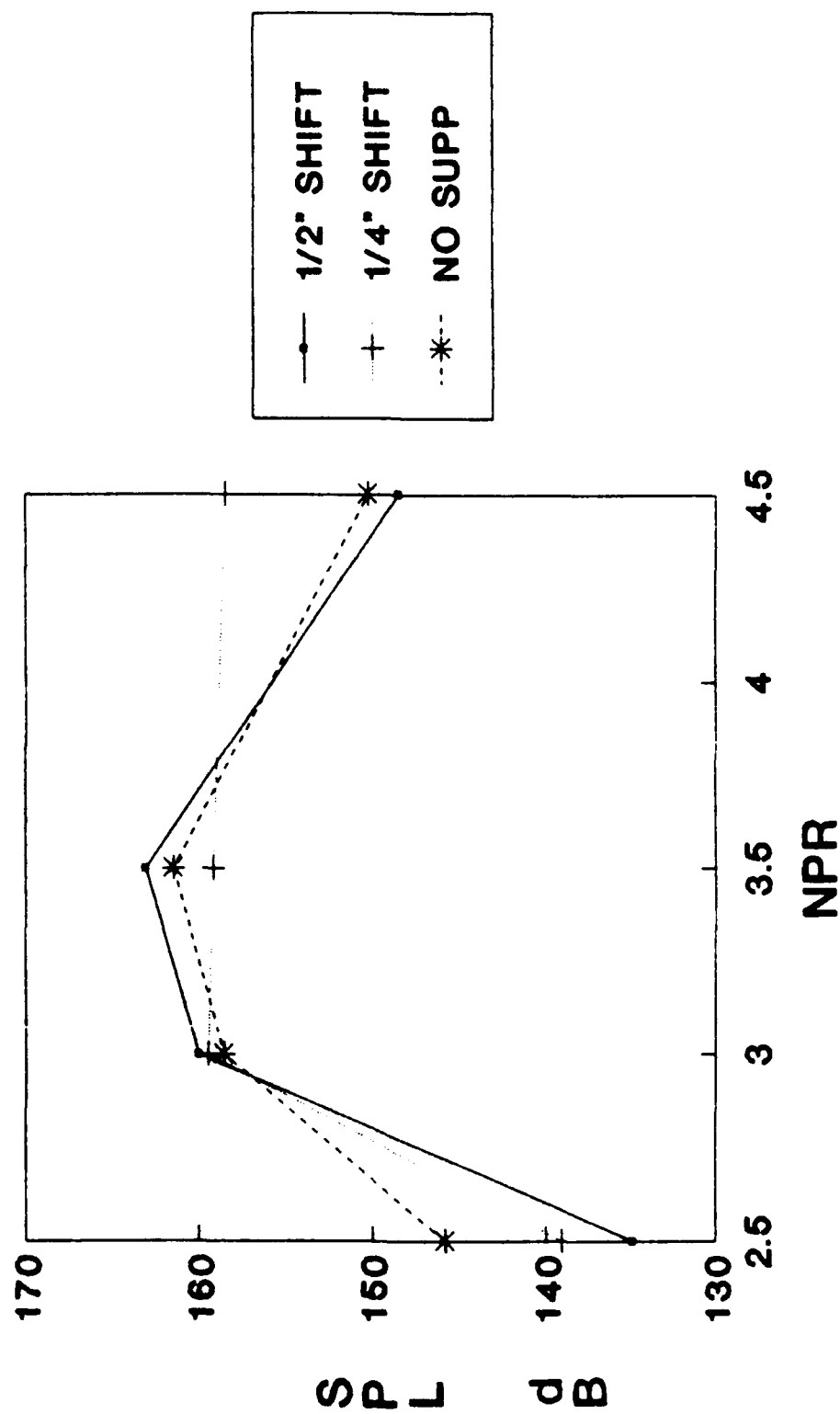


Figure 38. Axial Shift Suppression for Dual Axisymmetric Configurations

## TWO-DIMENSIONAL NOZZLE RESULTS

Two-dimensional 4.7% scale model nozzles were used to test screech suppression and nozzle orientation concepts. The single and twin baseline configurations were tested first followed by lateral spacing of the twin jets, secondary air jet, nozzle exit tab suppression, and axial shift suppression experiments. Two-dimensional nozzle orientation tests such as nozzle cant angle variation and pitch deflection variation were also studied.

### Single 2D Baseline Configuration

A single two-dimensional nozzle with a throat aspect ratio of 3.71 was tested over an NPR range of 2.0 to 5.0. The corresponding jet Mach number range is approximately 1.1 to 1.75. Acoustic spectra were recorded and reduced similar to the axisymmetric nozzle data. However, for most of the two-dimensional nozzle cases, the OASPL of the acoustic spectrum was used as the figure of merit.

Just as for the axisymmetric nozzle configurations, a modal frequency parameter chart was created to separate the various screech modes, and then a second plot of OASPL versus  $M_j$  was

created to quantify the analysis. This approach was used for the single rectangular nozzle and is shown in Figures 39 and 40.

In Figure 39, the modal frequency parameter is plotted versus jet Mach number. As was the case with the axisymmetric data, the frequencies of the dominant narrowband peaks were converted into a wavelength parameter. Instead of using the nozzle exit diameter, the nozzle throat height,  $h_t$ , was used to normalize the wavelength measurement. This modal frequency parameter showed the linear dependence of the various screech modes with jet Mach number.

The modal frequency plot for the single rectangular nozzle configuration clearly showed two different modes over the jet Mach number range. Zilz concluded that two "normal flapping" rectangular modes existed over the NPR range for a twin high aspect ratio nozzle configuration. He labelled these the Normal Symmetric (NS) and the Normal Antisymmetric (NA) modes (Figure 6).<sup>9</sup> Zilz found that for a twin rectangular high aspect ratio nozzle configuration, the NS mode occurred below design NPR and both the NS and NA modes occurred above design NPR. He was able to make these qualitative measurements using directivity instrumentation shown in Figure 41.<sup>9</sup>



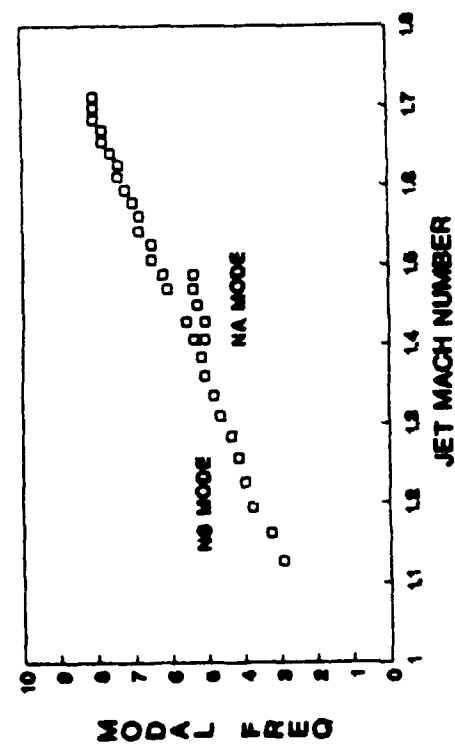


Figure 39. Single Two-dimensional Baseline  
(Modal Frequency Plot)

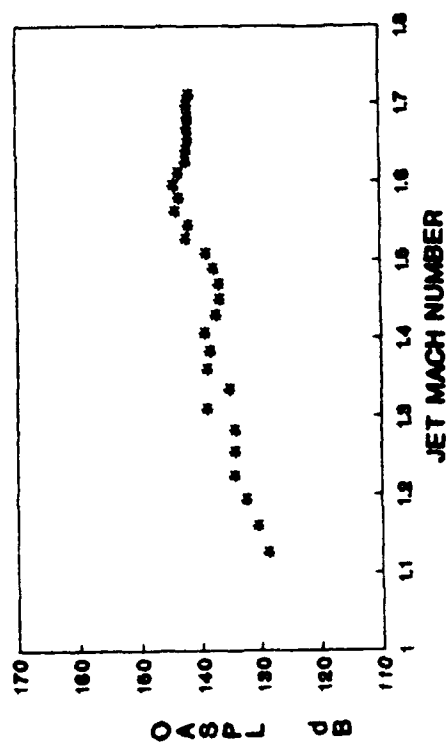


Figure 40. Single Two-dimensional Baseline  
(OASPL vs. Mach # Plot)

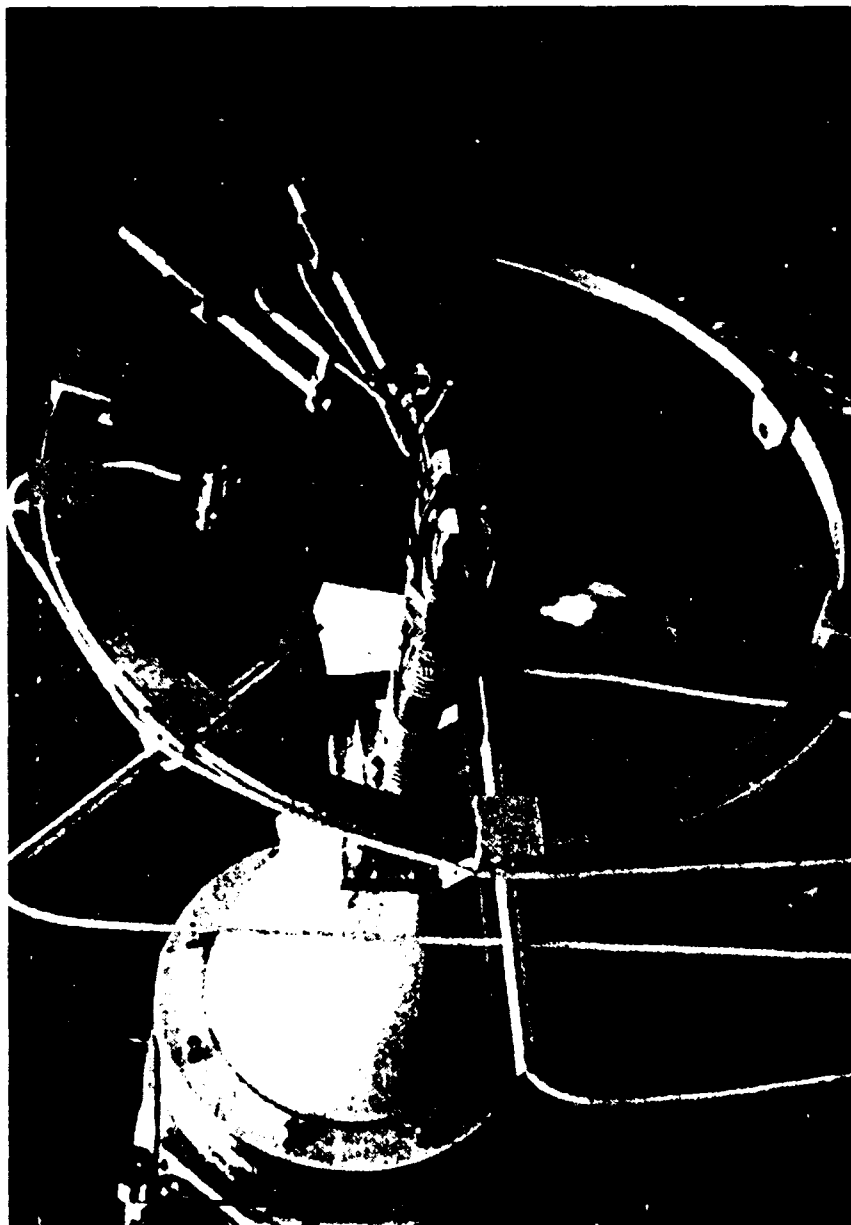


Figure 41. Directivity Instrumentation

Similar results were found for the single high aspect ratio rectangular nozzle of this test. A single mode occurred below the design jet Mach number of 1.4, and two modes occurred above this design jet Mach number. The two modes occurred between a jet Mach number of 1.4 and 1.5 transitioning into one mode beyond the jet Mach number of 1.5. Zilz concluded that when the NA mode was present just beyond the design Mach number, the OASPL decreased. Also, he concluded that after the NS mode became dominant again and the NA mode disappeared, the OASPL level increased steadily. These exact trends were seen in the single rectangular qualitative and quantitative results shown in Figures 39 and 40.

#### Twin 2D Baseline Configuration

The dual rectangular baseline configuration was comprised of two rectangular nozzles of the same type used for the single configuration. For this dual baseline configuration, a two-dimensional spacing ratio,  $s/w$ , of 3.25 was used. This spacing ratio is defined to be the center-to-center distance between the two nozzles divided by the width of a nozzle exit.

The qualitative and quantitative results for this configuration are shown in Figures 42 and 43. The OASPL

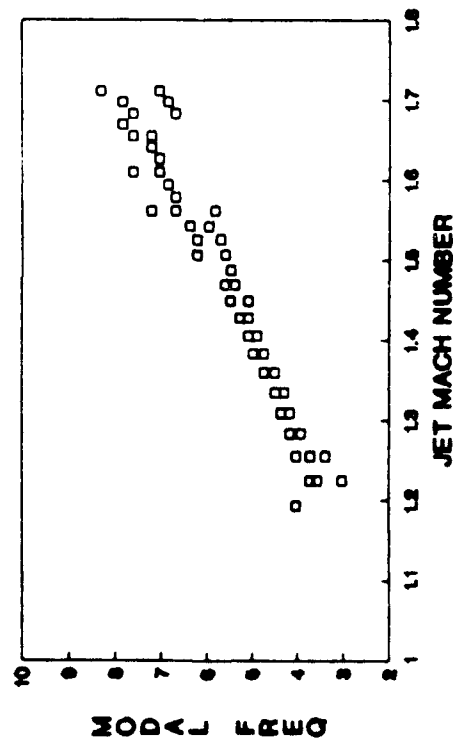


Figure 42. Dual Two-dimensional Baseline,  $s/w=3.25$   
(Modal Frequency Plot)

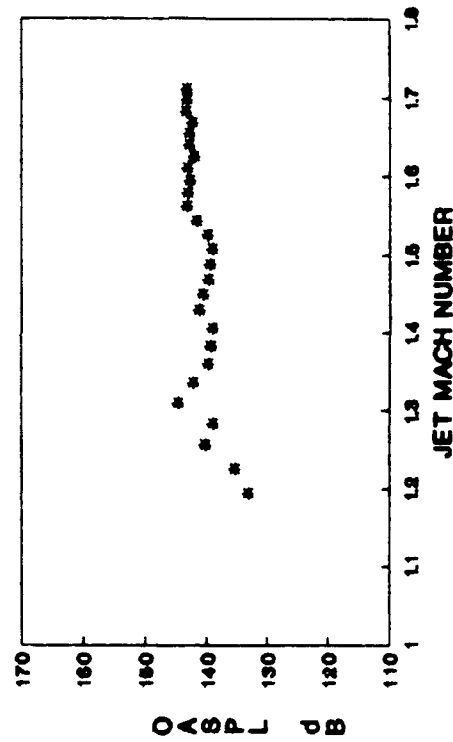


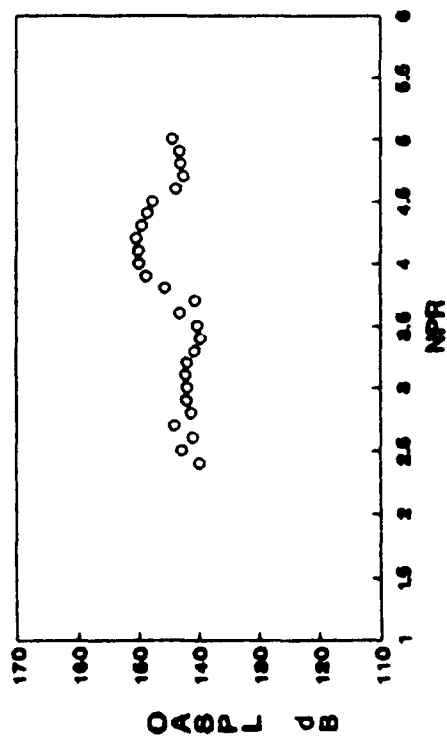
Figure 43. Dual Two-dimensional Baseline,  $s/w=3.25$   
(OASPL vs. Mach # Plot)

amplitudes for this case were similar in magnitude to the amplitudes for the single rectangular case. The OASPL decreased over the jet Mach number range just beyond the design Mach number suggesting that the NA mode was present in the design Mach number region. Also, the OASPL at the very overexpanded and underexpanded Mach numbers remained high suggesting that the NS mode existed over these Mach number regions.

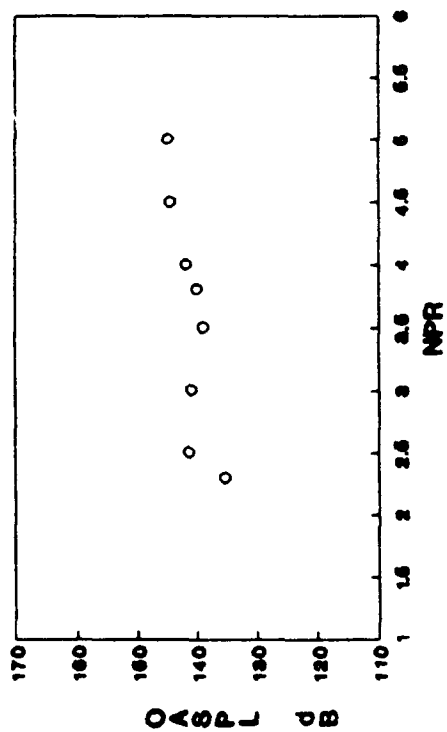
The qualitative results displayed the modal frequency variation with jet Mach number. These results were mixed for this configuration. The clarity and distinction between the various modes did not exist and did not follow the modal trends of the Zilz experiment. The two-dimensional nozzle spacing ratio ranges differed between the two experiments with the maximum  $s/w$  for the Zilz experiment being 3.20.

#### Twin 2D Lateral Spacing Suppression

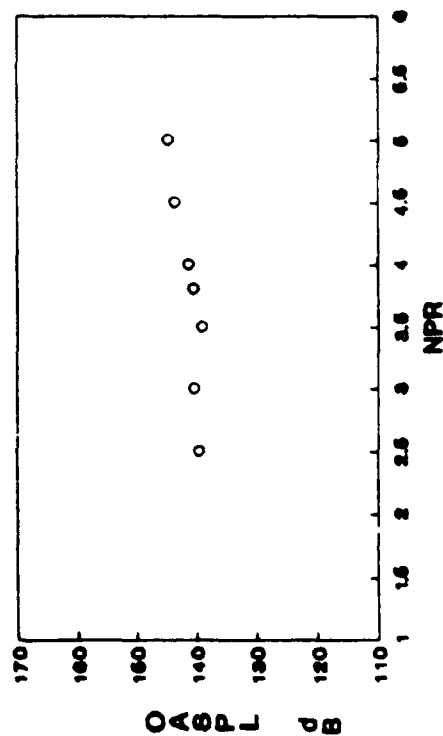
The twin two-dimensional nozzle baseline configuration was used to investigate the lateral spacing suppression technique. The baseline configuration was tested at nozzle spacing ratios of 2.75 to 7.00. The OASPL plots for each spacing ratio are seen in Figures 44 (a-k). OASPL trends similar to the single and twin baseline configurations existed for each of the different nozzle



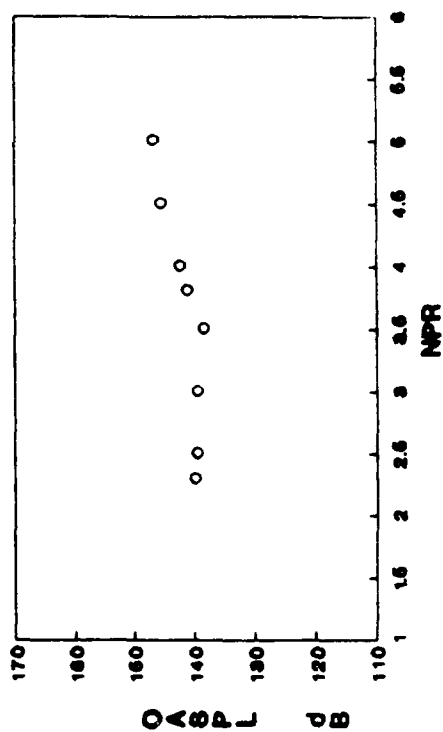
(a)  $s/w=2.75$



(b)  $s/w=3.00$

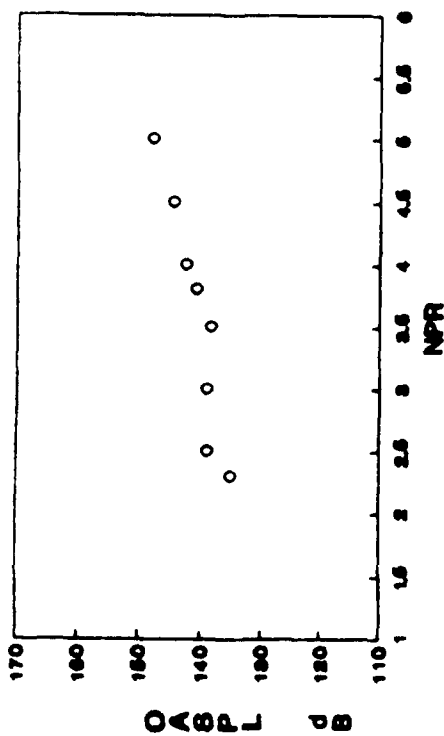


(c)  $s/w=3.25$



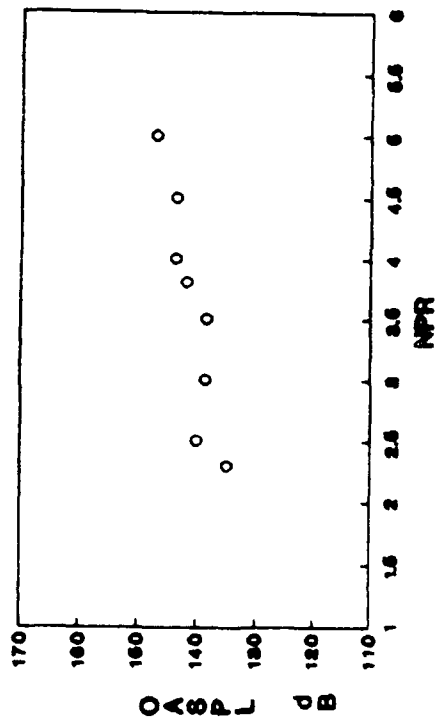
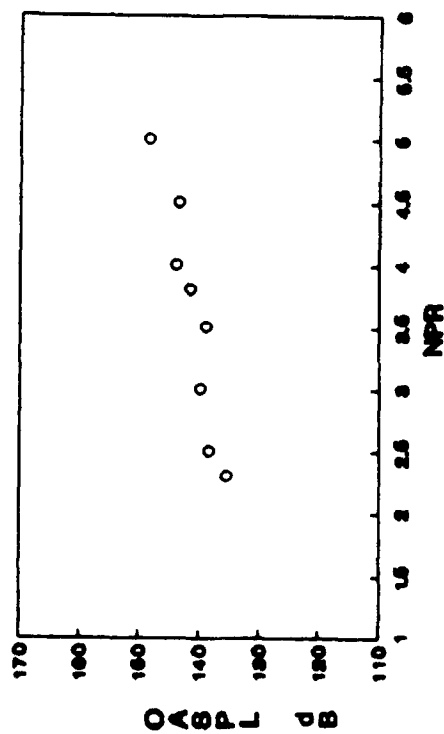
(d)  $s/w=3.50$

Figure 44 (a-k). OASPL versus NPR Plots for Various Spacing Ratios, ( $2.75 < s/w < 7.00$ )



(e)  $s/w=3.75$

(g)  $s/w=4.25$



(f)  $s/w=4.00$

(h)  $s/w=4.50$

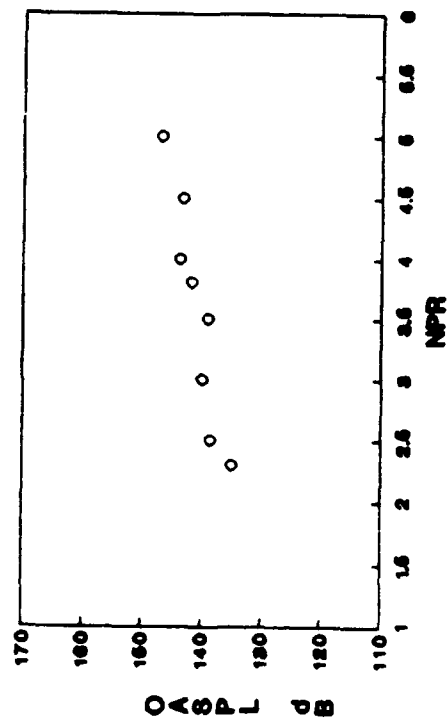
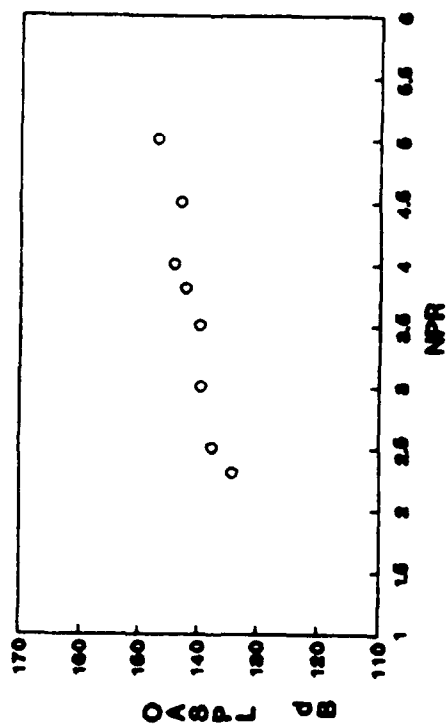
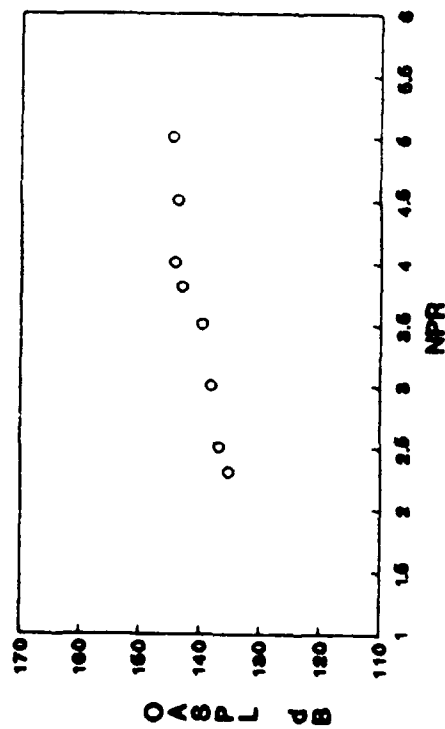


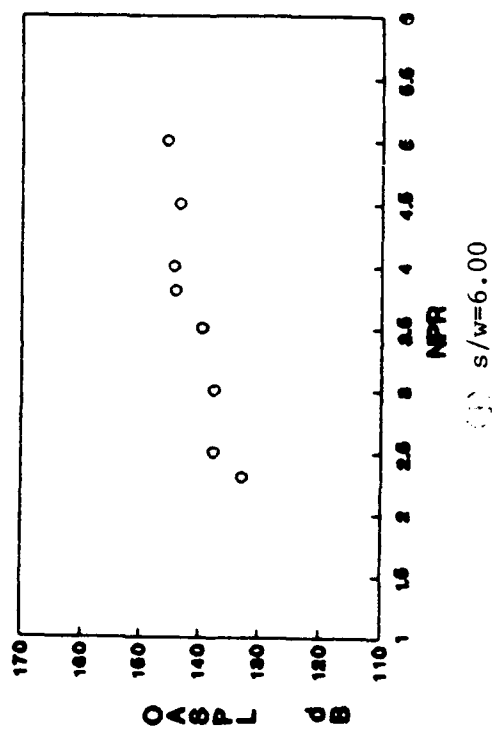
Figure 44 (Cont'd)



(i)  $s/w=5.00$



(k)  $s/w=7.00$



(j)  $s/w=6.00$

Figure 44 (Cont'd)



spacing ratio configurations. The OASPL decreased after the design NPR of 3.23 and then increased steadily over the NPR range beyond the NPR=3.5 condition. As shown previously, Zilz stated that the presence of the NA mode, in the region just after the design NPR, reduced the OASPL amplitudes. Beyond NPR=3.5, the NS mode was dominate and resulted in an increase in OASPL amplitudes.

In general, for this dual nozzle configuration over these NPR ranges, the OASPL amplitudes decreased with respect to nozzle spacing (Figure 45). Especially, for NPR conditions below the design NPR=3.23, the highest levels of OASPL occurred at the lowest spacing of  $s/w=2.75$ , and the lowest levels of OASPL occurred at the highest nozzle spacing of  $s/w=7.00$ . Since the NS mode was dominant below the design NPR, these results suggested that the NS mode was weakened and therefore the OASPL amplitudes reduced as the nozzles were separated further. For the NPR conditions of 2.5 and 3.0, at the nozzle spacing ratios of 4.0 and 4.5 respectively, the OASPL increased. This occurrence suggested that for this configuration at these NPR conditions, these spacings instigated higher interaction of the NS flapping mode which resulted in higher OASPL amplitudes.

At the higher NPR conditions above design of 3.5 and 4.5, the highest OASPL was again at the lowest nozzle spacing ratio of

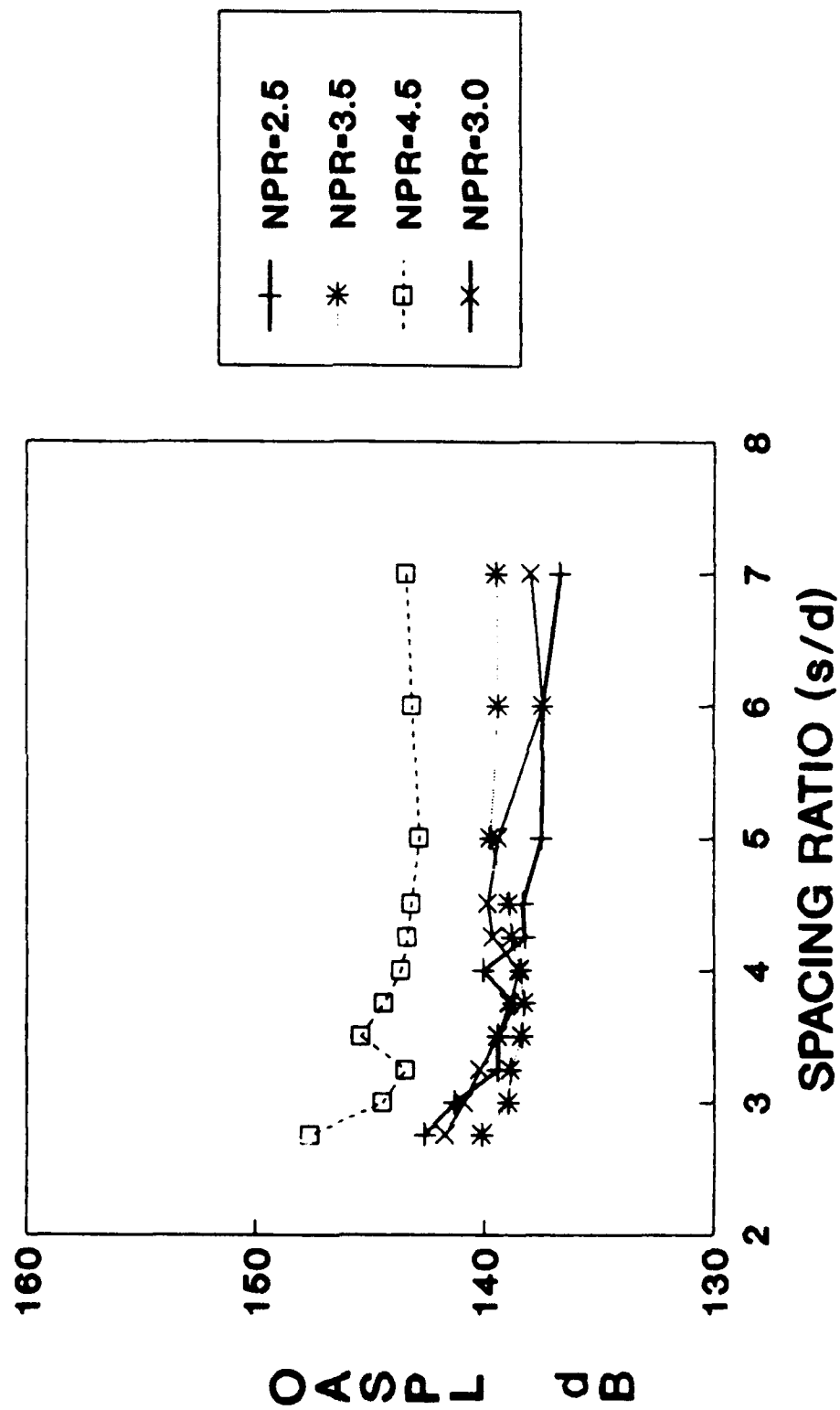


Figure 45. Lateral Spacing Suppression for Dual Two-dimensional Configurations, (OASPL vs. s/w)

2.75. At the NPR=3.5 setting, both the NA and NS modes were probably present. For spacing ratios of 2.75 to 3.75, OASPL decreased steadily, while for spacing ratios of 3.75 to 5.0, OASPL increased steadily. The OASPL amplitudes remained fairly constant for the spacing ratios of 5.0 to 7.0. This irregular trend of OASPL vs. spacing ratio suggested that the NA mode was dominant in the spacing range of 2.75 to 4.0, and that the NS mode was dominant in the spacing ratio range of 4.0 to 5.0. Concentrating on the NPR=3.5 condition at the higher spacing ratios, one can see a weak NA mode between NPR=3.0 and NPR=3.5. At the lower spacing ratios, a much stronger NA mode exists between 3.0 and 3.5.

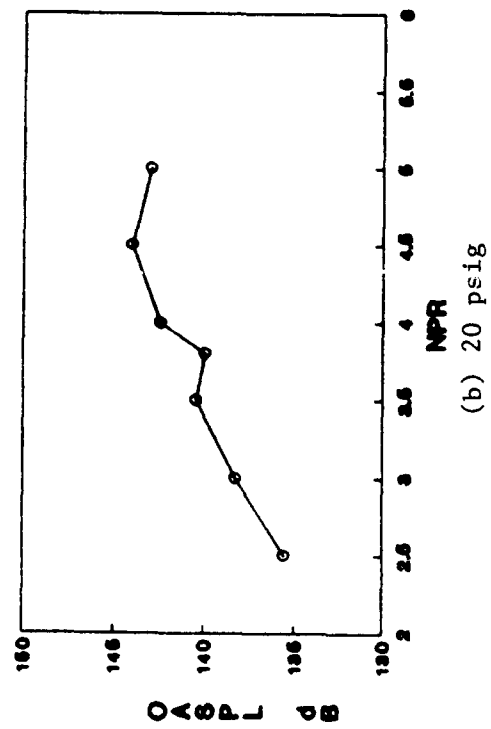
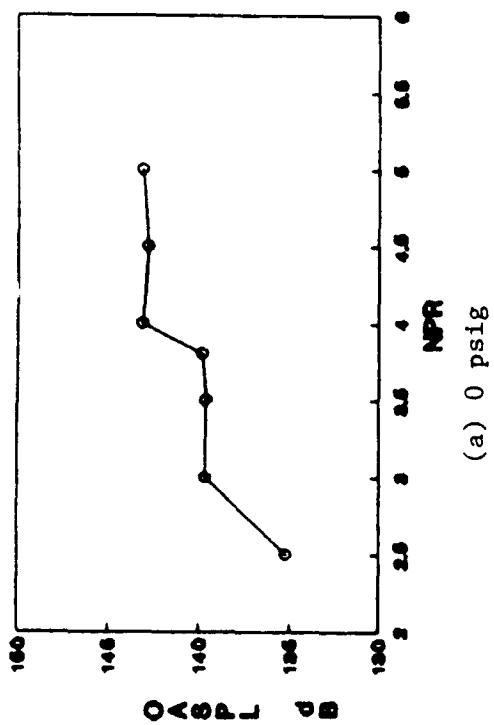
The highest NPR of 4.5 should have consisted of only NS mode characteristics and showed a general decrease in OASPL with nozzle spacing ratio. However, at the  $s/w=3.5$ , the OASPL increased sharply and then continued with the trend of decreasing OASPL. At this particular spacing, the NS mode interaction must have become stronger between the two jet plumes.

In conclusion, for lateral spacing suppression tests, the higher OASPL amplitudes occurred at the closest nozzle spacings. For NPRs below design, the lowest OASPL occurred at the highest spacing, and trends generally showed a decreasing OASPL level with increasing spacing. For NPRs above design, trends were

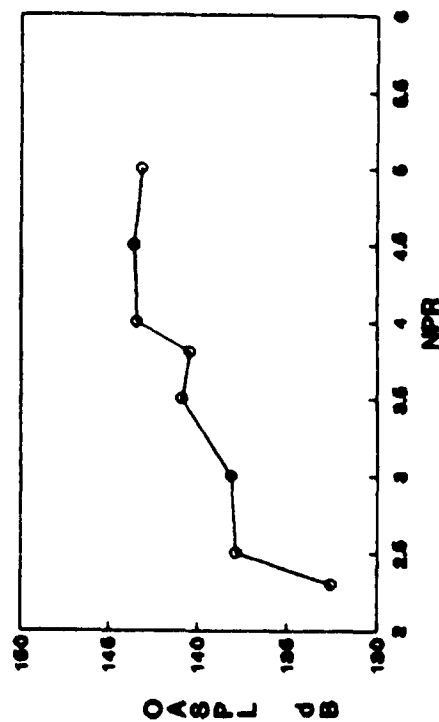
mixed especially for the NPR of 3.5 which most probably had both NA and NS mode interaction simultaneously.

#### Twin 2D Secondary Air Jet Suppression

A small air jet with a 0.125in (0.318cm) inside diameter was attached to one nozzle of the twin rectangular configuration. The baseline nozzle configuration was used with a spacing ratio of 3.25. The results were mixed for the single secondary air jet test. Over most of the NPR range, the OASPL amplitudes resulting from secondary air jet runs were higher than the amplitudes for the unsuppressed case (Figures 46 (a-d)). Some suppression of the screech amplitudes existed at the NPR=3.0 setting; however, these suppression deltas were minimal compared to the screech suppression achieved using the axisymmetric configuration (Figure 47). It is possible that at the closest spacing ratio of 2.75, a greater possibility of suppression could exist since OASPL amplitudes for that configuration were much higher than for the twin baseline configuration. Also, the secondary air jet technique may suppress the helical mode coupling of the axisymmetric configurations more effectively than the jet flapping type motion of the rectangular configurations.



(c) 40 psig



(d) 60 psig

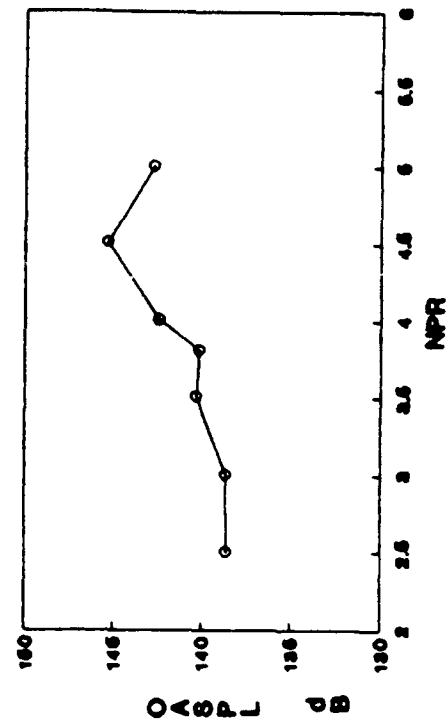


Figure 46 (a-d). OASPL versus NPR for Various Secondary Air Pressures, (0 psig - 60 psig)

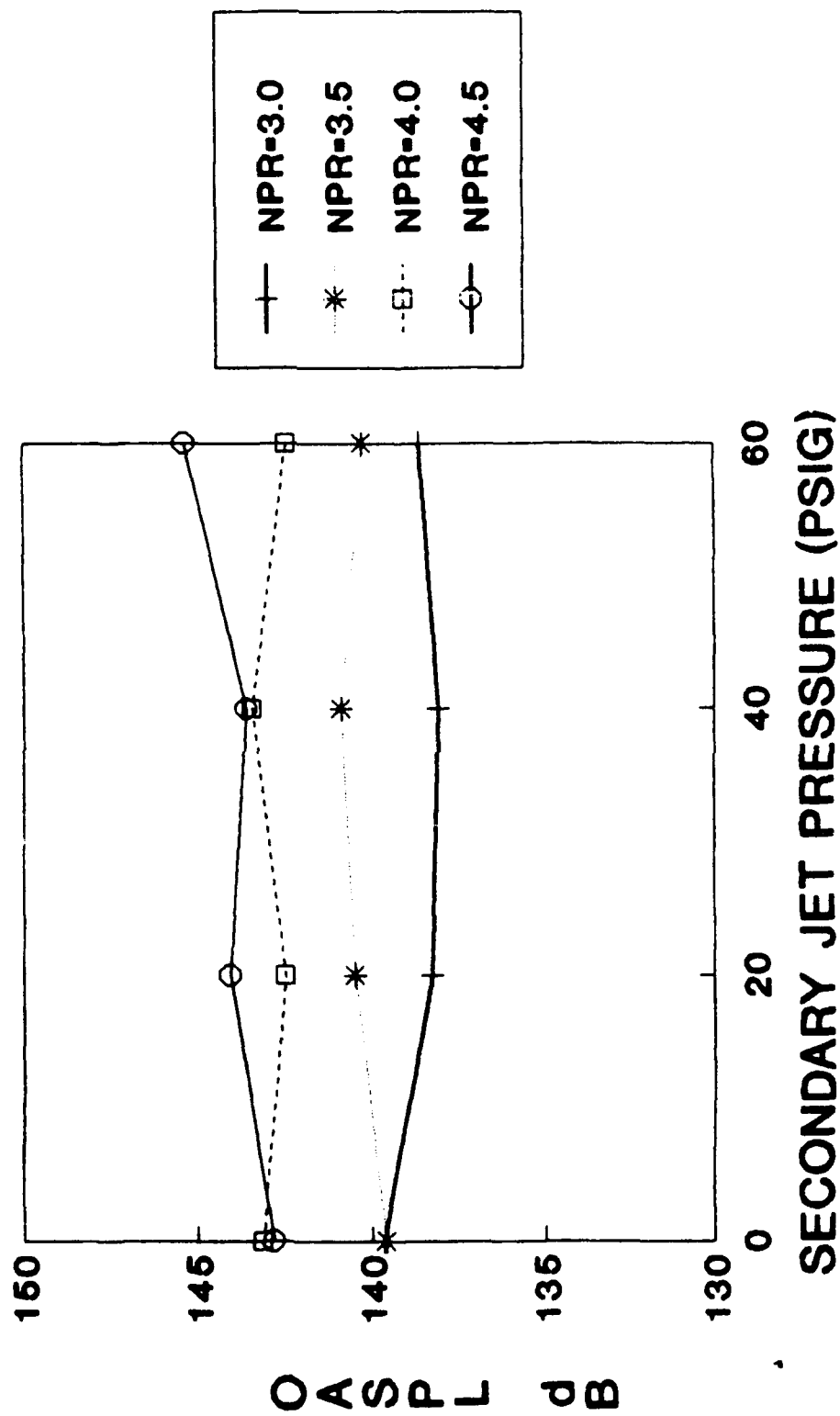


Figure 47. Secondary Air Suppression for Dual Two-dimensional Configurations

### Twin 2D Tab Suppression

Tab suppression tests were conducted for the two-dimensional configurations as was done for the axisymmetric configurations. One, two, and three tabs of the tab 3 variety were tested and are shown in the Appendix. These tab configurations were attached to one nozzle of the dual rectangular configuration, so that the characteristic jet flapping motion might be suppressed.

In Figure 48, a plot of OASPL versus NPR is shown. The OASPL increased with increasing NPR as expected due to the increasing strength of the shock cell structure with NPR. A design plot showing OASPL variation with the number of tabs is shown in Figure 49. Some screech reduction occurred for the underexpanded regions with the most screech suppression occurring for the 2-tab configuration. The 2-tab configuration has been favored by many researchers including Brown and Ahuja.<sup>13</sup> In a NASA report, the two authors concluded that the 2-tab configuration produced the highest jet mixing and actually reduced heating levels within the jet plume. In this cold test, the introduction of two tabs into the nozzle flow disrupted the normal jet flapping modes to an extent that OASPL amplitudes were reduced.

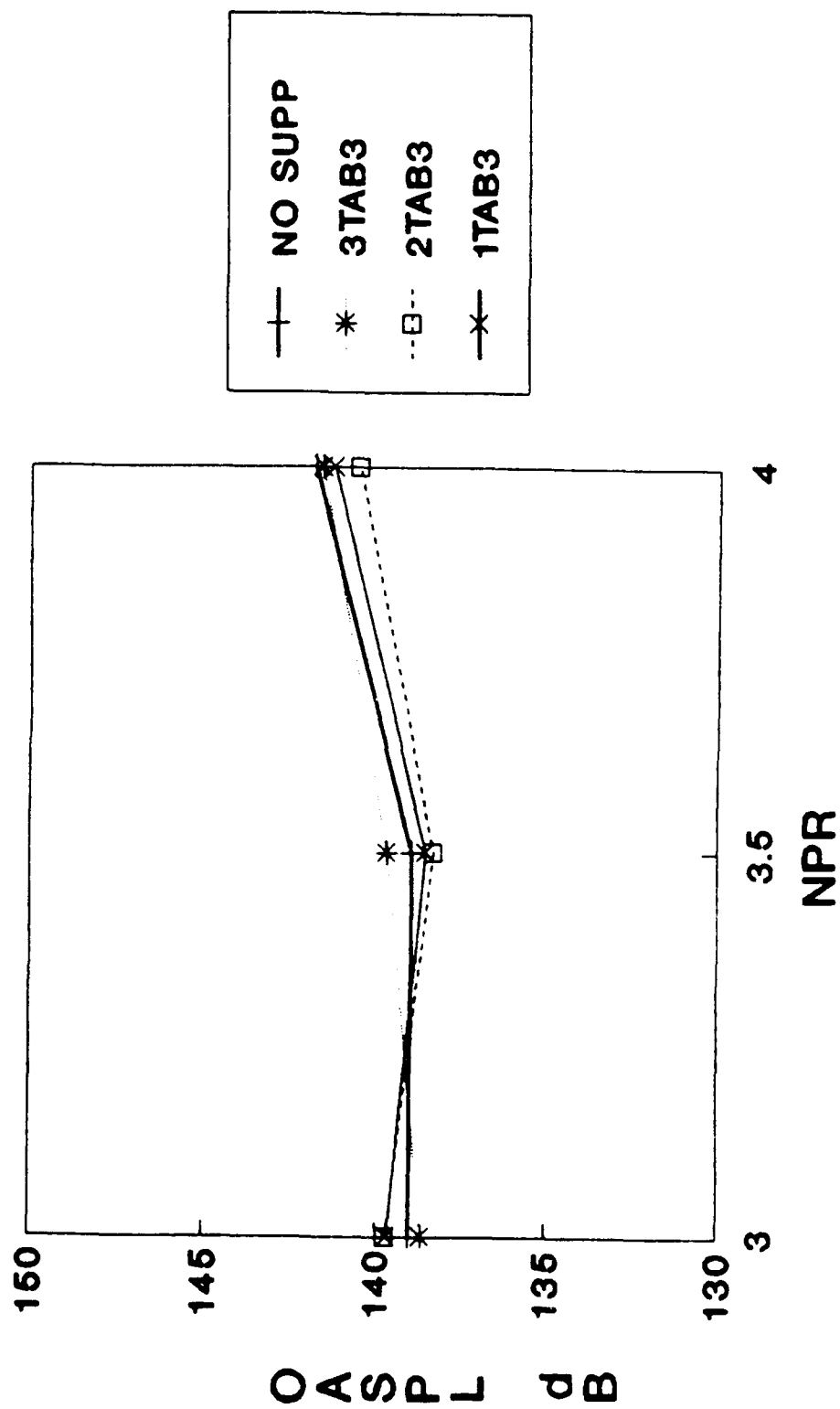


Figure 48. Tab Suppression for Dual Two-dimensional Configurations, (OASPL vs. NPR Plot)



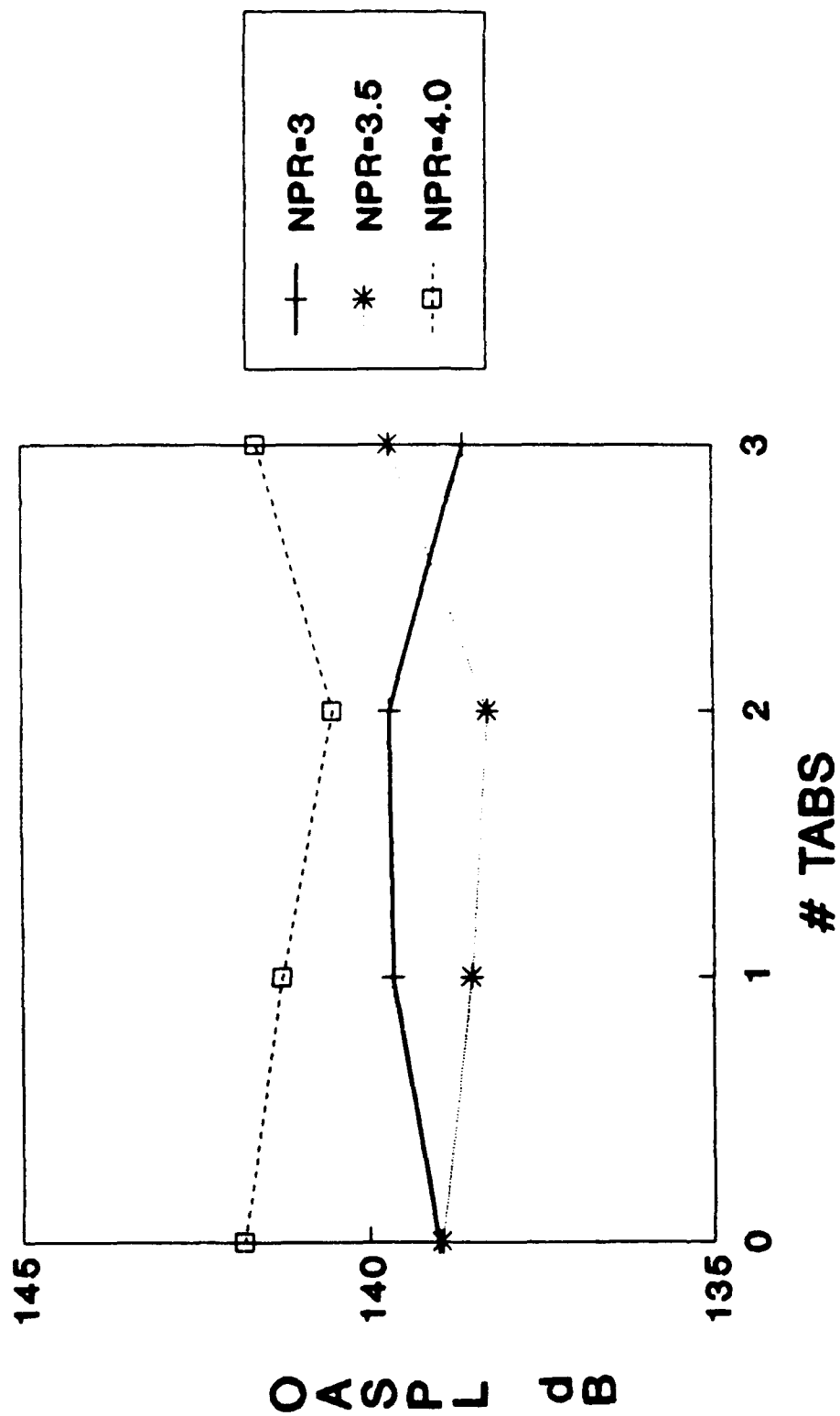


Figure 49. Tab Suppression for Dual Two-dimensional Configurations, (OASPL vs. # Tabs)

### Twin 2D Axial Shift Suppression

The final suppression concept tested was the axial shifting of one of the nozzles in the longitudinal direction. The incremental shift distances ranged from 0.25in (0.635cm) to 1.0in (2.54cm) (Appendix). As was the case for the axisymmetric nozzles, this shifting technique was thought to reduce the interaction of the screech modes and thus reduce the screech amplitudes. However, at nearly every NPR setting, the axial shift configurations resulted in higher levels of screech than the unsuppressed cases (Figure 50). This was particularly true at the very overexpanded and underexpanded NPR settings where the NS mode was dominant. The NS flapping mode was either enhanced or unchanged by the axial shifting of one nozzle.

### Twin 2D Cant Angle Orientation

Nozzle orientation which included canting and vectoring of the nozzles resulted in the following findings. The first nozzle orientation test consisted of canting the two-dimensional nozzles about the longitudinal axis (Appendix). Canting the nozzles from the 0° position to the 90° position essentially transformed the nozzle configuration from a high aspect ratio to a low aspect

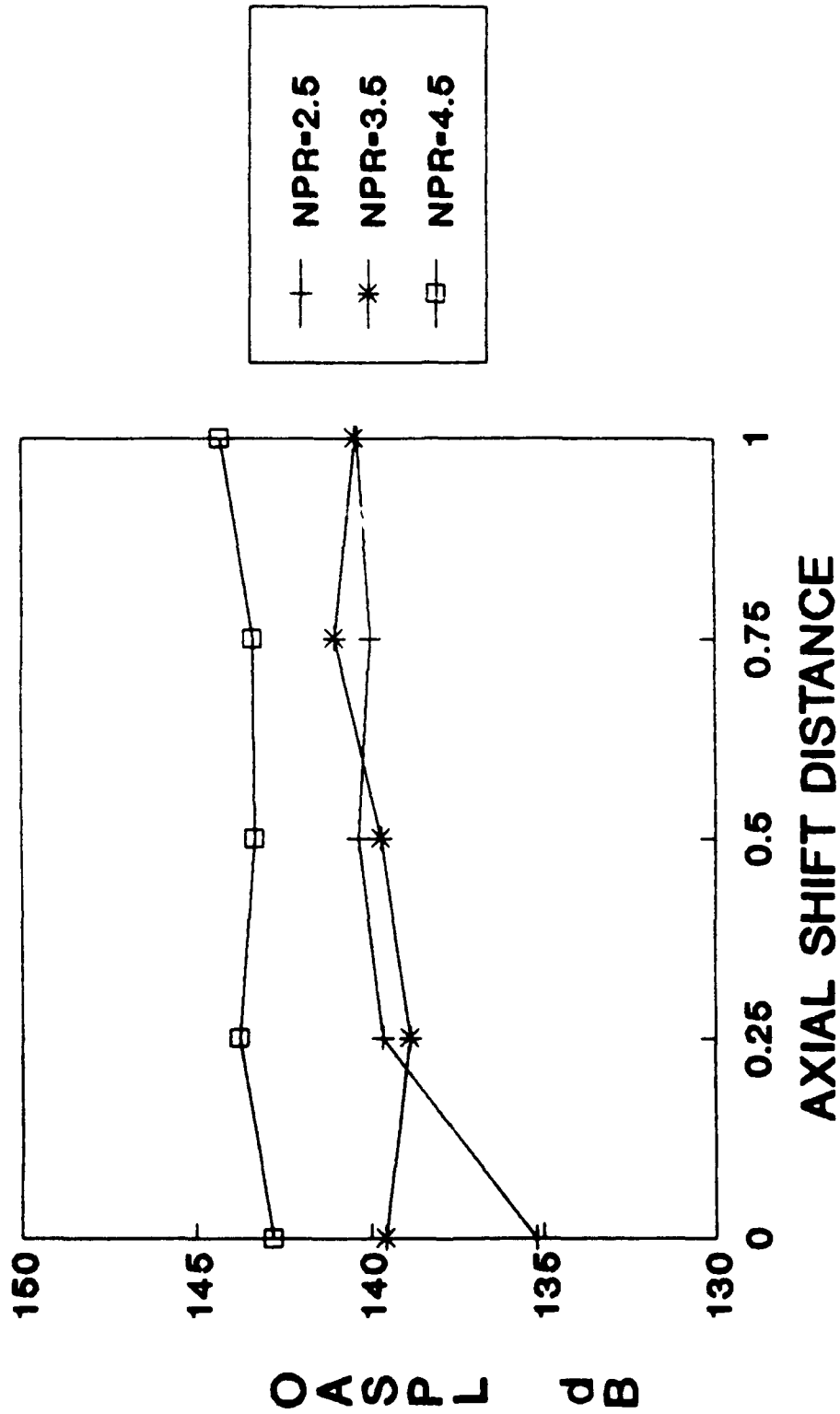


Figure 50. Axial Shift Suppression for Dual Two-dimensional Configurations, (OASPL vs. Axial Shift Distance)

ratio configuration. Over the NPR range, this transformation of the configuration resulted in increasing OASPL amplitudes (Figure 51). According to Zilz and Seiner, a low aspect ratio, rectangular nozzle will produce a lateral flapping motion as defined in Figure 6. The lateral flapping modes produce higher OASPL levels than do the normal flapping modes of the higher aspect ratio nozzles.<sup>9</sup> In Figure 52, a cant angle orientation design plot is presented. As the cant angle of the nozzles was increased, the OASPL for each NPR setting increased steadily. At the NPR=3.5 setting, the OASPL levels were the lowest due to the presence of the NA mode just after the design NPR=3.23 condition. These findings suggest that because high aspect ratio nozzles produce the normal flapping screech modes, high aspect ratio nozzles will produce lower screech amplitudes. A low aspect ratio configuration will produce higher screech amplitudes, since this configuration will produce lateral flapping screech modes.

#### Twin 2D Vectored Thrust

The second nozzle orientation was the vectoring of the twin two-dimensional baseline nozzles to a 10° and a 20° pitch setting. In Figure 53, pitch angles versus NPR range are represented. For the lower NPR values, the vectored nozzles produced the lower

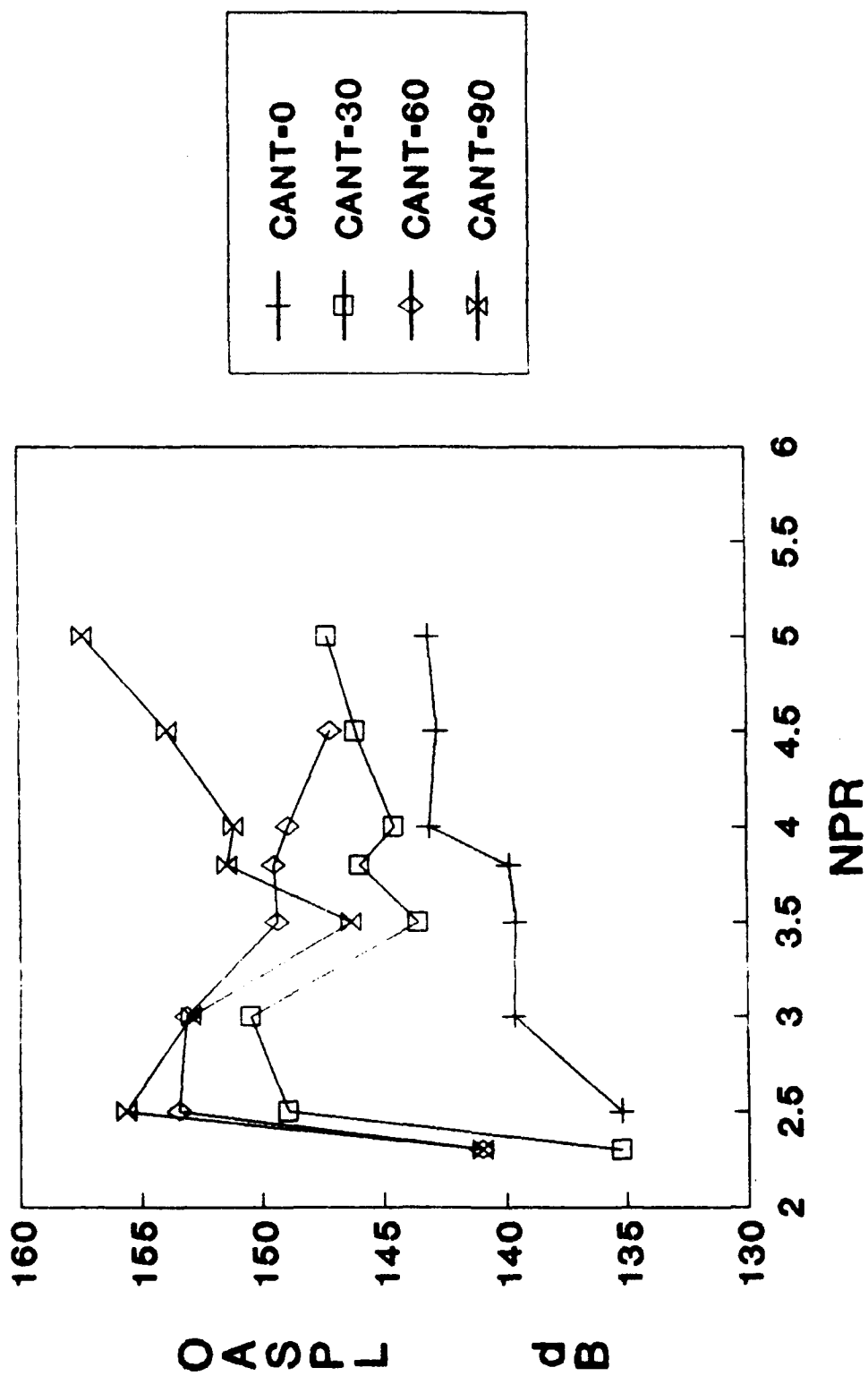


Figure 51. Cant Angle Comparison for Dual Two-dimensional Configurations, (OASPL vs. NPR Plot)

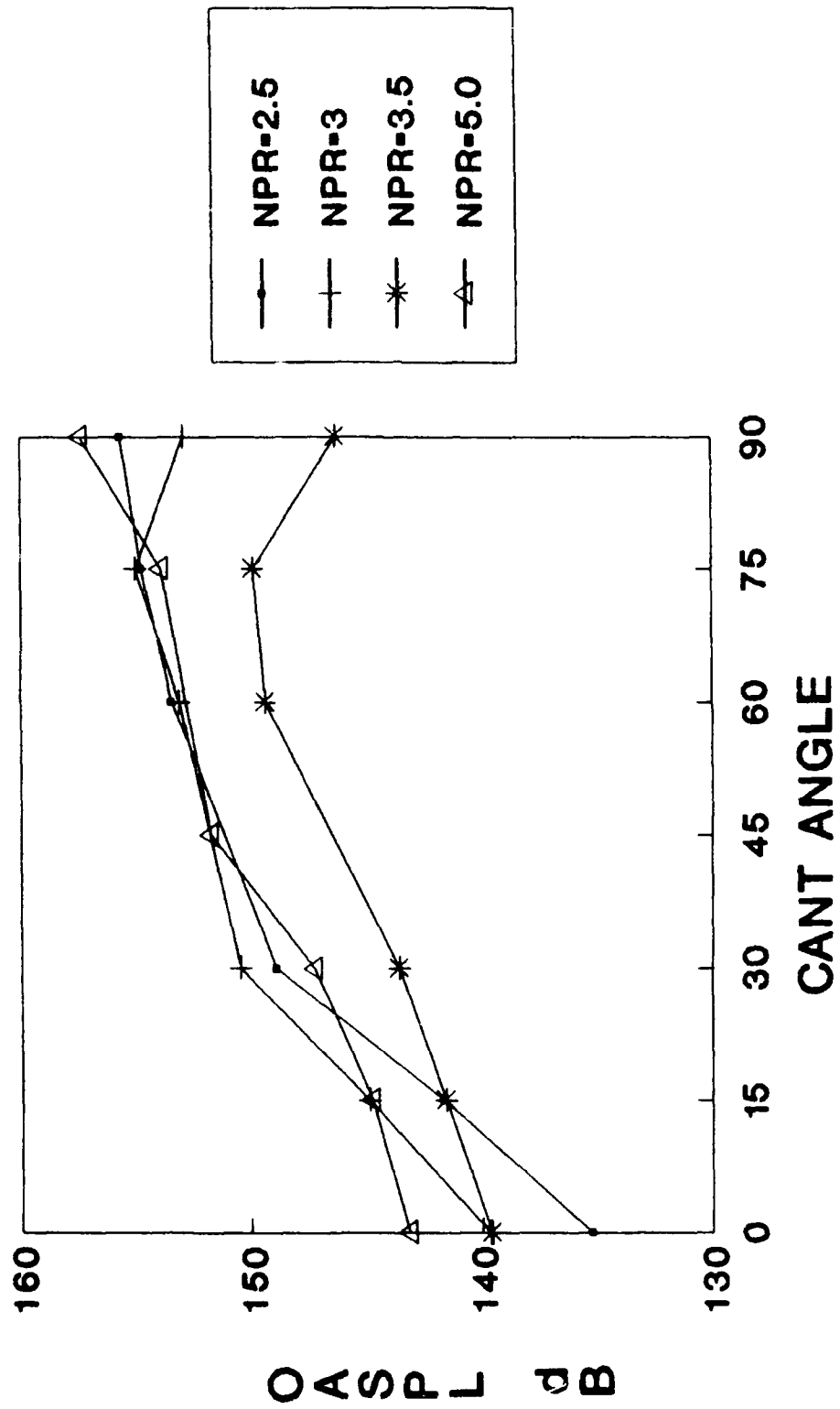


Figure 52. Cant Angle Effect  
(OASPL vs. Cant Angle Plot)

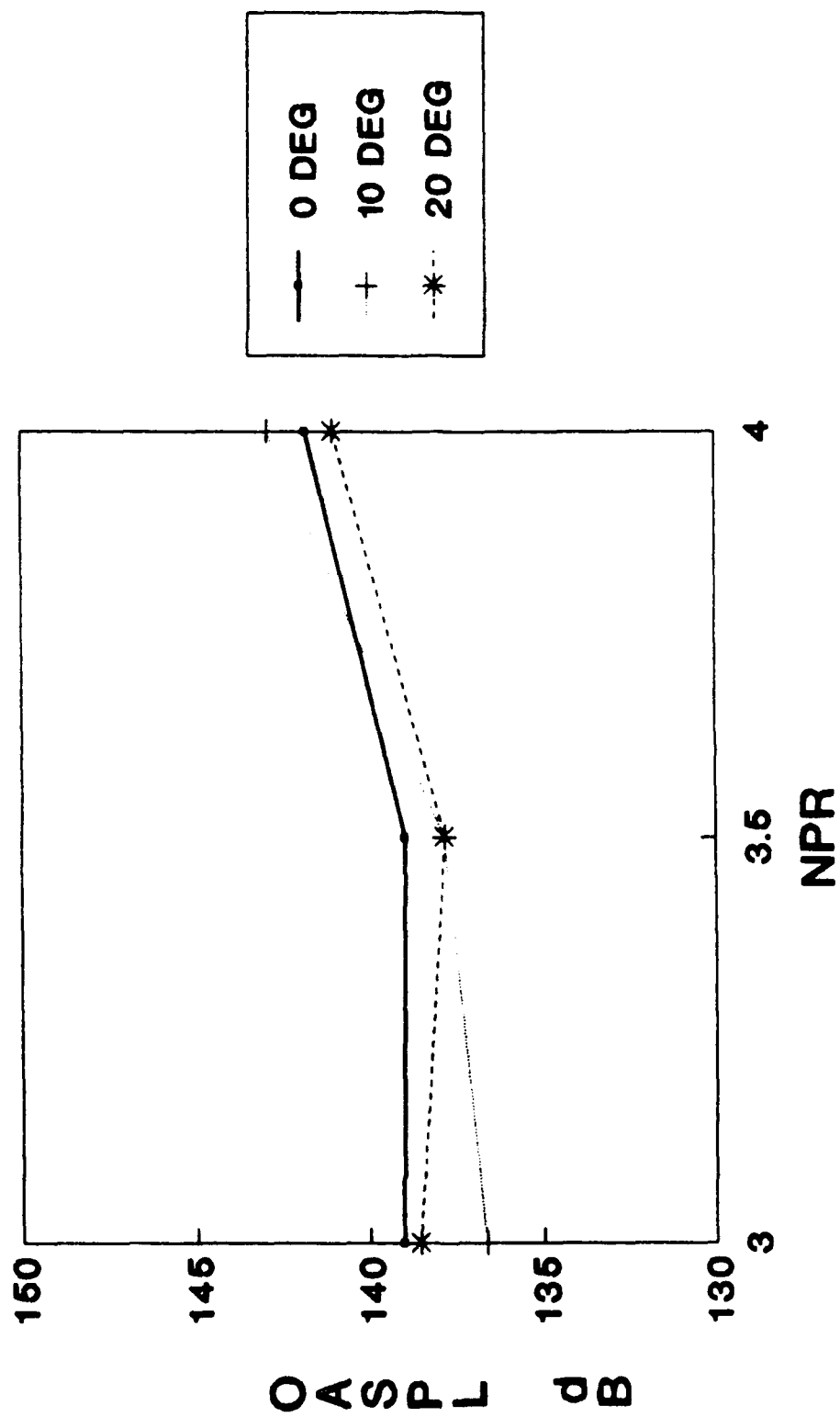


Figure 53. Vectoring Nozzle Effect  
(OASPL vs. NPR Plot)

OASPL amplitudes; however, at an NPR of 4.0, the 10° vectored nozzle produced the highest OASPL amplitude. During the test at the NPR=4.0 condition, the 10° nozzle was seen to have a large wave instability. In Figure 54, the SPL amplitudes of the discrete narrowband peaks are plotted versus pitch deflection. A 10° pitch setting increased screech amplitudes, while a 20° pitch setting decreased the screech amplitude especially at the highest NPR=4.0. The large vector angle seemed to restrict the normal flapping motion of the NS mode. This contributed to lower levels at the 20° pitch setting.



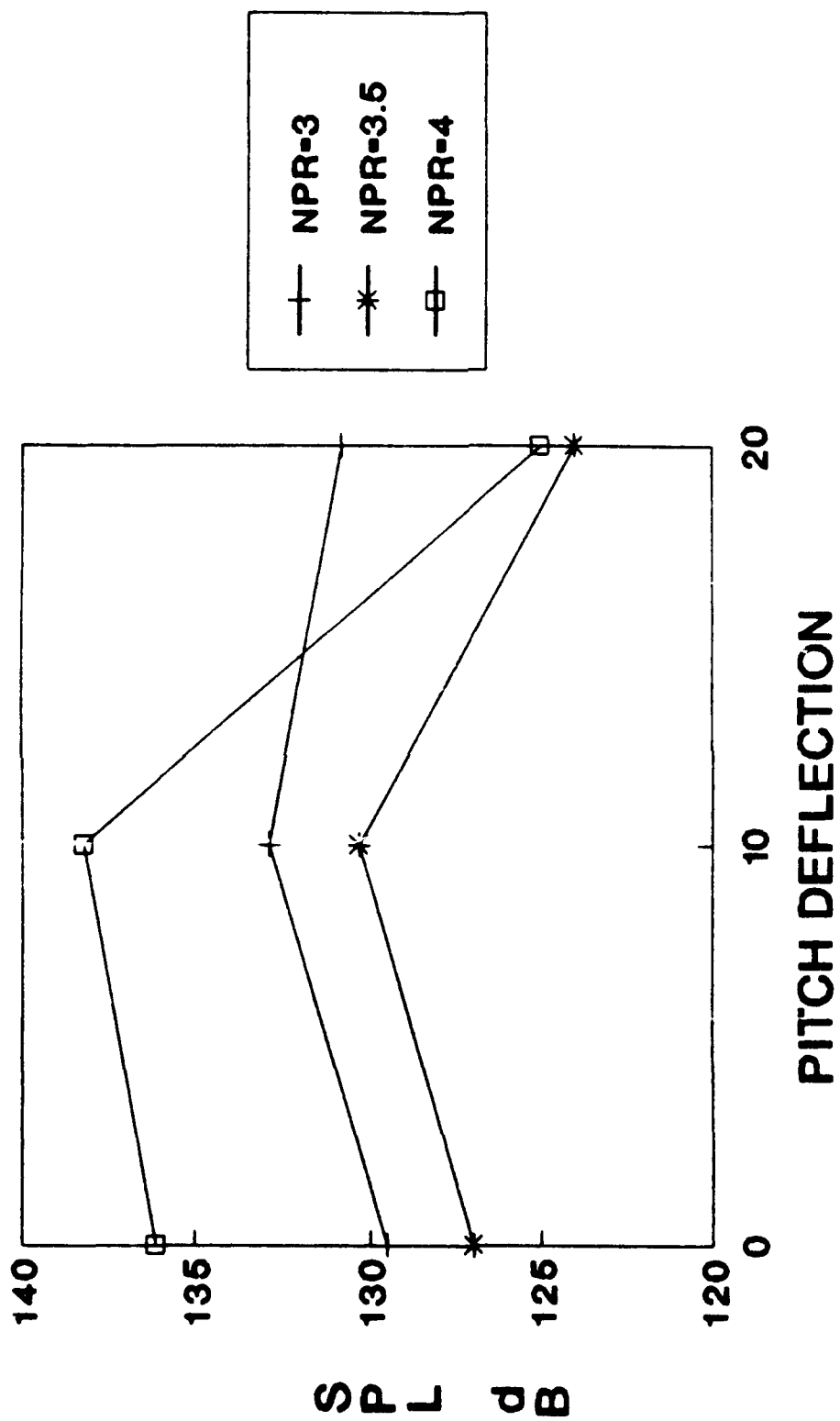


Figure 54. Vectoring Nozzle Effect  
(SPL vs. Pitch Deflection)

## CONCLUSIONS

Axisymmetric and two-dimensional nozzle configurations were tested using several different screech suppression concepts and nozzle orientations. The screech suppression techniques included lateral spacing, secondary air jet, tab suppression, and axial shift. For the two-dimensional nozzle configurations, nozzle orientations such as nozzle canting and pitch vectoring were used.

For the axisymmetric nozzle configurations, the following general nozzle design guidelines were determined:

(1). As the NPR was increased, the SPL amplitudes generally increased based on the stronger shock cell structure present in the jet plume.

(2). The twin configuration produced much higher screech amplitudes over a wider jet Mach number range than did the single nozzle due to the strong helical mode coupling between the jet plumes in the twin nozzle configuration.

(3). The modal frequency dependency on jet Mach number remained the same for the twin nozzle configuration at various nozzle to nozzle spacing ratios.

(4). Generally, the OAPSL amplitudes were highest at the lower nozzle spacing ratios and decreased as the nozzle spacing ratios were increased.

(5). The secondary air jet generally decreased SPL amplitudes with the greatest SPL reduction occurring for the highest secondary air jet pressure.

(6). Nozzle exit tabs reduced SPL amplitudes over the entire jet Mach number region. The tabs decoupled the helical mode interaction between the jets and in some cases resulted in a SPL amplitude reduction of 15 dB.

For the two-dimensional nozzle configurations, the following general nozzle design guidelines were determined:

(1). For the single rectangular nozzle and probably for the twin rectangular nozzle configuration, a single NS mode existed for the overexpanded nozzle conditions.

(2). Just beyond the design NPR condition, the NS and NA modes were present and this resulted in some reduction of OASPL. The NS mode became dominant at the very underexpanded conditions thus increasing the OASPL amplitudes.

(3). Lateral spacing tests showed that the highest OASPL amplitudes occurred at the closest nozzle spacing ratio of 2.75.

Also, for the overexpanded nozzle conditions, the lowest OASPL occurred at the largest nozzle spacing ratio. For the highest underexpanded condition of NPR=4.5, the general trend was a decrease in OASPL with an increase of nozzle spacing ratio. For the NPR condition of 3.5 just beyond the design NPR of 3.23, results were mixed probably due to NS and NA mode interaction.

(4). Some screech suppression was achieved using two exit tabs for the underexpanded NPR conditions. Further work is required in this area.

(5). The nozzle orientation technique of canting the nozzles from essentially a high aspect ratio configuration to a low aspect ratio configuration resulted in a large increase in OASPL amplitudes at every NPR condition. In the low aspect ratio configuration, lateral flapping modes are usually dominant and generally produce higher OASPL amplitudes.

(6). The nozzle orientation technique of pitching the nozzles resulted in an increase in OASPL at the 10° setting and then a large reduction in OASPL at the 20° setting especially at the high NPR conditions.

## REFERENCES

1. Davis, M. R., "Identification of Vortex Motions in Turbulent Mixing of Choked Jets," Experiments in Fluids 6, pp. 335-343, 1988.
2. Powell, A., "On the Mechanism of Choked Jet Noise," Proc. Phys. Soc., Vol. 66, Pt. 12B, pp. 1039-1056, 1953.
3. Seiner, John M., "Advances In High Speed Jet Aeroacoustics," AIAA-84-2275, 1984.
4. Davies, M. C. and Oldfield, D. E. S., "Tones From A Choked Axisymmetric Jet, 1. Cell Structure, Eddy Velocity and Source Locations, II. The Self-Excited Loop and Modes of Oscillation." Acoustica, Vol. 12, No. 4, pp. 257-277, 1962.
5. Norum, T. D., "Screech Suppression in Supersonic Jets," AIAA Journal, Vol. 21, No. 2, pp. 235-240, 1983.

6. Westley, R. and Woolley, J. H., "An Investigation of the Near Noise Fields of a Choked Axisymmetric Jet," AFSOR-UTIAS Symposium on Aerodynamic Noise, Toronto, 1968.

7. Seiner, J. M. and Norum, T. D., "Experiments of Shock Associated Noise on Supersonic Jets," AIAA-79-1526, 1979.

8. Seiner, J. M., Ponton, M. K., and Manning, J. C., "Acoustic Properties Associated with Rectangular Geometry Supersonic Nozzles," AIAA-86-1867, 1986.

9. Zilz, D. E., "Near-Field Acoustics of Supersonic Jets From Twin Two-Dimensional Nozzles," Thesis Notes, 1989.

10. Seiner, J. M., Manning, J. C., and Ponton, M. K., "Model and Full Scale Study of Twin Supersonic Plume Resonance," AIAA-87-0244, 1987.

11. Wlezien, R. W., "Nozzle Geometry Effects on Supersonic Jet Interaction," AIAA-87-2694, 1987.

12. Shaw, L., "Twin Jet Screech Suppression," AIAA-89-1140, 1989.

13. Brown, W. H. and Ahuja, K. K., "Shear Flow Control of Cold and Heated Rectangular Jets by Mechanical Tabs," NASA Contractor Report 182296, 1989.

## APPENDIX

### A.1 Single and Twin Axisymmetric Baseline Configurations:



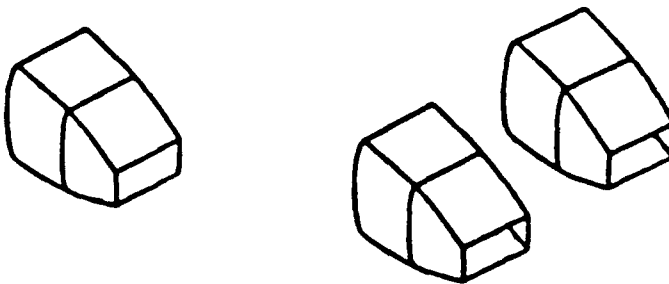
$$d = 1.0''$$

$$s/d = 2.25$$

$$A_e/A_t = 1.0$$

$$M_d = 1.0$$

### A.2 Single and Twin Two-Dimensional Baseline Configurations:



$$W_t, W_e = 1.82''$$

$$H_t = 0.49''$$

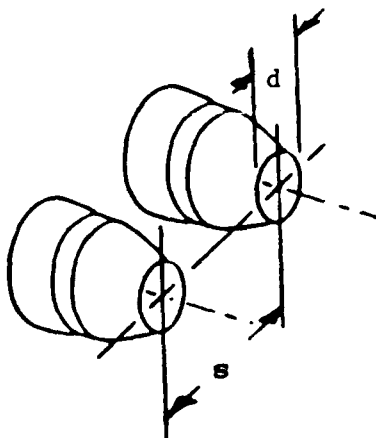
$$H_e = 0.55''$$

$$s/w = 3.25$$

$$A_e/A_t = 1.11$$

$$M_d = 1.4$$

### A.3 Lateral Spacing Suppression Configuration:



$$s/d \text{ range} = 2.25 - 7.0$$

$$s/w \text{ range} = 2.75 - 7.0$$

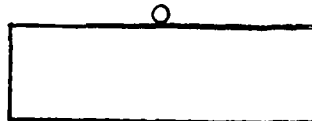
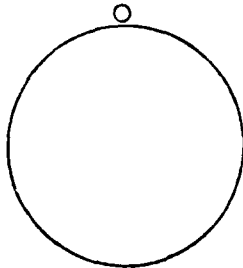


#### A.4 Secondary Air Jet Suppression Configuration:

$$s/d = 2.25$$

$$s/w = 3.25$$



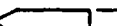
sec. pressure = 0., 10.,  
20., 30.,  
40., 50.,  
60. psig

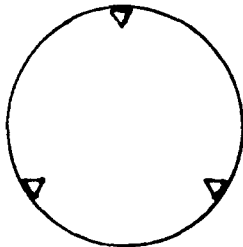


#### A.5 Tab Suppression Configuration:

$$s/d = 2.25$$

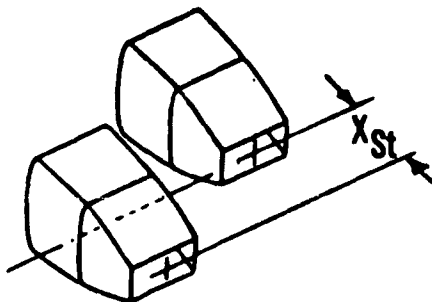
$$s/w = 3.25$$

tab 1  = 0.050"  
tab 2  = 0.100"  
tab 3  = 0.150"



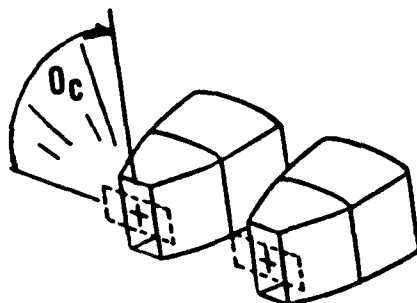
#### A.6 Axial Shift Suppression Configuration:

$$X_{st} = 0., .25, .5, .75, 1.0 "$$



A.7 2D Cant Angle Orientation Configuration:

$$\theta_c = 0^\circ, 15^\circ, 30^\circ, 45^\circ, 60^\circ, 75^\circ, 90^\circ$$



A.8 2D Vectored Thrust Orientation Configuration:

$$\delta_p = 0^\circ, 10^\circ, 20^\circ$$

